

UCSF

UC San Francisco Electronic Theses and Dissertations

Title

A Requirement for the GluA2 AMPA Receptor Subunit in Synaptic Homeostasis

Permalink

<https://escholarship.org/uc/item/6v51w2d1>

Author

Ancona Esselmann, Samantha Grace

Publication Date

2017

Peer reviewed|Thesis/dissertation

A Requirement for the GluA2 AMPA Receptor Subunit
in Synaptic Homeostasis

by

Samantha Ancona Esselmann

DISSERTATION

Submitted in partial satisfaction of the requirements for the degree of

DOCTOR OF PHILOSOPHY

in

Neuroscience

in the

GRADUATE DIVISION

of the

UNIVERSITY OF CALIFORNIA, SAN FRANCISCO

Dedicated to my grandfathers, Jon Mathews and Edward P. Ancona Jr.

“Somehow the unstable stuff of which we are composed has learned the trick of maintaining stability”

- Walter Cannon, *The Wisdom of the Body*

Acknowledgements

My thesis advisor and mentor, Roger Nicoll, has inspired me with his keen scientific mind from the moment I walked into his office to discuss a possible rotation in his lab. The pursuit of knowledge is, to him, uniquely thrilling and rewarding. I found that his scientific integrity and rigor set a wonderful standard for aspiring young scientists in the lab, me included. During my rotation, he was careful to check with me every Thursday after lab meetings to make sure that I deeply understood the material discussed and to chat about my own progress. Later, during the later years of my thesis project, as I became disheartened or disillusioned with troubleshooting or negative results, Roger reached out to me on a regular basis to check in and help me refocus my energy. I only wish I had learned sooner to believe in my own science and to discuss my own results and the state of the field more frequently with Roger. Working under his mentorship was an invaluable experience.

I am, similarly, so grateful to the entire Nicoll lab for their constant intellectual and personal support. I learned so much from the lab's many wonderful postdocs, including Wucheng Tao, John Gray, Bruce Herring, Maya Yamazaki, Nengyin Sheng, Jennifer Sun, and Salvatore Incontro. In particular, I want to acknowledge Argentina Lario-Lago for her forthright and faithful belief in open and reproducible science, as well as for her unshakeable friendship and devotion. I must also acknowledge Javier Díaz-Alonso, for his endless patience and mentorship, as well as for his offer to assist my project with *in utero* electroporations – a skill that is incredibly difficult to master. Finally, I wish to acknowledge Michael Bemben, who began his postdoc in the lab shortly before I began to wrap up my project. He saw holes in my project and immediately offered to step up and

help with difficult biochemical experiments that would have taken many months for me to complete. Argentina, Javier, and Michael were always open to talking through experimental ideas or troubleshooting, and for that I am eternally grateful. If possible, the graduate students in the Nicoll lab mentored me even more than the postdocs did. When I started my rotation, Adam Granger and Jon Levy taught me electrophysiology and contributed to the intellectual scope of my project. Kate Lovero was my lab roommate for over 2 years and she spent so much of her energy helping me troubleshoot my experiments, while encouraging me to study a different project on the side – exploring the role of catalytically-inactive matrix metalloprotein ADAM23. Quynh-Anh Nguyen was always helpful with my molecular biology and electrophysiology questions. Finally, I wish to thank my close friend, classmate and peer, Meryl Horn, who went through every stage of grad school with me. We've spent countless hours discussing our projects over the lab bench, coffee, or wine, and we are constantly pushing each other to strive for excellence in our lab work and in our extracurricular endeavors. Perhaps most critical to my work in the Nicoll lab is the technical assistance of Kirsten Bjorgan, Manuel Cerpas, and Dan Qin, in lab management, ordering supplies, making slice cultures, and genotyping mice.

The UCSF neuroscience community was a wonderful support system, all the way from the directors (Lou Reichardt, Roger Nicoll, then Anatol Kreitzer) and admin (Pat Veitch and Lucita Nacionales), to the students and postdocs in the program, including my classmates. Many in my class became very close, and I will forever treasure the friendships I formed with Mari Sosa, Tom Roseberry, David Leib, Karin Lin, and Jennifer Ortega, among many others. I will always look back fondly on our Latke nights, trips to the mountains, and adventures around the city. In the broader UCSF community, I wish to thank the graduate division communications director,

Jeannine Cuevas, for her unflinching kindness and her support of student outreach activities, especially her support of Carry the One Radio.

I had the great luck of having many peer mentors at UCSF, including Sama Ahmed and Allison Leaf. Sama – the immensely gifted founder of Carry the One Radio – was always encouraging and supportive, seeing leadership potential in me where I saw none. He helped me believe in myself. Allison was one of the co-founders of the Science Policy Group at UCSF who encouraged me to take on leadership of the science policy group after the original leadership graduated. I benefitted so much from my time with SPG where I learned about the intersection of science and policy.

I am also grateful to members of my thesis committee, who provided important feedback throughout my graduate career. My committee chair, Robert Edwards, always shared his sharp knowledge about molecular and cellular neurobiology and helped me to better understand various pitfalls of my techniques. Kevin Bender was a constant and supportive voice on my committee who helped encourage me in my pursuit of non-academic careers. He is also deeply knowledgeable about electrophysiology and encouraged me to delve more deeply into understanding the physiology of ion channels. Graeme Davis was both a member of my thesis committee as well as one of my rotation advisors, and I always enjoyed his philosophical take on the great mysteries of the brain. I wish to also acknowledge my other rotation advisor, Steve Finkbeiner, at the Gladstone institute for neurological disease, who opened my eyes to the world of neurodegenerative disease research. Gaia Skibinski was my postdoc mentor during my rotation in Dr. Finkbeiner's lab and she was a wonderful inspiration for both scientific rigor and personal organization strategies.

I must also thank and acknowledge my undergraduate mentors, including my undergraduate

laboratory volunteer advisor, Don Arnold, who provided so many fantastic opportunities and encouraged me to consider UCSF for graduate school. During my undergraduate work in the Arnold lab, I worked with graduate student Jason Junge, who trusted me to oversee much of the molecular biology and data analysis on his project. Most of what I know now about thinking strategically as a scientist comes from my time in the Arnold lab.

I thank my family for their unwavering support and encouragement over my entire education. My parents, Ted and Valerie, made sure to provide a rich intellectual home environment, while sending me to the public schools for which I was districted. They also made sure to be hands-off during my education so that I would learn to troubleshoot homework problems and personal scheduling on my own. I cannot emphasize enough how important these decisions were to making me the person I am today. I am so grateful, also, for the support I received from my grandparents, Edward and Dorothy Ancona, who provided a rich, international education and helped me dream big. My grandfather was a wonderful example to me of someone who managed to live a life that bridged his creative pursuits and scientific curiosity. My brother, Jon, provided a constant intellectual foil, and is always excited to discuss truly complex global, legal, economic, musical, or scientific issues. We share a unique humor and appreciation for knowledge and I could not have done this without him.

Finally, I acknowledge my husband, Axel, who has been with me over the past 10 years through thick and thin. He saw me morph into a professional oboist and then he encouraged me to pursue science when I decided to re-tool during my junior year of college. He always believed in me more than anyone (including myself) and constantly reminded me to stop doubting my abilities. I am

floored by his extensive knowledge about so many topics (no doubt gained from his podcast addiction), and I am humbled by his deep curiosity about the world. I am looking forward to the next chapters in our lives together.

Contributions

Outside-out electrophysiology experiments in chapter 3 were performed by Jon Levy in the Nicoll lab. *In utero* electroporations in chapter 3 were performed by Nicoll lab postdoc Javier Díaz Alonso. Biochemistry in chapter 3 was performed by Nicoll lab postdoc, Michael Bemben. Kir experiments in chapter 4 were performed by former Nicoll lab graduate student Seth Shipman. Kir2.1 characterization in chapter 4 was carried out by Meryl Horn.

The work in chapter 3 has been accepted by the Proceedings of the National Academy of Science and is reproduced with permission:

Ancona Esselmann, S.G., Diaz-Alonso, J., Levy, J.M., Bemben, M.A., Nicoll, R.A. (2017)
Synaptic homeostasis requires the membrane proximal carboxy tail of GluA2. Proc Natl Acad
Sci U S A.

ABSTRACT OF THE DISSERTATION

A Requirement for the GluA2 AMPA Receptor Subunit in Synaptic Homeostasis.

By Samantha Ancona Esselmann

Doctor of Philosophy in Neuroscience

University of California, San Francisco, 2017

AMPA-type glutamate receptors are known to play a critical role in both basal synaptic transmission and in acute forms of plasticity, such as LTP or LTD, but less is known about their role in neuronal homeostasis. A model for bidirectional synaptic scaling is emerging with the GluA2 AMPA receptor subunit playing a central role. Through my dissertation work, I found that GluA2, but not GluA1, is necessary for synaptic scaling-up, and I showed that GluA2 is also sufficient for mediating this phenomenon. Additionally, I discovered that the membrane-proximal C-terminal domain of GluA2 is required for scaling-up following chronic pharmacological silencing of network activity. Precisely how the GluA2 membrane-proximal C-terminal domain mediates synaptic insertion of AMPA receptors following chronic silencing remains to be elucidated. However, in probing the molecular mechanisms of synaptic homeostasis, we rely on tools and manipulations such as network-wide activity blockade that create highly artificial environments, and few studies have relied on the silencing of individual cells. I therefore employed 4 distinct strategies to chronically hyperpolarize or silence neurons to assess the intrinsic ability of a single neuron to engage synaptic scaling programs. I first hyperpolarized neurons with the inwardly-rectifying potassium channel, Kir2.1, after which I attempted to hyperpolarize neurons with more temporal control by expressing the inhibitory DREADD, hM4Di, and activating GIRK channels via CNO-mediated activation of the DREADD. I then employed a CRISPR/Cas9 strategy to eliminate all neuronal voltage dependent sodium channels. In the final series of experiments, I

set out to achieve tighter temporal control over the abolishment of sodium current. I therefore rescued with the skeletal sodium channel, Nav1.4, on this Nav-null background. Despite employing these four unique strategies to hyperpolarize or silence individual neurons, I observed no evidence for any cell-intrinsic scaling mechanisms. In fact, contrary to our expectations, it seemed that a more Hebbian, non-homeostatic, program overrode synaptic scaling.

Table of Contents

CHAPTER 1 – General Introduction	1
Abbreviations	2
Homeostasis – An Exposition.....	4
Information Processing in the Brain.....	5
Hebbian Plasticity – When Neurons Fire and Wire Together	6
Homeostatic Plasticity in the Brain.....	8
Mechanisms of Synaptic Scaling.....	10
AMPA Receptors in Synaptic Scaling.....	12
Synaptic Scaling – The Big Picture.....	17
CHAPTER 2 – Methods	19
Mouse genetics.....	20
Cloning and plasmid construction.....	20
In-utero electroporation.....	22
Toxins used in electrophysiology.....	22
Neuronal Transfection.....	23
Electrophysiology in slice cultures.....	23
Outside-out patches.....	25
Immunoblotting.....	25
Statistical analysis.....	26

CHAPTER 3 – Synaptic Scaling Requires the Membrane Proximal Carboxy Tail of GluA2. 27

Introduction.....28

Results.....30

 The GluA2 AMPAR subunit, but not GluA1, is necessary for homeostatic synaptic scaling following chronic activity blockade.....30

 The GluA2 AMPAR subunit is sufficient for homeostatic synaptic scaling following chronic activity blockade.....32

 The GluA2 C tail is critical for homeostatic synaptic scaling.....33

 The membrane proximal cytoplasmic tail of the GluA2 subunit is critical for homeostatic synaptic scaling.....34

 Specific membrane proximal cytoplasmic residues in the GluA2 AMPAR subunit are necessary for scaling.....35

 NMDA Receptors and Synaptic Scaling.....35

Discussion.....38

CHAPTER 4 – Cell-Intrinsic Synaptic Scaling 64

Introduction.....65

Results.....69

 Kir2.1 overexpression does not increase synaptic currents.....69

 Single-cell hyperpolarization with hM4Di and CNO does not increase quantal size.....71

 Genetic ablation of all neuronal voltage-sensitive sodium channels drives synaptic depression.....74

 Nav1.4 replacement and temporally-controlled single-cell silencing with μ -Conotoxin

GIIIB leads to synaptic depression.....	75
Discussion.....	77
<u>CHAPTER 5 – General Conclusions</u>	<u>102</u>
GluA2 is necessary and sufficient for the expression of postsynaptic scaling-up.....	103
The membrane-proximal GluA2 CTD is necessary for scaling.....	103
A single amino acid residue within the membrane proximal CTD of GluA2 is necessary for Scaling.....	106
Scaling in single neurons?	108
Future Directions	108
Concluding Remarks.....	111
<u>References</u>	<u>112</u>

List of Figures

CHAPTER 1

Figure 1 – GluA1 and GluA2 intracellular cytoplasmic tail amino acid sequences, with phosphorylation sites and protein interaction sequences	18
--	----

CHAPTER 3

Figure 1 – GluA2, not GluA1, is necessary for homeostatic synaptic scaling of quantal size.....	42
Figure 2 - GluA2 is sufficient to support synaptic scaling in the absence of other AMPAR subunits.....	44
Figure 3 – The cytoplasmic tail of GluA2 subunit is critical for homeostatic synaptic scaling....	46
Figure 4 – Membrane-proximal cytoplasmic tail of GluA2 is critical for synaptic scaling.....	48
Figure 5 – A specific residue in the membrane proximal CTD of the GluA2 AMPAR subunit is necessary for scaling.....	50
Figure S1 The effects of chronic activity blockade on synchronous EPSC size in GluA2-lacking neurons.	52
Figure S2 – GluA1 shRNA validation.....	54
Figure S3 – The effects of chronic activity blockade on synchronous EPSC size in GluA2(Q) replacement neurons.....	56
Figure S4 – The effects of chronic activity blockade on synchronous EPSC size in GluA2-truncation rescued neurons.....	58
Figure S5 – Evidence for robust synaptic scaling of NMDA Receptors.....	60

Figure S6 – AMPAR synaptic accumulation after NMDAR ablation is not occluded by TTX-mediated synaptic scaling.....	62
--	----

CHAPTER 4

Figure 1 – pCaggs-mCherry-IRES-Kir2.1 characterization.	78
Figure 2 – Synaptic effects of long-term overexpression of pCaggs-mCherry-IRES-Kir2.1.....	80
Figure 3 – Synaptic effects of pCaggs-mCherry-IRES-Kir2.1 early overexpression from DIV4-DIV7.....	82
Figure 4 – Synaptic effects of late pCaggs-mCherry-IRES-Kir2.1 overexpression from DIV9-DIV 12.....	84
Figure 5 – Characterization of acute effects of synthetic ligand CNO on Vm of inhibitory DREADD hM4Di-transfected cells.....	86
Figure 6 – Synaptic effects of inhibitory DREADD hM4di and synthetic ligand CNO.....	88
Figure 7 – Synaptic effects of long-term sodium channel genetic ablation.....	90
Figure 8 – Nav1.4 replacement experiment design.....	92
Figure 9 – Acute characterization of skeletal sodium channel replacement on nNav 1.X CRISPR background.....	94
Figure 10 – Acute characterization of skeletal sodium channel replacement on nNav 1.X CRISPR background, with Nav1.4-specific Conotoxin block.....	96
Figure 11 – Synaptic (AMPA) characterization of Nav 1.4 replacement and chronic Conotoxin block.....	98
Figure 12 – Synaptic (NMDA) characterization of Nav 1.4 replacement and chronic Conotoxin block.....	100

Chapter 1

General Introduction

Abbreviations

ACSF – artificial cerebrospinal fluid

AMPA - α -amino-3-hydroxy-5-methyl-4-isoxazolepropionic acid

AMPA - receptor activated by α -amino-3-hydroxy-5-methyl-4-isoxazolepropionic acid

APV - (2*R*)-amino-5-phosphonovaleric acid

ATD – amino terminal domain

ATP – adenosine triphosphate

CA - *cornu ammonis*

cDNA - complementary deoxyribonucleic acid

CNO – clozapine-N-oxide, inert synthetic ligand to activate hM4Di.

CNS – central nervous system

CRISPR – clustered regularly interspaced short palindromic repeats

CTD/C-tail – carboxy terminal domain (CTD and C-tail used interchangeably)

DREADD – designer receptors exclusively activated by designer drugs

DIV – days in vitro

EPSC – excitatory post synaptic current

GFP – green fluorescent protein

GluA2 – glutamate receptor 2

GluA1 – glutamate receptor 1

GRIP1 – glutamate receptor interacting protein 1

gRNA – guide RNA (CRISPR)

GTP – guanosine triphosphate

HBSS – hank's buffered saline solution

HEK – human embryonic kidney

HEPES – *N*-2-hydroxyethylpiperazine-*N*-2-ethanesulfonic acid.

hM4Di – engineered human muscarinic type 4 inhibitory GPCR

Kir2.1 – inwardly rectifying potassium channel 2.1, encoded by the KCNJ2 gene.

KO – knockout

LTD – long term depression

LTP – long term potentiation

mCherry – a red fluorescent protein

MEM - minimum essential medium

mRNA – messenger ribonucleic acid

Nav – voltage sensitive sodium channel

NMDA – *N*-methyl-D-aspartate

NMDAR – receptor activated by *N*-methyl-D-aspartate

PBS – phosphate buffered saline

PCR – polymerase chain reaction

PDZ – postsynaptic density zone

PSD95 – postsynaptic density protein 95

R.I. – rectification index

RNA – ribonucleic acid

shRNA – short hairpin RNA

TTX – tetrodotoxin

WT – wildtype

“Plus ça change, plus c'est la même chose.”
- Jean-Baptiste Alphonse Karr

“The more things change, the more things stay the same,” quipped the French satirist, Jean-Baptiste Alphonse Karr in the January 1849 issue of his journal *Les Guêpes* (“The Wasps”). Karr – referring to the curious way in which turbulent political upheavals often manage to, perversely, cement the *status quo* – had little idea that a student (150 years in the future, on a different continent, studying neurobiology rather than human nature) would quote this particular epigram to set the stage for her dissertation on molecular mechanisms of synaptic homeostasis. Yet here we are (and I think Karr would be thrilled).

Homeostasis – *an exposition*

From the Ancient Greek words for “the same” (*homoios*) and “standing still” (*stasis*), emerges the modern concept of “homeostasis,” a word brimming with etymological tedium and biological mysticism. Building on Claude Bernard’s 1854 theory of ‘*la fixité du milieu interieur*’ (“the constancy of the internal environment”), Walter Bradford Cannon decided to coin the term “homeostasis” in 1926 when he required a word that communicated something beyond an isolated biochemical “equilibrium” (Cannon, 1932; Woods and Ramsay, 2007). When applied to the biologically-inert thermostat, for example, homeostasis describes the ability of that machine to 1) sense the ambient temperature, 2) assess if the ambient temperature falls within a pre-approved set of parameters, and 3) if the ambient temperature is not within these parameters, implement the appropriate negative feedback (i.e. air-conditioning or heater) to return the ambient temperature to within acceptable bounds. Indeed, words like *thermostat*, *heliostat*, or *cryostat* employ the very same root suffix as homeostasis, and all contain negative feedback programs. For a biological being, however, maintaining a physiological *status quo* necessitates a system of immense complexity wherein both normal and pathological perturbations to an organelle, cell, cell-layer,

organ, or organ system, are automatically counteracted (Cannon, 1932; Woods and Ramsay, 2007). In studying the molecular complexities of the brain, it becomes clear that a homeostatic program exists (and *must* exist!) to reign in the natural tendencies of our neural circuitry toward excess. But before we embark into the dense and disorienting jungle of neuronal homeostasis, we must first touch base with the building blocks of neurophysiology.

Information Processing in the Brain

Neuroscientists like to compare and contrast nervous systems with computers (hardware and software). Concepts like circuits, recursive functions, if/then logic statements, electricity, gates, storage, memory, encoding, recall, signal, and resistance, among many others, are common to both lexicons. But many of these comparisons are easier to make at a macro level, between large neural circuits and central processing units, and a fundamental understanding of basic neural function requires a departure from an *in silico* world to an *in vivo* world. In the brain, the essential building blocks of neural circuits are individual biological units, called cells – neurons, specifically – that propagate both electrical and chemical signals and are supported by a vast and varied network of glia. There are billions of neurons in any given mammalian brain, and these neurons form trillions of connections with each other, called synapses.

Of the two types of synapses – chemical and electrical – it is the former that facilitates most of what we think of as information transfer within the brain. When an activated neuron fires an action potential (an all-or-none propagation of membrane depolarization), the depolarizing action potential travels along an axon away from the cell body, and invades the presynaptic terminal,

resulting in the priming and release of vesicles packed with neurotransmitters such as glutamate, acetylcholine, GABA, or dopamine. These neurotransmitters then diffuse across the synaptic cleft and activate their corresponding receptors in the postsynaptic membrane, initiating an ionotropic or metabotropic signal in the postsynaptic cell depending on the specific neurotransmitter-receptor pair. These chemical signals can be transmuted rapidly back into electrical signals by the postsynaptic ionotropic receptors that, when activated, open to allow ion flow, which alters local membrane polarization. Canonical excitatory neurotransmitters like glutamate activate certain receptors that allow the flow of cations into the neuron, which serves to depolarize the postsynaptic terminal. These depolarizing potentials then propagate along the dendrite to the cell body and may elicit a new action potential if threshold is reached, thus completing the electrical-chemical-electrical signal transduction from one neuron to another. But how do a few different neurotransmitters and their receptors inform higher-level cognition? How are perceptual cues processed? How are complex muscle movements orchestrated? How do we form memories?

Hebbian Plasticity – When Neurons Fire and Wire Together

Of particular interest to our lab, is the role of specific neurotransmitters and their corresponding receptors in what is widely believed to be the cellular manifestation of memory formation: the potentiation of synapses. Falling under the umbrella of synaptic plasticity, the potentiation or diminution of synaptic strength were largely theoretical phenomena until the early 1970s, when a study called “Long-lasting potentiation of synaptic transmission in the dentate area of the anaesthetized rabbit following stimulation of the perforant path,” demonstrated an hours-long potentiation of excitatory postsynaptic potentials (EPSPs) in a part of the brain called the

hippocampus following high-frequency stimulation, that was soon dubbed “long-term potentiation” or LTP (Bliss and Lomo, 1973). Belonging to the brain’s limbic system, the hippocampus – so-called because of its uncanny resemblance to the sea horse¹ – plays critically important roles in memory consolidation and recall, and consists primarily of two interlocking specializations, the *Cornu Ammonis* regions (CA1-4) and the Dentate Gyrus. Because the Bliss and Lomo study was performed in the hippocampus, which is known to be required for the formation of memories (Scoville and Milner, 1957), LTP became an attractive candidate for a physical expression of memory formation. Since the first description of LTP in the 1970s, countless scientists have scrambled to uncover the molecules and signaling cascades involved in the phenomenon, with a clear consensus emerging around key players, including NMDARs (*N*-methyl-D-aspartate receptors), AMPARs (α -amino-3-hydroxy-5-methyl-4-isoxazolepropionic acid receptors), and CAMKII (Ca^{2+} /calmodulin-dependent protein kinase II) among others (Collingridge et al., 1983; Giese et al., 1998; Nicoll, 2017; Pettit et al., 1994; Sheng and Kim, 2002).

Briefly, in the well-studied form of postsynaptic LTP that occurs at the hippocampal CA3-CA1 synapse, calcium influx through NMDARs – occurring after coincident postsynaptic depolarization and presynaptic vesicle release – is necessary to initiate a cascade of downstream events, including the activation of CAMKII (Nicoll, 2017). The activation of CAMKII has recently been shown to be a necessary step for the lasting structural enlargement of the postsynaptic specialization (Matsuzaki et al., 2004; Nicoll, 2017). Specific AMPAR subunits, as well as specific residues in their intracellular C-tails, were long thought to be necessary for the postsynaptic

¹ “*Hippos*” is the Greek word for horse, and *kampos* is an ancient Greek word for sea monster.

expression of LTP, as AMPARs are rapidly inserted into the synapse after a potentiating signal (Lee et al., 2003; Lee et al., 2010; Roche et al., 1996; Shi et al., 2001; Zamanillo et al., 1999). However, recent evidence from our lab suggests there is neither a specific AMPA subunit requirement nor an absolute requirement for any AMPARs in LTP expression (Granger et al., 2013). Instead, it seems a large reserve pool of ionotropic glutamate receptors (iGluRs) in the extrasynaptic membrane is required, and this pool may consist entirely of GluA1 homomers, GluA2 homomers, or even Kainate receptors, and still support LTP independent of receptor or subunit type (Granger et al., 2013; Penn et al., 2017).

Long Term Depression (or LTD) – the other side of the same coin – is an NMDAR-dependent weakening of synaptic connections through the rapid and sustained removal of AMPARs from synapses after a low frequency stimulation protocol (Granger and Nicoll, 2014; Malenka and Bear, 2004). Both LTP and LTD are types of “Hebbian Plasticity,” so-called because in the mid-20th century, Donald Hebb imagined a basic framework for encoding memories into synaptic strength, and described it in his book, “The Organization of Behavior,” as follows:

Let us assume that the persistence or repetition of a reverberatory activity (or "trace") tends to induce lasting cellular changes that add to its stability.[...] When an axon of cell A is near enough to excite a cell B and repeatedly or persistently takes part in firing it, some growth process or metabolic change takes place in one or both cells such that A's efficiency, as one of the cells firing B, is increased. (Hebb, 1949)

Homeostatic Plasticity in the Brain

More recently, Hebbian plasticity has been summarized with the epigrammatic, “cells that fire together wire together,” and describes a system that favors positive feedback: LTP, for example,

causes a strengthening of synaptic connections and simultaneously increases the probability of the same synapse being further potentiated. But the problem with this model – if it existed alone – is that neurons, and the information encoded therein, would eventually become saturated in either direction, trending toward runaway activity or quiescence (Fox and Stryker, 2017; Turrigiano and Nelson, 2004). If every synapse in a neuron were simultaneously potentiated, the relative weight and import of signals from individual synapses would be lost to the background noise (Watt and Desai, 2010). Without a mechanism to prevent runaway positive feedback of Hebbian programs like LTP or LTD, our brain’s ability to access and interpret the most critically important information would be lost. Luckily for us, Hebbian plasticity does not exist alone in a vacuum, but coordinates with a different form of plasticity that returns neurons to a set-point of activity. This is called “homeostatic plasticity” (see also the theory of “metaplasticity” - (Bear, 2003; Bienenstock et al., 1982)).

Homeostatic plasticity works globally to prevent, or counteract, the saturation of synaptic strength through negative feedback programs, such as 1) the homeostatic insertion and removal of postsynaptic receptors, 2) the modulation of presynaptic neurotransmitter release (Harris et al., 2015; Lindskog et al., 2010; Muller et al., 2012; Paradis et al., 2001; Younger et al., 2013), or 3) the adjustment of relative ion channel abundance and patterns of expression (Parrish et al., 2014) (Davis, 2013; Turrigiano et al., 1994). In each of these scenarios, as long as the neuron is able to return to some predetermined set-point of activity in the presence of a normal or pathological perturbation, the program is thought to be homeostatic (Abbott and Nelson, 2000; Davis, 2013). However, for the purposes of this dissertation, I focus on the first of these three mechanisms: homeostatic modulation of postsynaptic receptor abundance.

Mechanisms of Synaptic Scaling

In the late 1990s, two groups first demonstrated a bidirectional scaling of quantal amplitude in cultured mammalian neurons (O'Brien et al., 1998; Turrigiano et al., 1998). Chronically silencing (for 24-48 hours) cortical cultures with saturating concentrations of the sodium channel blocker, tetrodotoxin (TTX), elicited a compensatory global increase in quantal size via the insertion of AMPARs, while chronic excitation of these cultures with the competitive GABA_A receptor antagonist, bicuculline, caused a compensatory decrease in quantal size via putative removal of synaptic AMPARs (Turrigiano et al., 1998). It was later confirmed that there was also an NMDAR component to bidirectional synaptic scaling (Goold and Nicoll, 2010; Watt et al., 2000).

Subsequently, several molecules that might mediate scaling upstream of synaptic AMPAR insertion have been proposed, including BDNF, TNF-alpha, Retinoic acid, Arc/Arg3.1, L-Type calcium channels, and the calcium/calmodulin-dependent protein kinases (CAM-Kinases) (Aoto et al., 2008; Groth et al., 2011; Rutherford et al., 1998; Shepherd et al., 2006; Stellwagen and Malenka, 2006; Thiagarajan et al., 2005). Early scaling studies in mammalian cultures identified a role for BDNF, whereby exogenous BDNF blocked scaling, a BDNF receptor blocker induced scaling, and BDNF had the opposite effect on quantal amplitudes in interneurons, suggesting a role in maintaining the excitation/ inhibition balance in neural circuits (Rutherford et al., 1998).

One smaller branch of scaling research has explored the co-opting of traditional immune signaling molecules in nervous system function², where TNF- α is secreted by glia – possibly in response to

² In Harris et al., 2015, a member of the peptidoglycan pattern recognition receptor family (PGRP-LC) is necessary for the induction and expression of a presynaptic form of homeostatic plasticity at the fly neuromuscular junction (Harris, N., Braiser, D. J., Dickman, D. K., Fetter, R. D., Tong,

extracellular levels of glutamate – to control synaptic scaling in neurons (Stellwagen and Malenka, 2006). That same year, immediate early gene Arc was found to control levels of surface AMPARs homeostatically, supposedly working to optimally maintain surface levels and subunit composition for subsequent and coincident Hebbian forms of plasticity (Shepherd et al., 2006). Soon after, a study exploring the role of Retinoic Acid (RA) in scaling, found that 1) activity blockade increased RA synthesis, 2) acute RA application enhanced synaptic transmission through local translation and synaptic incorporation of GluA1, and 3) knocking-down RA’s nuclear receptor, RAR α , blocked synaptic scaling (Aoto et al., 2008). Another group observed a preferential synaptic insertion of GluA1 homomers following block of L-type Ca²⁺ channels with Nifedipine, causing loss of Ca²⁺ entry and a resultant “increase in vesicle pool size and turnover rate” (Thiagarajan et al., 2005).³ Finally, multiple groups have described a role for CAMKK and its downstream kinase, CAMKIV, in bi-directional synaptic scaling (Gainey et al., 2009; Goold and Nicoll, 2010). However, the field remains unsettled as to which scaling programs are the most physiologically relevant, and no group has mechanistically linked any of these upstream players with downstream AMPAR accumulation.

A., and Davis, G. W. (2015). The Innate Immune Receptor PGRP-LC Controls Presynaptic Homeostatic Plasticity. *Neuron* 88, 1157-1164, *ibid.*)

³ Worth mentioning here – although not discussed further in this dissertation – is that Ca²⁺-permeable AMPARs are thought to play a role in synaptic scaling of interneurons, as surface levels of GluA4 have been shown to increase in PV+ hippocampal interneurons following chronic network excitation (Chang, M. C., Park, J. M., Pelkey, K. A., Grabenstatter, H. L., Xu, D., Linden, D. J., Sutula, T. P., McBain, C. J., and Worley, P. F. (2010). Narp regulates homeostatic scaling of excitatory synapses on parvalbumin-expressing interneurons. *Nat Neurosci* 13, 1090-1097.). The preponderance of GluA1 and GluA4 AMPAR subunits and absence of GluA2 in interneurons of MGE*-origin renders these AMPARs Ca²⁺-Permeable, and thus inwardly-rectifying (Matta, J. A., Pelkey, K. A., Craig, M. T., Chittajallu, R., Jeffries, B. W., and McBain, C. J. (2013). Developmental origin dictates interneuron AMPA and NMDA receptor subunit composition and plasticity. *Ibid.* 16, 1032-1041.) *MGE refers to the Medial Ganglionic Eminence.

Importantly, the mechanism or mechanisms by which a neuron (or neurons) senses changing activity remains unclear, which I address in chapter 4. It is possible that neurons sense their own firing rate and respond with a global increase or decrease in synaptic strength (Ibata et al., 2008). Conversely, it is also possible that hyper-local perturbations – i.e. at the level of individual spines – induce local protein translation and synaptic AMPAR incorporation (Sutton et al., 2006). Finally, it may be that widespread changes in network activity are required for scaling, involving soluble molecules like BDNF, TNF-alpha, or Retinoic Acid (Aoto et al., 2008; Rutherford et al., 1998; Stellwagen and Malenka, 2006). It is equally possible that all of these scaling programs coordinate to ensure a robust homeostatic response in the presence of a perturbation, and are not mutually exclusive.

AMPA Receptors in Synaptic Scaling

As so much controversy exists concerning the upstream mediators and signaling pathways, it is perhaps easier to focus on the AMPA receptors themselves when dissecting mechanisms of scaling. After all, if the necessary AMPAR subunit(s) can be found, and the critical domain(s) identified, perhaps one might work backwards to identify putative interacting proteins. However, the field is also divided in this matter. While a handful of groups have identified a specific requirement for the GluA2 AMPAR subunit in bidirectional synaptic scaling (Gainey et al., 2009; Gainey et al., 2015; Goold and Nicoll, 2010; Shipman et al., 2013), others have either directly or indirectly found a requirement for GluA1 (Garcia-Bereguian et al., 2013; Groth et al., 2011; Letellier et al., 2014; Lindskog et al., 2010; Soares et al., 2013), or no specific requirement for any individual AMPAR subunit (Altimimi and Stellwagen, 2013).

In the mammalian CNS, there are four AMPA receptor subunits, GluA1, GluA2, GluA3, and GluA4 (Hollmann and Heinemann, 1994; Keinänen et al., 1990) and each has a unique role and pattern of expression within the brain (Lu et al., 2009; Wenthold et al., 1996). Responsible for most rapid, excitatory synaptic transmission in the CNS, AMPARs are activated by glutamate binding, allowing flow of cations including Na⁺, Ca²⁺, and K⁺ – although the Ca²⁺ permeability is governed by the subunit composition (Sommer et al., 1991) – and display a characteristic rapid desensitization (Armstrong et al., 2006). AMPARs are formed as a heteromeric or homomeric combinations of four subunits, each subunit containing a single glutamate binding pocket, a large extracellular amino terminal domain (ATD), four membrane-associated domains (M1–4) including one (M2) re-entrant loop which forms the pore, and a small cytoplasmic carboxy terminal domain (CTD) (Rosenmund et al., 1998; Sobolevsky et al., 2009). The vast majority of AMPA receptors in the brain contain the GluA2 subunit, and in the hippocampus and neocortex, pyramidal neurons express AMPARs formed by GluA2 and GluA1, while most remaining AMPARs are GluA2/GluA3 heteromers. Notably, GluA1A2 heteromers form approximately 80% of the synaptic pool and up to 95% of extrasynaptic surface receptors in hippocampal CA1 pyramidal neurons (Lu et al., 2009; Wenthold et al., 1996).

Within GluA2, a glutamine (Q) in the pore region undergoes RNA editing to an arginine (R), which confers receptor-impermeability to Ca²⁺ ions and a decreased single-channel conductance (Greger et al., 2003; Greger et al., 2007). Another unique feature of GluA2-containing AMPARs is a linear current-voltage relationship, as current through GluA2-lacking AMPARs is blocked between 0 and +40mV by intracellular positively charged polyamines, which become lodged in the pore during membrane depolarization. Thus, GluA2-lacking receptors display “inward rectification,”

and this current-voltage relationship serves as a useful tool for determining the relative abundance of GluA2-lacking vs. GluA2-containing receptors in a cell (Panicker et al., 2008).

AMPA receptor intracellular C-tails carry the most sequence divergence, and this heterogeneity could point to putative protein interactions involved in synaptic scaling (Figure 1). Amino acid residues in the GluA1 C-tail were thought to play a critical role in LTP until it was shown that LTP was preserved in the absence of GluA1 (Granger et al., 2013), although rebuttals to this finding have focused on the highly artificial environment created by the *GRIA1-3^{fl/fl}* manipulation. Perhaps because of the preponderance of studies showing a specific requirement for the GluA1 C-tail in LTP, there was increasing interest developing around the role of the GluA2 C-tail in scaling. Indeed, a role for GluA2 in single cell scaling-down was described in 2010, whereby germline knockout of GluA2, but not GluA1, blocked scaling-down following chronic single-cell optogenetic excitation, with no effect on NMDAR scaling (Goold and Nicoll, 2010). In 2009, the Turrigiano lab reported a requirement in dissociated cultures of cortical neurons for the GluA2 subunit in scaling-up following chronic activity blockade (Gainey et al., 2009). By overexpressing a short GluA2 C-tail peptide and rescuing a GluA2 knockdown with a chimeric GluA2-GluA1 subunit (GluA2 + GluA1 C-tail), the authors showed a specific requirement for GluA2 in scaling-up. Years later, a subsequent study was published from the same lab in which the authors demonstrate a requirement for specific residues in the distal GluA2 C-tail, implicating phosphorylation sites within the GRIP/PICK binding domain in scaling-up, although this is not consistent with our results, for reasons described in chapters 3 and 5 (Gainey et al., 2015).

Within the GluA2 C-tail, a number of protein binding or phosphorylation sites have been identified (Figure 1). Of the proteins thought to interact with the GluA2 C-tail, I discuss the following in chapters 3 and 5: Band4.1, AP2 adapter complex (AP2), *N*-Ethylmaleimide-Sensitive Fusion protein (NSF), Protein Interacting with C Kinase-1 (PICK1), and Glutamate Receptor Interacting Protein-1 (GRIP1). Of the known phosphorylation sites in the GluA2 and GluA1 C-tails, the following are discussed in chapter 3: GluA2 880S, GluA1 816S, and GluA1 818S.

NSF is a hexameric ATPase involved in membrane fusion events and found to have a putative role in the delivery of AMPARs to synapses via binding of the GluA2 membrane proximal C-tail (Noel et al., 1999; Osten et al., 1998). It was shown that when the GluA2-NSF interaction is blocked, endocytosis of AMPARs increases, suggesting a role for NSF in stabilizing GluA2-containing AMPARs at the surface (Braithwaite et al., 2002). In the same study, the authors identified a counteracting role of GRIP1, which binds the distal C-tail of GluA2 and was thought to act by stabilizing an intracellular reserve pool of GluA2-containing AMPARs for subsequent surface recycling, which would support homeostatic scaling. The importance of this GRIP1/GluA2 interaction in synaptic scaling was demonstrated again in 2015, when the GRIP1/GluA2 interaction was blocked by mutating residues in the distal GluA2 C-tail or knocking down GRIP1. Both manipulations blocked scaling-up after chronic network silencing (Gainey et al., 2015). The authors concluded that GRIP1 and PICK1 compete for binding of one region within the GluA2 C-tail (in which GRIP works to promote scaling while PICK blocks scaling), and that the relative binding of these proteins is governed by the phosphorylation state of distal GluA2 C-tail serines and tyrosines (Dong et al., 1999; Gainey et al., 2015). Further evidence for the role of PICK1 in a homeostatic internalization of AMPARs came from a study showing that PICK1 germline

knockout occludes scaling-up but has no effect on scaling-down (Anggono et al., 2011). Finally, the AP2 binding site in the proximal GluA2 C-tail overlaps significantly with the NSF binding site⁴, and a competitive interaction between NSF and AP2 has been proposed, in which NSF works to bring AMPARs to the surface and AP2 is helping to coordinate clathrin-mediated endocytosis of AMPAR-containing vesicles (Lee et al., 2002). How this push and pull between endocytosis and surface delivery could play out in scaling remains to be explored.

Given the prevailing controversy surrounding AMPAR subunit specificity in synaptic homeostasis, the aim of my graduate work was to determine the AMPAR subunit or subunits and corresponding amino acid residues necessary for the expression of synaptic scaling-up following chronic activity blockade. I also hoped to determine if any AMPA receptor is sufficient for the expression of scaling, in the absence of all endogenous AMPARs. To achieve these goals, I used either short-hairpin RNAs or a Cre-Lox system to remove endogenous AMPAR subunits, in combination with single-cell molecular replacement. For the Cre-Lox experiments, I used mice with floxed GluA1, GluA2, and GluA3 genes (*GRIA1-3^{fl/fl}*) which allows for the complete genetic deletion of endogenous AMPARs with expression of the Cre recombinase. The *GRIA1-3^{fl/fl}* mice were characterized in a previous study (Lu et al., 2009), and provide a clean genetic background on which I can rescue with individual transfected AMPAR subunits to explore their role in synaptic scaling (Granger et al., 2013).

⁴ Peptides that were previously shown to interfere with NSF binding the GluA2 C-tail also work to interfere with the AP2-GluA2 interaction, suggesting their binding sites overlap. Lee, S. H., Liu, L., Wang, Y. T., and Sheng, M. (2002). Clathrin adaptor AP2 and NSF interact with overlapping sites of GluR2 and play distinct roles in AMPA receptor trafficking and hippocampal LTD. *Neuron* 36, 661-674.

Synaptic Scaling – The Big Picture

In chapter 3 of this dissertation, I describe experiments exploring AMPA receptor subunit necessity and sufficiency in synaptic scaling following chronic activity blockade, and provide evidence that the GluA2 AMPAR subunit is both necessary and sufficient for scaling. I also identify a specific region in the membrane proximal GluA2 C-tail that is necessary for scaling, which is at odds with the GluA2 scaling literature to date (Gainey et al., 2015). In chapter 4, I take a step back and ask a much more fundamental question: when we silence activity in an entire network of neurons – thereby blocking programs of activity-dependent competition – are we observing physiologically-relevant molecular mechanisms that govern scaling? To address this, I designed a series of experiments in which I reduce or eliminate the capability of an individual neuron to fire action potentials, and I examine the effects of these manipulations on synaptic scaling programs. I found that individually silenced or hyperpolarized neurons either scaled-down synaptic activity or did not change, suggesting that chronic network-wide activity blockade may not tell the whole story.

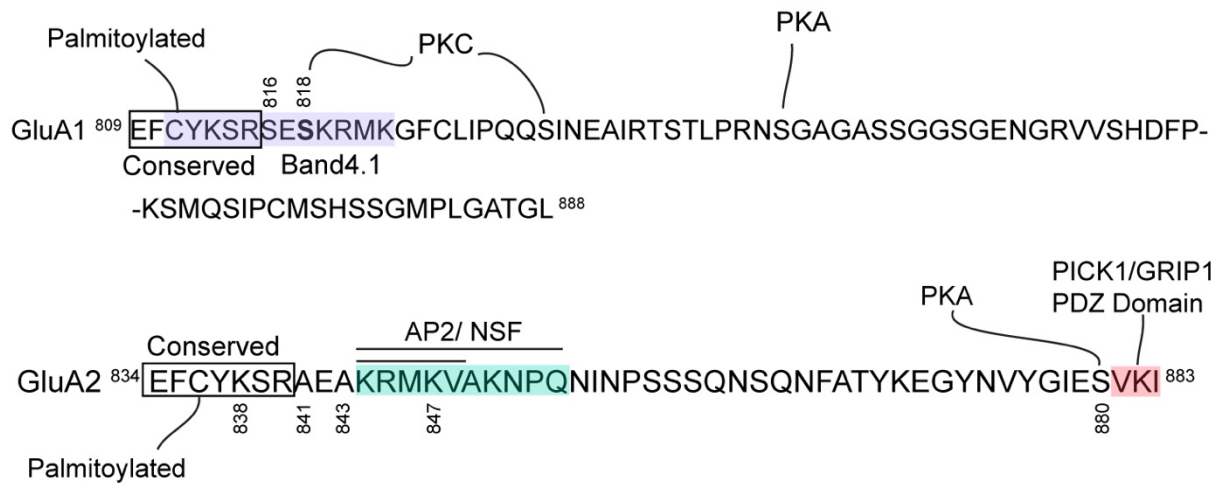


Figure 1. GluA1 and GluA2 intracellular cytoplasmic tail amino acid sequences, with phosphorylation and protein interaction sequences labeled.

Chapter 2

Methods

Mouse genetics

All animals were housed according to the IACUC guidelines at the University of California, San Francisco. Mice with the *GRIA1*^{fl/fl}, *GRIA2*^{fl/fl}, and *GRIA3*^{fl/fl} (*GRIA1-3*^{fl/fl}) were generated and genotyped as previously described (Lu et al., 2009).

Cloning and plasmid construction

For mouse sodium channel CRISPRs, the following guide RNA (gRNA) targeting sequences were used (5' to 3'), from Horn, M. et al 2017 in review at Cell Reports: Mouse Nav1.1, 1.2, and 1.3: TCCACTCCCCACACAGCACG; Nav1.6: GCTGCTGCAGAATGAGAAGA; For rat sodium channel CRISPR, the consensus sequence GACCATGTGGGACTGCATGG is present in Nav1.1, 1.2, 1.3 and 1.6, which we targeted with a single CRISPR, with the gRNA sequence (5' to 3'): GACCATGTGGGACTGCATGGAGG. Other consensus sequences were targeted with other CRISPR Nav1.X gRNAs, but were not found to adequately ablate sodium currents (data not shown). GluN1 gRNA sequence: AACCAGGCCAATAAGCGACA was validated previously in (Incontro et al., 2014)

All AMPAR constructs and Cre:GFP were cloned into the pFUGW expression plasmid by PCR and In-Fusion® HD Cloning System (Invitrogen). pFUGW-GluA2 constructs were co-expressed with GFP behind an internal ribosomal entry site (IRES). Knockdown constructs targeting GluA2 (shGluA2, target sequence: 5' GGAGCACTCCTTAGCTTGA 3') and GluA1 (shGluA1, target sequence: 5' GGAATCCGAAAGATTGGT 3') were expressed from an H1 promoter in pFHUGW along with GFP expressed from the Ubiquitin promoter to mark the

transfected cell. AMPAR subunit truncations, chimeras, and mutation constructs, were generated by overlap extension PCR. GluA2 Δ C ended in amino acid 838, with the last 4 amino-acids being FCYK. GluA2 Δ 847 ended with the sequence KRMK. GluA2 A841S contained the proximal C-tail sequence EFCYKSRSEAKRMK. GluA2 A843S contained the proximal C-tail sequence EFCYKSRAESKRMK, and GluA2 A841S, A843S contained the proximal C-tail sequence EFCYKSRSESKRMK. Chimeric AMPAR constructs were made by swapping C-tail sequences of GluA1 and GluA2.

pCAGGs-mCherry-IRES-Kir2.1 construct was cloned by infusing[®] Kir2.1 PCR product after IRES into pCAGGs-mCherry-IRES construct. pCAGGs-Kir2.1-T2A-TdTomato construct was kindly donated by Massimo Scanziani (Xue et al., 2014).

pCAGGs-mCherry-IRES-hM4Di was cloned by infusing[®] hM4D(Gi) PCR product after the IRES into pCAGGs-mCherry-IRES construct. Original pcDNA5/FRT-HA-hM4D(Gi) was a gift from Bryan Roth (Addgene plasmid #45548) (Armbruster et al., 2007).

To clone CRISPR constructs, gRNAs were ligated into pX458 using the InFusionHD cloning system in a bicistronic plasmid containing the human-optimized Cas9. For targeting all neuronal sodium channels in mouse slices, bullets were triple coated with the gRNA/Cas9 construct containing gRNA targeting Nav1.1, Nav1.2, Nav1.3 and a vector containing the gRNA targeting Nav1.6, along with a cell fill (pCAGGS-mCherry) to identify transfected cells. For targeting all neuronal sodium channels in rat slices, bullets were double coated with the gRNA/Cas9 construct taoning the gRNA targeting Nav1.1, Nav1.2, Nav1.3, Nav1.6 and a cell fill (pCAGGS-mCherry).

For overexpression of skeletal sodium channel, we co-coated rat Nav CRISPR gRNA with Nav1.4 rNav1.4-pBsta, which we procured courtesy of the Julius lab.

In utero electroporation

For in utero electroporations, at embryonic day 15.5 (~E15.5) pregnant *GRIA1-3^{fl/fl}* mice were anesthetized with 2.5% isoflurane in O₂ and injected with buprenorphine for analgesic. Embryos within the uterus were temporarily removed from the abdomen and injected with 2 µl of mixed plasmid DNA into the left ventricle via a beveled micropipette. Each embryo was electroporated with 5x50 millisecond, 35 volt pulses. The positive electrode was placed in the lower right hemisphere and the negative electrode placed in the upper left hemisphere. Following electroporation, the embryos were sutured into the abdomen, and sacrificed on postnatal day 6-9 (P6-9) for organotypic slice cultures. For further detail on electroporation, please see (Navarro-Quiroga et al., 2007).

Toxins used in Electrophysiology

Clozapine-*N*-Oxide (CNO) was ordered from Sigma Aldrich (cat# C0832-5MG) and was initially dissolved in Dimethyl Sulfoxide (DMSO) at 20 mM and later added to slice culture medium or bath perfusion at 2 µM final concentration.

Tetrodotoxin (TTX) was ordered from Fisher Scientific (Cat# NC0066215) and dissolved in water to 1mM. It was later added to slice culture medium at 1 µM final concentration.

μ -Conotoxin GIIIB was ordered from VWR International (# H-9015.0500BA) and dissolved in water to an initial stock concentration of 600 μ M. μ -Conotoxin GIIIB was added to slice culture medium or bath perfusion at 600 nM final concentration.

Neuronal Transfection

Sparse biolistic transfections of organotypic slice cultures were performed as previously described (Schnell et al., 2002). Briefly, 50-100 μ g total of mixed plasmid DNA was coated on 1 μ M-diameter gold particles in 0.5 mM spermidine, precipitated with 0.1 mM CaCl_2 , and washed 4x in pure ethanol. The gold particles were coated onto PVC tubing, dried using ultra-pure N_2 gas, and stored at 4 degrees in desiccant. DNA-coated bullets were shot with a Helios Gene Gun (BioRad).

Electrophysiology in Slice Cultures

Dual whole-cell recordings in area CA1 were done by simultaneously recording responses from a fluorescent transfected neuron and neighboring untransfected control neuron. Dual whole-cell recordings measuring strontium evoked aEPSCs used an extracellular solution bubbled with 95% O_2 / 5% CO_2 consisting of (in mM) 119 NaCl, 2.5 KCl, 4 SrCl₂ (substituted with 4 CaCl₂ in synchronous EPSC recordings), 4 MgSO₄, 1 NaH₂PO₄, 26.2 NaHCO₃, 11 Glucose. 100 μ M picrotoxin was added to block inhibitory currents and in synchronous EPSC experiments, 2 μ M 2-Chloroadenosine was used to control epileptiform activity. For voltage clamp experiments, intracellular solution contained 135 CsMeSO₄, 8 NaCl, 10 HEPES, 0.3 EGTA, 5 QX314-Cl, 4

MgATP, 0.3 Na₃GTP, 0.1 spermine. For current clamp experiments, intracellular solution contained 135 mM KMeS, 10mM NaCl, 2mM MgCl₂, 1mM EGTA, 10mM HEPES, 14mM phosphocreatine, 4mM Mg-ATP, and 0.3mM Na-GTP. KMeS internal was used for all current clamp experiments, including experiments to measure membrane potentials and rheobase currents in Kir2.1 transfected cells, hM4Di experiments confirming acute efficacy of CNO application, and nNav 1.X CRISPR experiments. In Kir2.1 rheobase experiments, current was pulsed in gradually increasing amounts for 500ms until a single action potential was reliably elicited (this is the rheobase current). In nNav 1.X CRISPR action potential rise time and height experiments, the start of the action potential was the point at which the action potential reached 10% of its maximum slope.

Cultures were either untreated or chronically incubated for 48 hours with 1 μ M TTX and recordings were made after washing off TTX in the recording bath ACSF for >5 minutes unless otherwise indicated. For asynchronous EPSC recordings, a bipolar stimulation electrode (FHC) was placed in stratum radiatum, and stimulation was increased from 0.2 Hz to 2 Hz to increase the frequency of Sr²⁺-evoked responses (Oliet et al., 1996). Sr²⁺-evoked aEPSCs were analyzed off-line with custom software (IGOR Pro), and in all cases at least 100 quantal events per cell were used in the analysis. In all scale bars used for aEPSC sample traces, scale bars represent 5pA and 20 ms unless otherwise noted. Responses were collected with a Multiclamp 700A amplifier (Axon Instruments), filtered at 2 kHz, and digitized at 10 kHz. To examine AMPAR rectification, 100 μ M D-AP5 was washed-in to block NMDA receptors. Rectification was calculated as the ratio of the slopes of the lines connecting AMPA EPSC amplitude from 0 to +40 mV and from -70 mV to

0 mV. This calculation can be taken as follows: $R.I. = 7(I_{40} - I_0)/4(I_0 - I_{70})$ where I_x represent EPSC amplitude at x mV.

Outside-out Patches

Outside-out patches were taken from CA1 cells by obtaining whole-cell access to CA1 pyramidal neurons at -70 mV with a $4-5$ M Ω patch pipette, then slowly pulling the pipette away from the soma until a high-resistance seal reformed. HEPES-aCSF containing (in mM): 150 NaCl, 2.5 KCl, 10 HEPES, 10 glucose, 1 MgCl₂, 2 CaCl₂, 0.1 D-AP5, 0.1 picrotoxin, 0.1 cyclothiazide, and 0.5 μ M TTX was then perfused over the tip of the pipette. Glutamate currents were evoked by perfusing HEPES-ACSF containing 1 mM L-glutamic. A ValveLink 8 (AutoMate Scientific Inc.) was used for fast perfusion of control, and glutamate containing HEPES-aCSF. Voltage ramps from -70 mV to $+40$ mV were generated in the presence and absence of glutamate. The glutamate-activated current was obtained by subtraction. Rectification was calculated as in synaptic experiments.

Immunoblotting

HEK293T cells were maintained and transfected as previously described (Bemben et al., 2014). Cells were washed in PBS and resuspended directly in SDS-PAGE sample buffer and subjected to Western blotting. Membranes were blocked with blotting grade buffer (Bio-Rad, Cat No. 170-6404). Antibodies used in the study were GluA1 (Rb, Synaptic Systems, Cat No. 182 103) and Actin (MS, ABM, Cat No. G043).

Statistical Analysis

For all experiments involving un-paired data, including all outside-out patch data, a Mann-Whitney U-test was used. For rectification experiments, a Kruskal-Wallis test with Dunn correction for multiple comparisons was used. For all experiments using paired data, a two-tailed Wilcoxon signed-rank test was used. Data analysis was carried out in Igor Pro (Wavemetrics), Excel (Microsoft), and Graphpad (Prism).

Chapter 3

Synaptic scaling requires the
membrane-proximal carboxy
tail of GluA2

Introduction

In the vertebrate central nervous system, AMPA receptors (AMPA receptors) mediate the majority of fast excitatory synaptic transmission, and are formed as tetrameric combinations of four subunits (GluA1-4). Each subunit is differentially expressed over development and throughout the brain, and obeys distinct trafficking patterns during both basal activity and plasticity (Huganir and Nicoll, 2013; Malinow and Malenka, 2002). Numerous studies have explored the putative AMPAR subunit specificity in acute forms of plasticity, including both long-term potentiation (LTP) and long-term depression (LTD) (Collingridge et al., 2004; Huganir and Nicoll, 2013; Malinow and Malenka, 2002; Sheng and Kim, 2002). However, recent evidence suggests that there is no absolute requirement for a specific AMPAR subunit in supporting LTP (Granger et al., 2013) or LTD (Granger and Nicoll, 2014). In contrast, there has been comparatively little exploration of possible AMPAR subunit requirements in slower, homeostatic forms of plasticity.

First demonstrated in experiments characterizing the effects of chronic activity suppression in cultured cortical neurons (O'Brien et al., 1998; Turrigiano et al., 1998), synaptic scaling is now an established phenomenon in excitatory neurons, in which chronic changes in neural activity induce counteracting changes in postsynaptic neurotransmitter receptor abundance, contributing to the restoration of baseline neuronal output (Turrigiano, 2008). Previous studies implicate the GluA2 AMPAR subunit in both cell-autonomous and network-wide synaptic scaling in pyramidal cells of the visual cortex and hippocampus (Gainey et al., 2009; Gainey et al., 2015; Goold and Nicoll, 2010) (but see (Altimimi and Stellwagen, 2013)). However, other lines of evidence suggest that GluA2-lacking, or calcium permeable, AMPARs are preferentially trafficked to the synapse during scaling ((Aoto et al., 2008; Groth et al., 2011; Soares et al., 2013; Thiagarajan et al., 2005) but see (Gainey et al., 2009)).

Here, we set out to find the AMPAR subunit and specific regions within it required to support scaling-up. To achieve this, we employed a variety of molecular replacement techniques, replacing endogenous AMPARs with chimeric AMPAR subunits, or subunits containing point mutations within identified critical regions. We first explored the requirement for the individual AMPAR subunits GluA1 and GluA2 in synaptic scaling, as the vast majority of endogenous AMPARs in CA1 pyramidal neurons are GluA1A2 heteromers (Lu et al., 2009; Wenthold et al., 1996). We found a requirement for GluA2, but not GluA1, in scaling-up of postsynaptic currents in rodent hippocampal pyramidal neurons in organotypic slice culture, consistent with previous observations from dissociated cultures of cortical neurons. Additionally, we found that AMPAR subunits lacking the GluA2 cytoplasmic C-terminal domain (CTD) failed to support scaling-up, while both wild-type GluA2 and chimeric subunits containing the GluA2 CTD were sufficient to support scaling. In neurons expressing only GluA2(Q) homomers, scaling-up remained intact, indicating that GluA2 is sufficient to support scaling-up. Most surprisingly, we found no requirement for the distal GluA2 CTD in scaling-up, despite evidence from previous studies that have found the distal CTD to be important (Gainey et al., 2015). Instead, we identified a specific amino acid sequence within the membrane proximal GluA2 CTD to be necessary and sufficient for scaling, and we demonstrate that point mutations within the region disrupt the ability of the GluA2 subunit to support scaling, suggesting a previously undescribed interaction.

Results

The GluA2 AMPAR subunit, but not GluA1, is necessary for homeostatic synaptic scaling following chronic activity blockade

Previous studies exploring the necessity of the GluA2 AMPAR subunit in synaptic scaling have relied primarily on recording miniature excitatory post-synaptic currents (mEPSCs) in dissociated cultures of cortical rodent neurons. Here, we have instead turned to organotypic hippocampal slice cultures, a system which is also pharmacologically accessible, but allows us to use evoked stimulation of CA3 inputs onto CA1 pyramidal neurons, more closely modeling the input these cells receive *in vivo*. Organotypic slices were prepared from P6–P8 animals and biolistically transfected with a gene gun the following day, a technique which results in a very sparse transfection, to investigate effects of cell-autonomous genetic manipulations (Fig. 1A). We first set out to verify in slice culture that, as in dissociated culture, synaptic AMPAR content scales up following chronic network silencing with saturating concentrations of tetrodotoxin (1 μ M TTX). Using a bipolar electrode, we stimulated Schaffer Collateral axons from CA3 and recorded both synchronous and asynchronous excitatory postsynaptic currents (aEPSCs) in CA1 pyramidal neurons. aEPSC recordings were made in the presence of 4 mM extracellular strontium, which resulted in desynchronization of vesicle release from the presynaptic terminal, allowing for analysis of discrete aEPSCs (Fig. 1B, asterisks). For asynchronous recordings, a train of 3 stimuli spaced 500 ms apart was used to elicit aEPSCs, and following each stimulus artifact a period of 50 ms containing a synchronous component of the EPSC was not analyzed (Fig. 1B, gray bars). As expected, aEPSCs scale up by approximately 40% in wild-type neurons following chronic activity blockade (Fig. 1B). It has been reported that GluA2-lacking receptors, which generate strongly inwardly-rectifying currents, are recruited to the synapse following scaling-up ((Aoto et

al., 2008; Groth et al., 2011; Soares et al., 2013; Thiagarajan et al., 2005), but see (Gainey et al., 2009)). However, the rectification index (R.I.) of evoked synaptic AMPAR currents was unaltered following protracted (>72 hours) TTX exposure (Fig. 1C). We also examined the rectification of extrasynaptic AMPAR currents from somatic outside out patches (Fig. 1D) by generating I/V curves. Compared to the dramatic rectification seen in GluA2-lacking cells (broken line in Fig. 1D), the curves from control cells (black line) and those exposed to TTX (green line), were very similar, although there was slight, but significant, decrease in R.I. (Fig. 1D, bar graph, inset).

We then sought to confirm the role for GluA2 in scaling, a requirement that has been described previously in dissociated cultures of cortical neurons. We first confirmed the efficacy of our short hairpin RNA (shRNA) knockdown of the GluA2 subunit by comparing the R.I. of evoked EPSCs from shRNA transfected cells and neighboring control cells (Shipman et al., 2013). Expression of the shRNA for 7-9 days resulted in EPSCs that were strongly rectifying (Fig. 1E). In all the following experiments we simultaneously recorded aEPSCs in a transfected neuron and a neighboring control neuron. By monitoring the control cells we could verify the presence of normal scaling in each of our experiments. We confirmed that scaling is absent in neurons expressing the shRNA (Fig. 1F and 1I), as the size of the aEPSCs in untransfected cells (clear bars) is increased following TTX treatment, while the size of aEPSCs recorded from the shRNA expressing cells treated in TTX (salmon colored bars) are no different from those not treated with TTX (gray bars). The scaling of aEPSC amplitudes is fully restored with the co-transfection of an RNAi-insensitive GluA2 (insensitivity to the shRNA is denoted by an asterisk* appended to the subunit name, Fig. 1G and 1I). Additionally, the relative amplitude of synchronous EPSCs in GluA2-lacking cells compared to neighboring controls is not maintained following chronic network silencing (Fig. S1) further verifying the requirement for GluA2 in scaling-up (Fig. S1 and S3B).

Is the GluA1 AMPAR subunit required for scaling-up? To test this possibility we biolistically transfected an shRNA targeting the GluA1 subunit (Fig. S2) and examined the effect of chronic activity blockade with TTX. The scaling-up of aEPSCs in GluA1 lacking cells was the same as that observed in untransfected cells (Fig. 1H and I). These data confirm the necessity of GluA2, but not GluA1, in scaling of excitatory synaptic currents. The finding that scaling-up is intact in the absence of GluA1, raises the possibility that GluA2 may be sufficient for this phenomenon.

The GluA2 AMPAR subunit is sufficient for homeostatic synaptic scaling following chronic activity blockade

Next we asked whether GluA2 is alone sufficient for synaptic scaling, in the absence of all endogenous AMPAR subunits native to hippocampal pyramidal neurons. To address this question, we used a molecular replacement strategy with conditional knockout mice homozygous for floxed GluA1, GluA2, and GluA3 (*GRIA1-3^{fl/fl}*) from which we generated slice cultures between postnatal days 6 and 9. We then sparsely transfected Cre recombinase along with the unedited rectifying GluA2 subunit GluA2(Q) using biolistic transfection on the day after cultures were made (Fig. 2A). We used GluA2(Q), rather than the GluA2(R), because neurons only expressing GluA2(R) generate little AMPAR current (Lu et al., 2009). This strategy allows for a complete replacement of endogenous heteromeric AMPARs with GluA2 homomers in transfected cells, confirmed by measuring the rectification index (Fig. 2B).

In this null background GluA2(Q) rescued approximately 70% of synchronous excitatory current amplitude at -70mV, relative to neighboring untransfected control cells (Fig. S3A). Cells expressing only homomeric GluA2(Q) receptors exhibited normal scaling-up following chronic

silencing (Fig. 2C). This data with aEPSCs is supported by synchronous EPSC experiments (See Fig. S3A and B). Additionally, GluA1 replacement on the *GRIA1-3^{fl/fl}* + Cre background was unable to support scaling-up following chronic silencing (Fig. 2D). These results further support a model in which GluA2 is not only necessary for the synaptic expression of scaling but is also sufficient.

The GluA2 C tail is critical for homeostatic synaptic scaling

Previous studies suggest that the GluA2 CTD may be integral for the scaling pathway. Thus, dialysis of a GluA2 CTD peptide into the cell blocked scaling (Gainey et al., 2009), presumably by acting in a dominant negative fashion. Further evidence pointed to a homeostatic mechanism by which GRIP interacts with the distal GluA2 CTD (Gainey et al., 2015). To clarify further the role of the GluA2 CTD in scaling we performed a series of experiments replacing endogenous GluA2 with GluA1-GluA2 chimeric subunits or with a CTD-truncated GluA2.

In neurons expressing GluA2 shRNA we rescued synaptic currents with chimeric, truncated, or mutated AMPAR subunits that were RNAi-insensitive (marked with *) to assess the role of the GluA2 CTD in scaling. First, we rescued with chimeric AMPAR subunits in which the CTDs of the GluA1 and GluA2 were swapped (GluA1A2CTD and GluA2*A1CTD) (Fig. 3A and B). We confirmed the synaptic incorporation of the GluA2*A1CTD, by the loss of rectification (Fig. 3F). Despite its targeting to the synapse this chimera was unable to rescue scaling, indicating a requirement for the GluA2 CTD (Fig. 3C and E). The possibility remained that the GluA2 CTD was not sufficient to restore scaling in the absence of the rest of the GluA2 subunit. However,

when we rescued with GluA2 CTD appended to GluA1, scaling was rescued (Fig. 3D and E), confirming the key role of the GluA2 CTD in scaling-up.

The membrane proximal cytoplasmic tail of the GluA2 subunit is critical for homeostatic synaptic scaling

What domain of the CTD of GluA2 is required for scaling? To address this, we designed a series of truncations (Fig. 4A and 4B). In neurons expressing a construct in which the entire CTD of GluA2 (GluA2* Δ CTD) is deleted, homeostatic scaling was absent (Fig. 4C, 4F and see S4). However, this negative result could be due to a failure of GluA2 Δ *CTD to form functional receptors or an inability for it to traffic to the synapse. To address this concern we quantified the synaptic rectification index of evoked EPSCs (Fig. 4G). The fact that rectification was the same as in control cells indicates that this receptor is functional and traffics to the synapse. These findings establish the necessity of the GluA2 CTD in scaling.

We next re-introduced sections of the GluA2 CTD to the GluA2* Δ CTD construct, adding back 9 amino acids to the membrane proximal region (MPR) of the CTD (Fig. 4A and 4B). Surprisingly, this replacement subunit, GluA2* Δ 847 (so-called because the CTD is truncated following K847) was able to fully rescue scaling-up of aEPSCs (Fig. 4D, 4F and see S4). This result – in which scaling is rescued with a GluA2 subunit lacking the majority of the CTD – appears to be at odds with previous results in which phosphorylation of a distal serine 880, or replacement of the distal serine with glutamate to mimic phosphorylation, blocked scaling-up (Gainey et al., 2015). We therefore carried out a series of experiments in which we mutated serine 880 to glutamate (GluA2*S880E). In our hands robust scaling occurred with this mutation (Fig. 4E and 4F).

Specific membrane proximal cytoplasmic residues in the GluA2 AMPAR subunit are necessary for scaling

After establishing a requirement for the MPR of GluA2 CTD in scaling, we set out to determine the role of specific residues. Examination of this region (Fig. 5A and 5B) reveals that the only difference between GluA2 and GluA1 are two alanines in GluA2 (A841 and A843) instead of two serines in GluA1 (S816 and S818). We therefore focused on these two residues. In all of the following experiments we quantified R.I. of the evoked EPSCs to ensure that the constructs all successfully trafficked to the synapse (Fig. 5H). Mutating the two alanines in RNAi-proofed GluA2 to “GluA1-like” serines (GluA2* A841S, A843S) abolished scaling (Fig. 5C and 5G). Additionally, scaling was also absent when the same mutations were made in the truncated GluA2 (GluA2* Δ 847) (Fig. S6). These results establish the requirement for either one or both membrane proximal alanines for scaling. Next, we tested the requirement for these two residues individually. Surprisingly, scaling was restored when endogenous GluA2 was replaced with GluA2* A841S (Fig. 5D and 5G) but not when replaced with GluA2* A843S (Fig. 5E and 5G), indicating a specific role or requirement for A843 of GluA2. If this alanine is critical for homeostasis one might predict that mutating the equivalent serine in GluA1 (S818) to an alanine would rescue scaling. Indeed, we found that this construct (GluA2*A1CTD S818A) rescued scaling (Fig. 5F and 5G).

NMDA Receptors and Synaptic Scaling

Of note, in the course of these experiments, we became curious about the role of NMDA receptors in AMPAR-mediated synaptic scaling, as we observed – largely by chance – a very significant decrease in the AMPA/NMDA ratio after chronic TTX treatment (Figure S5). This result seemed

to suggest that not only was the NMDAR synaptic component scaling-up in response to chronic network silencing (shown previously (Watt et al., 2000)), but also that it was scaling-up more than the AMPAR-mediated component. If AMPA scaled-up more than NMDA, one would expect to see an increase in the AMPA/NMDA ratio. If AMPA and NMDA scaled-up to a similar degree, one would expect a maintenance of the AMPA/NMDA ratio. One of the more likely scenarios, supported by a handful of previous experiments (Perez-Otano and Ehlers, 2005), would involve the formation of silent synapses with chronic, pharmacological network silencing. Silent synapses are known to contain NMDA receptors but no AMPA receptors (Kerchner and Nicoll, 2008), which could explain the dramatic reduction in AMPA/NMDA ratio. In support of this model, Arendt et al. found evidence of the formation of silent synapses with chronic TTX treatment, and a subsequent massively-potentiated LTP (Arendt et al., 2013) (i.e. more silent synapses allows for a larger LTP). This result argues for a mechanism by which a neuron is able to “turn up the volume” after chronic network-wide silencing, such that it becomes exquisitely more sensitive to subsequent activity.

While this result was intriguing, it would be outside the scope of our original aims to pursue it further. Further experiments may elucidate the mechanisms by which silent synapses form with TTX incubation, or the mechanisms by which NMDARs are able to respond so robustly to homeostatic molecular programs. For example, one might explore possible subunit requirements in NMDAR-scaling, as there are known activity-dependent maturation programs for NMDAR subunits, namely, the activity-dependent switch from the GluN2B subunit, which prevents premature synapse maturation, to the GluN2A subunit, which promotes maturation (Gray et al., 2011). Genetic ablation of these two subunits has distinct physiological effects: GluN2A deletion results in an increase in mEPSC (AMPA) amplitude without a concomitant increase in frequency,

while GluN2B deletion results in higher mEPSC frequency with no change in amplitude (Gray et al., 2011). One group reported an activity-dependent switch from GluN2B to GluN2A subunits following prolonged activity deprivation, although no change in AMPA/NMDA ratio was reported in this study (Soares et al., 2013). Of interest, these activity-dependent subunit switches are known to influence synaptic AMPAR levels, and studies exploring the requirement for NMDARs during development have found no requirement for NMDARs in synapse formation, instead finding a role for NMDARs in blocking recruitment of AMPARs to immature synapses (Adesnik et al., 2008). Consistent, low-grade activation of NMDARs blocks early synapse maturation and discrete bursts of activity seem to induce the formation of functional synapses.

In light of this, we decided to test the possibility that NMDARs were somehow involved in the TTX-induced scaling-up of synaptic AMPARs. To explore this possibility, we genetically ablated NMDARs using our lab's previously validated GluN1 CRISPR (Incontro et al., 2014), resulting in a complete abolishment of NMDARs, as the GluN1 subunit is obligatory for receptor formation (Figure S6). Both TTX incubation and genetic ablation of NMDARs are known to, individually, cause an increase in AMPARs at synapses (Adesnik et al., 2008), so we wondered if NMDAR ablation could occlude the scaling-up of AMPAR-mediated EPSCs with TTX incubation.

If NMDAR control of synaptic AMPAR occupation was solely responsible for gating the TTX-induced scaling-up of AMPARs, we would expect a genetic ablation of NMDARs to occlude scaling-up. Instead, we found that after 48 hours of TTX incubation – on the background of the GluN1 CRISPR – scaling-up was not occluded (Figure S6A), which suggests that scaling-up of AMPARs does not depend entirely on the activity of NMDARs. NMDAR ablation with GluN1

CRISPR after 3 weeks of gRNA with Cas9 expression was confirmed by recording NMDAR currents (Figure S6B). While these results are preliminary, they indicate that the AMPAR enhancement following NMDAR ablation is a distinct phenomenon from AMPAR scaling up following chronic TTX treatment. Further work is needed to elucidate the ways AMPARs can be regulated by NMDARs (Explanation in Figure S6C and S6D).

Discussion

Using molecular replacement strategies to dissect the role of specific AMPAR subunits and associated subdomains necessary for scaling, we have established that the GluA2 subunit is both necessary and sufficient for homeostatic scaling. In addition, we identify a specific and novel role for the GluA2 CTD. While previous reports have implicated the CTD of GluA2 in homeostasis (Gainey et al., 2009; Gainey et al., 2015), our results define a critical residue in the membrane-proximal region of the CTD. Contrary to a previous report (Gainey et al., 2015), we could find no requirement for more distal sequences or specific residues therein. Perhaps the difference in results is due to the preparation: we used hippocampal slice culture, while the previous study used dissociated visual cortical neurons. Finally, we identified a specific uncharged residue, S843, within the membrane-proximal CTD of the GluA2 subunit that, when mutated, renders the GluA2 CTD unable to support scaling following chronic silencing. Together, these results reinforce the crucial role of the GluA2 subunit in bidirectional synaptic scaling, and suggest a novel molecular interaction mediating the phenomenon.

Previous attempts to establish specific AMPAR subunit contributions to synaptic scaling are conflicting. Several studies have reported evidence of an increase in the relative abundance of GluA1 homomers after long-term incubation in TTX ((Aoto et al., 2008; Groth et al., 2011; Soares et al., 2013; Thiagarajan et al., 2005), but see (Gainey et al., 2009)), while other reports have found little evidence that *any* AMPAR subunit is, alone, necessary for scaling (Altimimi and Stellwagen, 2013). We attempt to address these discrepancies by protracted incubation (>72 hours) of organotypic hippocampal slice cultures with TTX to assay both synaptic and surface rectification, finding no change in synaptic rectification and a very small, but significant, decrease in the rectification of extrasynaptic AMPARs. These findings make it highly unlikely that GluA2-lacking receptors play an appreciable role in scaling.

An intriguing question arises that we were unable to resolve within the scope of this study: given the otherwise striking similarity between the MPR of the GluA1 and GluA2 subunits, how might the presence of a single uncharged amino acid (A843) – or the absence of a polar amino acid – confer such markedly distinct synaptic trafficking behavior? We speculate that there exists some unique interaction between an effector protein and the proximal GluA2 CTD that is blocked by a polar serine residue, either through phosphorylation or steric hindrance. Intriguingly, few protein interactions have been described within the MPR of the GluA2 CTD. Previously, the MPR of the GluA1 subunit has been found to interact with 4.1N (also known as Band 4.1), a neuronally-enriched FERM-domain cytoskeletal-associated protein from the 4.1 family of membrane organizers that coordinates synaptic receptors with the actin cytoskeleton (Chen et al., 2005; Hoover and Bryant, 2000). Germline knockout of both 4.1N and 4.1G (but not 4.1B), two closely related members of the 4.1 family, does not grossly perturb glutamatergic synapses, which points

to a possible functional redundancy within the family of proteins (Wozny et al., 2009). However, there is little evidence of any interaction between 4.1N and GluA2. Several groups have investigated interactions between ionotropic glutamate receptor subunits and 4.1N, with initial evidence pointing toward a necessary sequence in the membrane-proximal GluA1 CTD (Shen et al., 2000). Subsequent studies identified interactions with another AMPAR subunit, GluA4, as well as the kainate receptor subunits, GluK1 and GluK2 (Coleman et al., 2003; Copits and Swanson, 2013), but no group has definitively ruled out interactions with GluA2. Intriguingly, however, it was recently found that post-translational modifications to the MPR in the cytoplasmic tail of GluK2 – a region with some sequence similarity to the homologous region in the AMPAR membrane proximal C-tails – can dramatically impact the association between these receptor subunits and 4.1N (Copits and Swanson, 2013). The palmitoylation of GluK2 within this membrane-proximal sequence promoted association with 4.1N, while the activation of PKC and the subsequent phosphorylation of the GluK2 MPR at a serine residue proximal to a series of positively charged amino acids served to decrease the interaction with 4.1N. These post-translational modifications of ionotropic glutamate receptors to govern the differential association with 4.1N, control activity-dependent receptor endocytosis, and, thus, could provide a possible mechanism by which AMPAR identity and abundance are regulated in forms of synaptic homeostasis.

Other possible “scaling effector” proteins include the AP2 adapter complex, as well as NSF, which are known to interact with a specific stretch of amino acids in the GluA2 CTD (Lee et al., 2002) (Anggono and Huganir, 2012), but these proteins are unlikely to play a role in scaling, as a partial

truncation of the GluA2 CTD (“ Δ 847”) that eliminates these binding sites – either in part or in their entirety – does not block scaling-up.

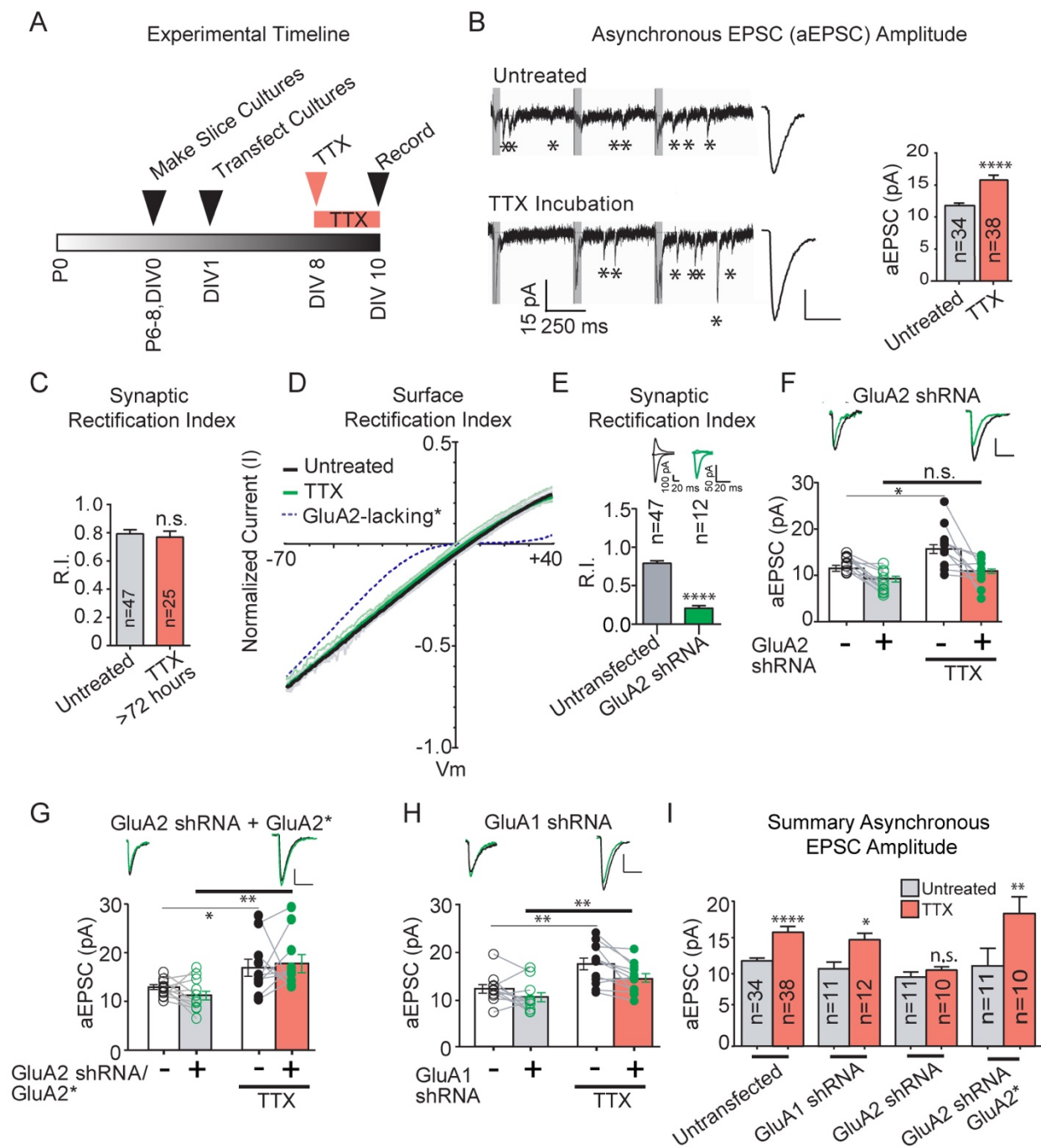


Figure 1. GluA2, not GluA1, is necessary for homeostatic synaptic scaling of quantal size.

(A) Timeline of organotypic culture preparation, TTX incubation, and recording for rat experiments. (B) Left: sample traces of asynchronous EPSCs (aEPSCs) from whole cell recordings in 4 mM extracellular strontium with 2 Hz stimulation following 48 hours of either no treatment (top) or 48 hours of treatment with 1 μ M TTX (bottom) showing a scaling-up of aEPSC amplitude with treatment. Grey box is synchronous component of EPSC that is not analyzed. Right: averaged aEPSCs from TTX-treated and untreated control neurons. Bar graph contains averaged aEPSC amplitudes. (C) Synaptic rectification of AMPARs with or without chronic TTX treatment (>72 hours, see methods). (D) Surface rectification of AMPARs with and without chronic TTX treatment. (E) Synaptic rectification of paired AMPA EPSCs in control neurons and neighboring neurons transfected with a short-hairpin RNA against GluA2. (F) Paired asynchronous recordings without and with preceding chronic TTX treatment in control neurons and neighboring neurons transfected with GluA2 shRNA. Black=control. Green=transfected. Untreated sample traces are top left and TTX-treated sample traces are top right. (G) shRNA-insensitive GluA2 rescue: treatment conditions are the same as (F). Asterisk indicates shRNA resistance. (H) GluA1 shRNA: treatment conditions are the same as (F). (I) Summary bar graph indicating unpaired scaling data, within the same transfection conditions. Significance measured across treatment conditions (color-coded from Fig. 1F-H). All scale bars for aEPSC sample traces represent 5 pA and 20 ms unless otherwise noted. *p<0.05; **p<0.01; ****p<0.0001, n.s. not significant.

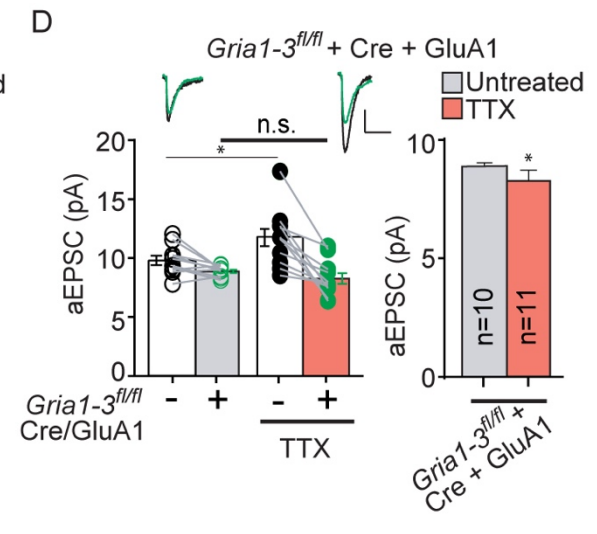
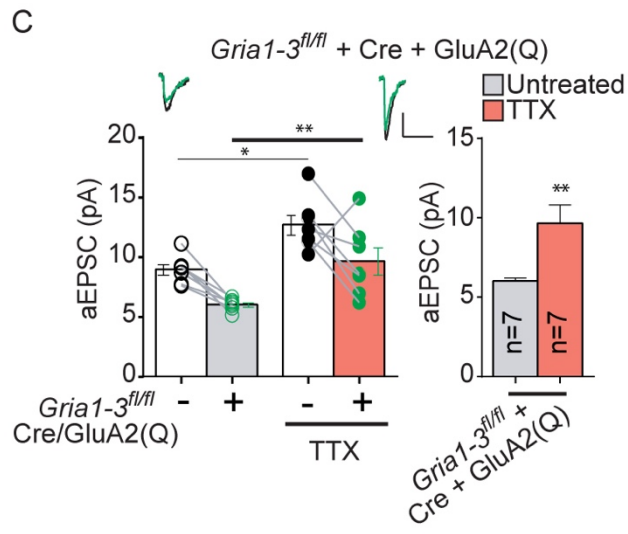
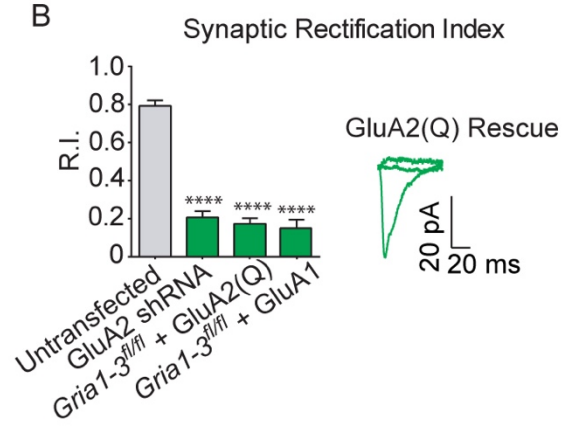
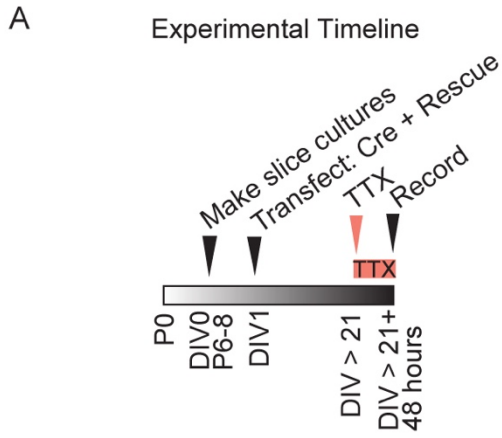
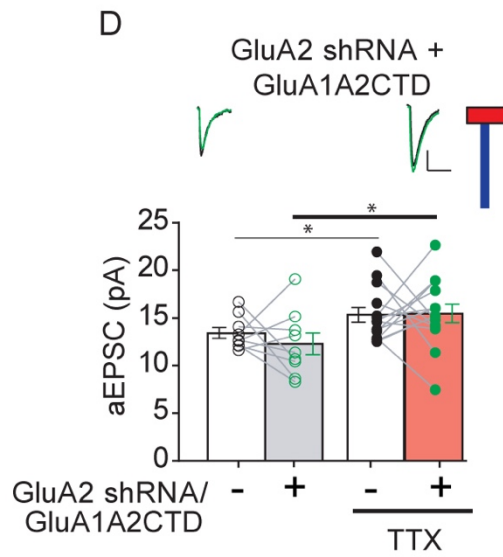
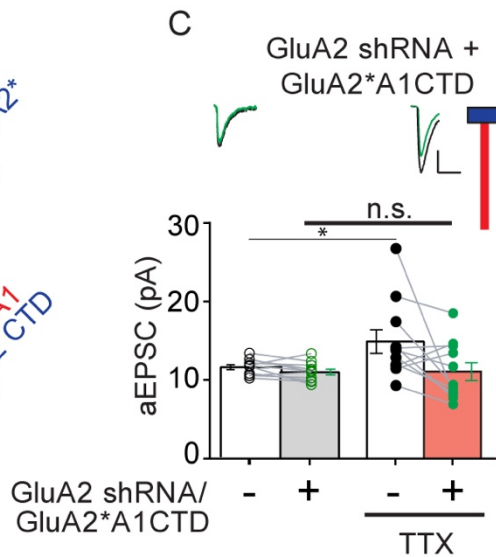
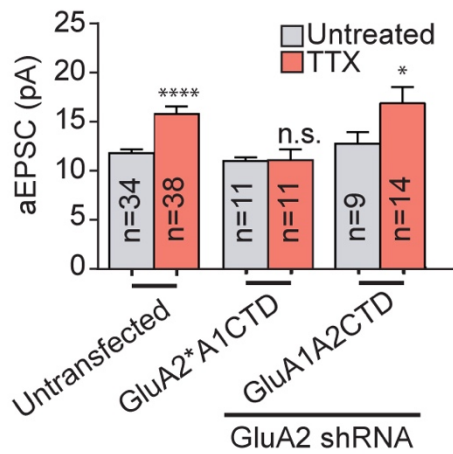


Figure 2. GluA2 is sufficient to support synaptic scaling in the absence of other AMPAR subunits. (A) Timeline of organotypic slice culture preparation, TTX incubation, and recording for GluA2(Q) replacement experiments. (B) Synaptic rectification of paired AMPA EPSCs in *GRIA1-3^{fl/fl}* control neurons and neighboring neurons transfected with Cre and GluA2(Q) or Cre and GluA1. GluA2 shRNA synaptic rectification in rat slice is shown for comparison. Scale bars represent 20 pA and 20 ms. (C) Paired asynchronous recordings without and with preceding chronic TTX treatment in *GRIA1-3^{fl/fl}* control neurons and neighboring *GRIA1-3^{fl/fl}* neurons transfected with Cre + GluA2(Q). Right: within-transfection condition summary bar graph. (D) Paired asynchronous recordings without and with preceding chronic TTX treatment in *GRIA1-3^{fl/fl}* control neurons and neighboring *GRIA1-3^{fl/fl}* neurons transfected *in utero* with Cre + GluA1. *p<0.05; **p<0.01; ****p<0.0001, n.s. not significant.

A GluA1 IEFQYKSRSESKRMK...GATGL
 GluA2 IEFQYKSRAEA KRMK...IESVKI



E Summary Asynchronous EPSC Amplitude



F Synaptic Rectification Index

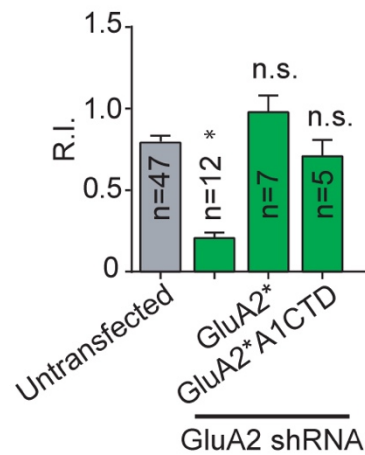


Figure 3. The cytoplasmic tail of GluA2 subunit is critical for homeostatic synaptic scaling. (A) Endogenous GluA1 and GluA2 C-tail amino acid sequence. (B) Schematic diagram of endogenous GluA1 and GluA2 AMPAR subunits next to schemata of chimeric AMPARs with swapped C-tails. Red indicates GluA1 subunit origin. Blue indicates GluA2 subunit origin. Boxes indicate amino terminal domains (ATDs) and transmembrane (TM) regions of AMPARs, while vertical lines indicate intracellular C-tails. (C) Paired asynchronous recordings without and with preceding chronic TTX treatment in control neurons and neighboring neurons transfected with GluA2 shRNA and shRNA-insensitive AMPAR chimeric subunit called “GluA2*A1CTD”. (D) GluA2 shRNA + shRNA-insensitive AMPAR chimeric subunit called “GluA1A2CTD”. Treatment conditions are the same as in Fig. 3C. (E) Summary bar graph indicating unpaired scaling data, within the same transfection conditions. Significance measured across treatment conditions (color-coded from Fig. 3C and D). (F) Comparing synaptic rectification of chimeric AMPAR GluA2*A1CTD (and therefore pore residue conferring calcium and intracellular polyamine block is present) to cells transfected with GluA2 shRNA for comparison and to cells transfected with GluA2 shRNA + full-length shRNA-insensitive GluA2. All scale bars for aEPSC sample traces represent 5 pA and 20 ms unless otherwise noted. * $p < 0.05$; **** $p < 0.0001$, n.s. not significant.

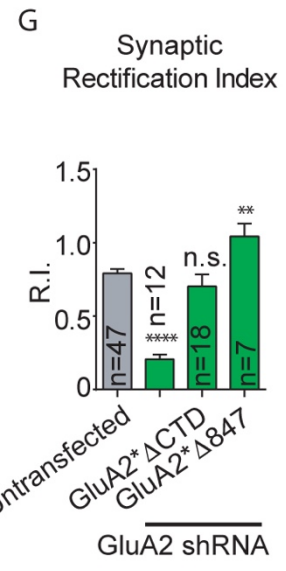
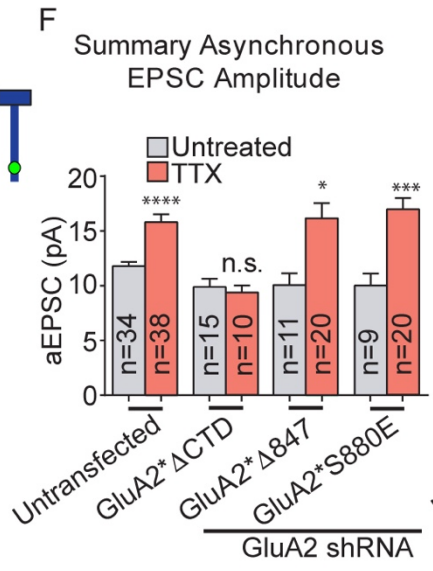
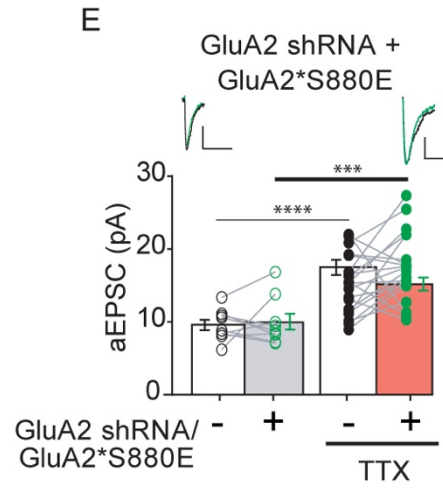
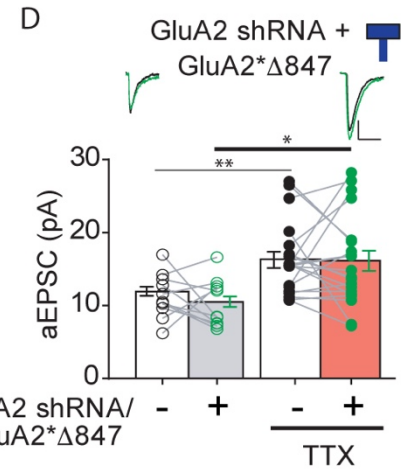
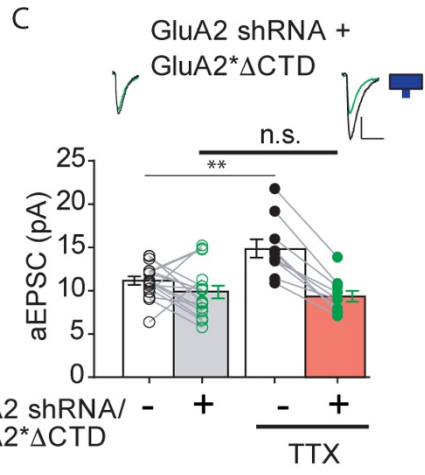
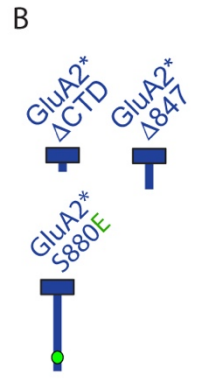


Figure 4. Membrane-proximal cytoplasmic tail of GluA2 is critical for synaptic scaling.

(A) Endogenous GluA1 and GluA2 C-tail amino acid sequences, and GluA2 C-tail sequences with truncations ($\Delta 838$, $\Delta 847$) or point mutation (S880E, large arrowhead indicates location of phosphomimetic point mutation). Box in membrane-proximal sequence illustrates region with divergent sequence in the first 14 amino acids of AMPAR C-tails. (B) Schematic diagram of truncated or mutated GluA2 subunits. Blue indicates GluA2 subunit origin. Green dot indicates location of specific S880E point mutation. (C) Paired asynchronous recordings without and with preceding chronic TTX treatment in control neurons and neighboring neurons transfected with GluA2 shRNA and shRNA-insensitive AMPAR chimeric subunit called “GluA2* $\Delta 838$ ”. (D) GluA2 shRNA + shRNA-insensitive AMPAR chimeric subunit called “GluA2* $\Delta 847$ ”. Treatment conditions are the same as in Fig. 4C. (E) GluA2 shRNA + shRNA-insensitive AMPAR chimeric subunit called “GluA2*S880E”. Treatment conditions are the same as in Fig. 4C. (F) Summary bar graph indicating unpaired scaling data, within the same transfection condition. Significance measured across treatment conditions (color-coded from Fig. 4 C-F). (G) Compares synaptic rectification of truncated or mutated GluA2 subunits to cells transfected with GluA2 shRNA. All scale bars for aEPSC sample traces represent 5 pA and 20 ms unless otherwise noted. * $p < 0.05$; ** $p < 0.01$; *** $p < 0.001$; **** $p < 0.0001$, n.s. not significant.

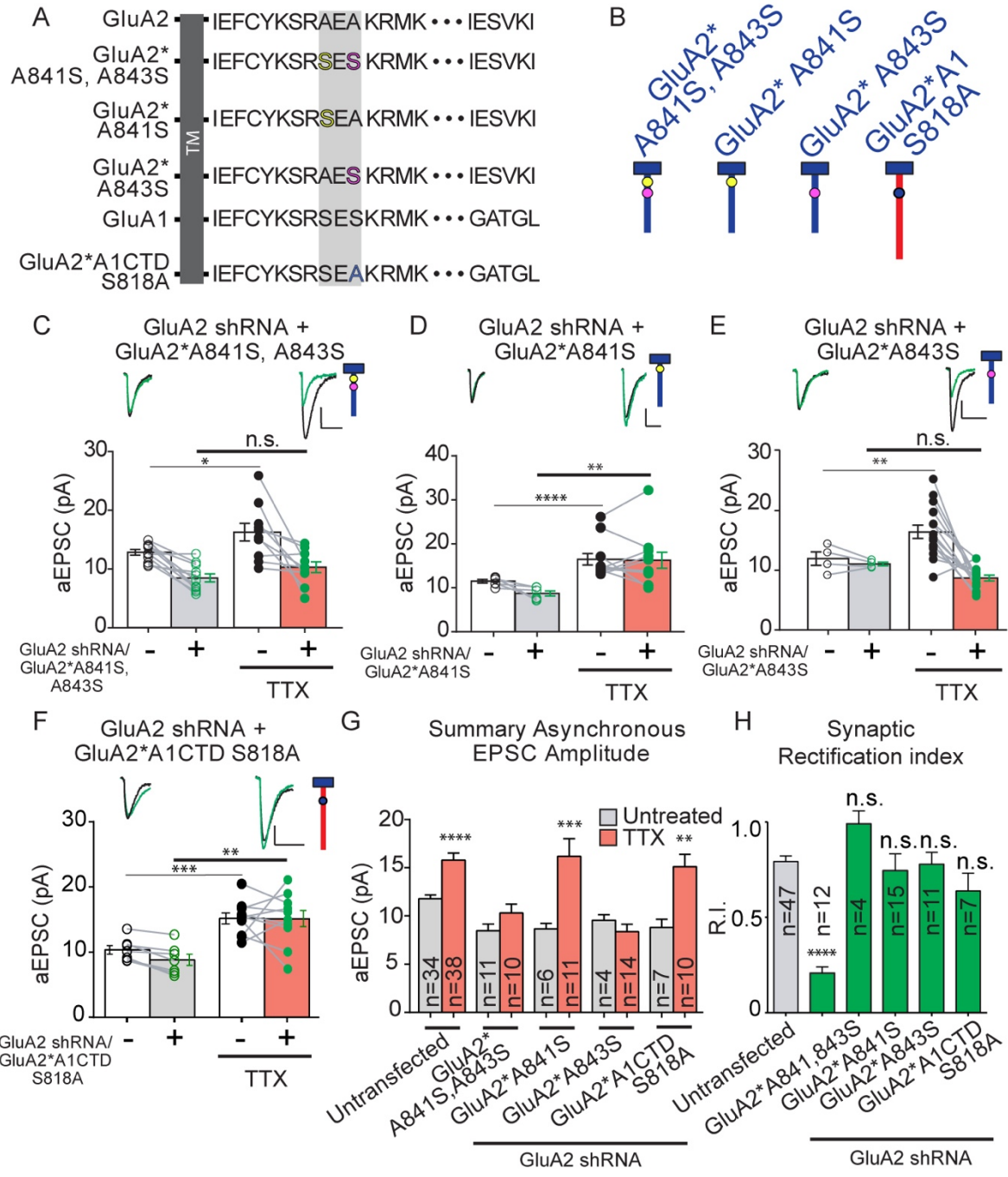
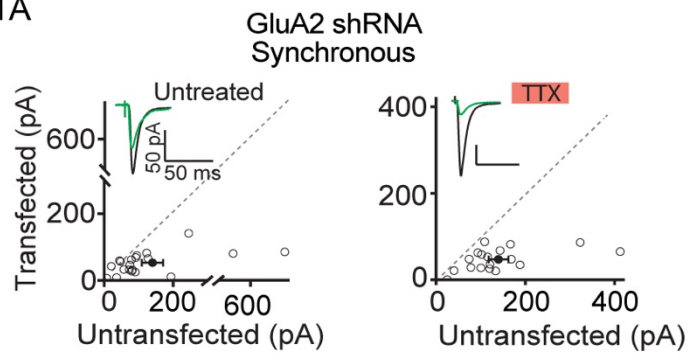


Figure 5. A specific residue in the membrane proximal CTD of the GluA2 AMPAR subunit is necessary for scaling. (A) Endogenous GluA1 and GluA2 C-tail amino acid sequences, and GluA2 or chimeric AMPAR C-tail sequences with point mutations. Box in membrane-proximal sequence illustrates region with divergent sequence in the first 14 amino acids of AMPAR C-tails, as well as location of mutations. Point mutations are color-coded to match Fig. 5B. (B) Schematic diagram of truncated or mutated GluA subunits. Blue and red indicate GluA2 and GluA1 subunit origin, respectively. (C) Paired asynchronous recordings without and with preceding chronic TTX treatment in control neurons and neighboring neurons transfected with GluA2 shRNA and shRNA-insensitive AMPAR chimeric subunit called “GluA2* A841S, A843S”. Schematic of GluA2 replacement receptor repeated in top right. (D) GluA2 shRNA + shRNA-insensitive AMPAR chimeric subunit called “GluA2* A841S”. Treatment conditions are the same as in Fig. 5C. (E) GluA2 shRNA + shRNA-insensitive AMPAR chimeric subunit called “GluA2* A843S”. Treatment conditions are the same as in Fig. 5C. (F) GluA2 shRNA + shRNA-insensitive AMPAR chimeric subunit called “GluA2* A1CTD S818A”. Treatment conditions are the same as in Fig. 5C. (G) Summary bar graph indicating unpaired scaling data, within the same transfection conditions. Significance measured across treatment conditions (color-coded from Fig. 5C-F). (G) Comparing synaptic rectification of mutated GluA2 or chimeric subunits to cells transfected with GluA2. All scale bars for aEPSC sample traces represent 5 pA and 20 ms unless otherwise noted. * $p < 0.05$; ** $p < 0.01$; *** $p < 0.001$; **** $p < 0.0001$, n.s. not significant.

S1A



S1B

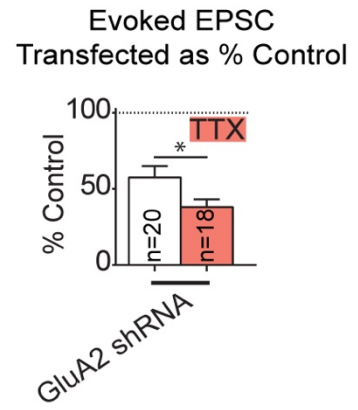
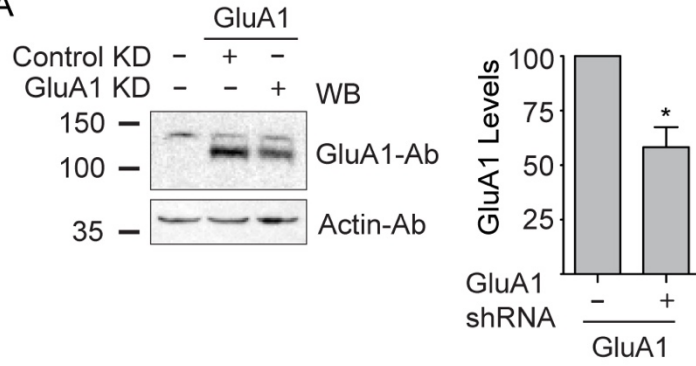


Figure S1. The effects of chronic activity blockade on synchronous EPSC size in GluA2-lacking neurons. (A) Paired synchronous recordings without and with preceding chronic TTX treatment in control neurons and neighboring neurons transfected with GluA2. (B) Summary graph of percent control (data from S1A). Amplitude deficit in EPSCs of GluA2-lacking neurons was exacerbated by TTX, not preserved, suggesting an inability to scale-up. * $p < 0.05$; *** $p < 0.001$.

S2A



S2B

GluA1 shRNA
AMPA EPSC (8-10div) Untreated
Rat organotypic hippocampal cultures

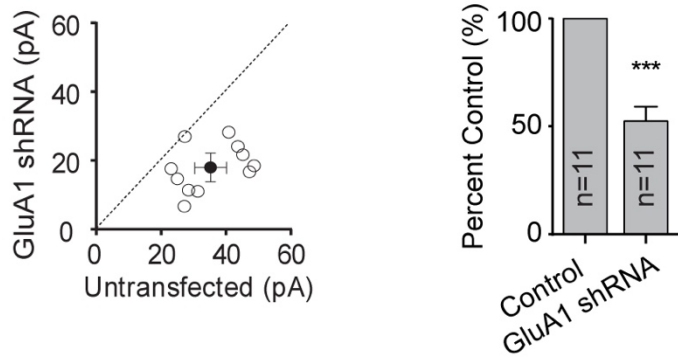
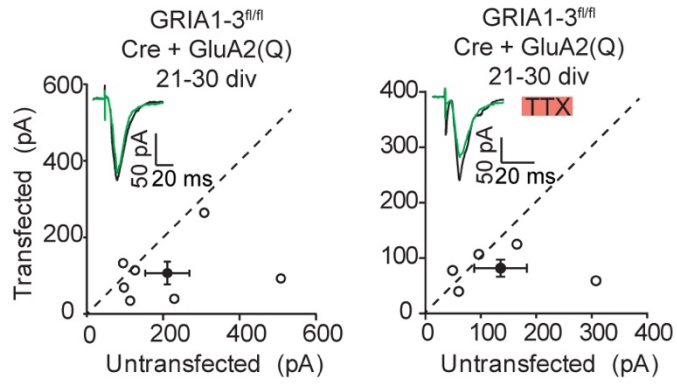


Figure S2. GluA1 shRNA validation. (A) Immunoblot analysis of GluA1 transfected in HEK293T cells. Total GluA1 lysate levels (means \pm s.e.m.) normalized to control (n = 3). Immunoblots were probed with indicated antibodies. WB, Western blot; Ab, antibody. (B) Paired EPSC recordings of GluA1 shRNA-transfected and neighboring untransfected neurons confirms expected EPSC phenotype for pyramidal neurons in the hippocampus completely lacking the GluA1 subunit. Remaining EPSC is from GluA2/3. * $p < 0.05$; *** $p < 0.001$.

S3A



S3B

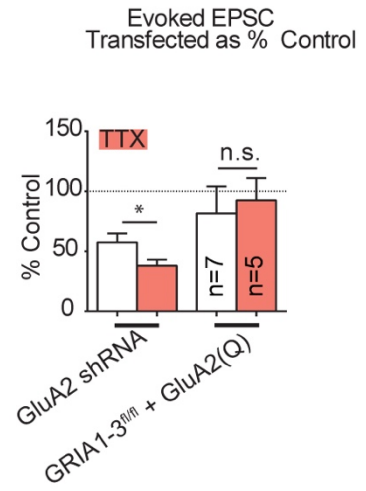
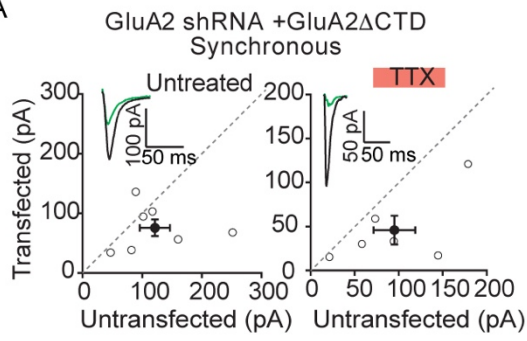
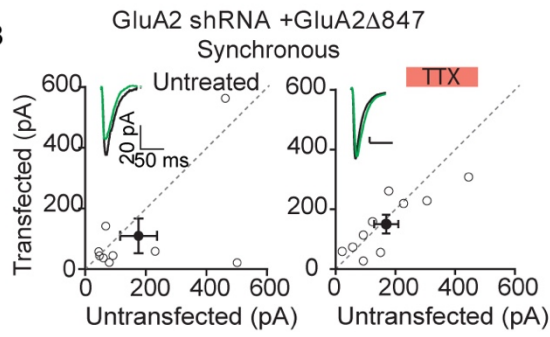


Figure S3. The effects of chronic activity blockade on synchronous EPSC size in GluA2(Q) replacement neurons. (A) Similar to figure S1 – paired synchronous recordings without and with preceding chronic TTX treatment in control *GRIA1-3^{fl/fl}* neurons and neighboring *GRIA1-3^{fl/fl}* neurons transfected with Cre + GluA2(Q) cDNA. In control conditions GluA2(Q) rescues 70% of the AMPAR EPSC (Fig. A). If GluA2(Q) receptors are unable to scale in TTX, we would expect the rescue to be less than 70%, because the control cells would scale, increasing the difference between the two cells. We found that the relative EPSC size was preserved when these experiments were repeated with TTX. (B) Summary graph of percent control (data from A). Amplitude deficit in EPSCs of GluA2-replacement neurons was preserved by TTX, suggesting a preservation of scaling-up. GluA2 shRNA % control data included for reference. * $p > 0.05$; n.s. not significant.

S4A



S4B



S4C

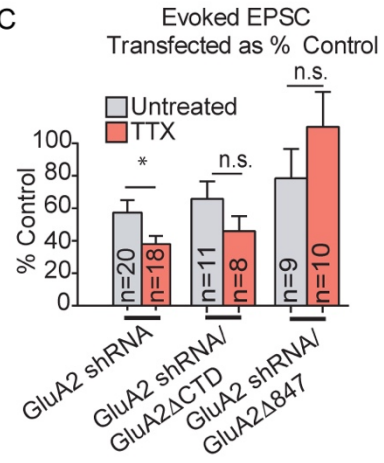
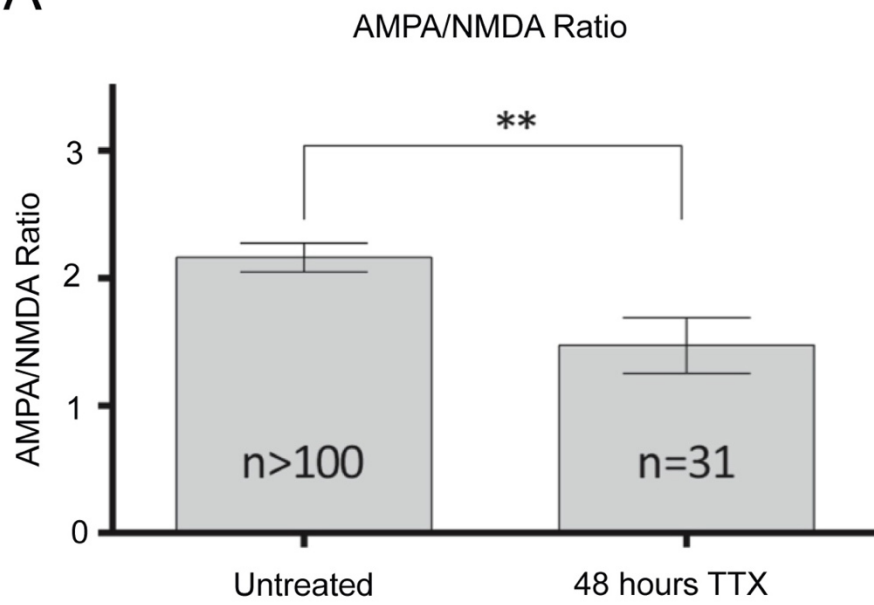


Figure S4. The effects of chronic activity blockade on synchronous EPSC size in GluA2-truncation rescued neurons. (A) Similar to figures S1A and S3A – paired synchronous recordings without and with preceding chronic TTX treatment in control neurons and neighboring neurons transfected with the GluA2 shRNA and GluA2 Δ 838 insensitive to the shRNA. (B) Paired synchronous recordings without and with preceding chronic TTX treatment in control neurons and neighboring neurons transfected with the GluA2 shRNA and GluA2 Δ 847 insensitive to the shRNA. (C) Summary graph of percent control (data from S4A, B). GluA2 shRNA % control data included for reference. * $p > 0.05$; n.s. not significant.

A



B

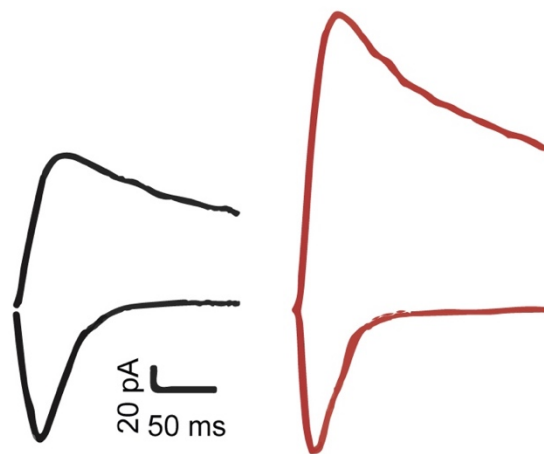
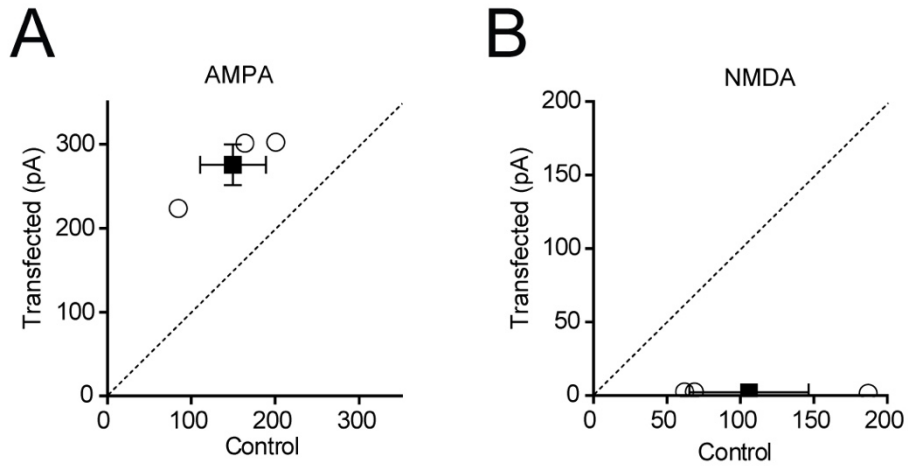


Figure S5. Evidence for robust synaptic scaling of NMDA Receptors. (A) AMPA/NMDA ratio in over 100 untreated neurons and 31 TTX treated neurons between DIV7-9. Summary graph includes mean \pm s.e.m., $p < 0.01$ (Mann-Whitney t-test). (B) Sample traces of both untreated (black trace) and TTX treated (red trace) synaptic currents recorded at +40mV and -70mV to sample NMDA and AMPA currents, respectively (NMDA taken 100 ms after stimulation at which point there is no remaining AMPA component). ** $p < 0.01$.

GluN1 CRISPR 1 μ M TTX 48 Hours



Alternate possibilities (AMPA)

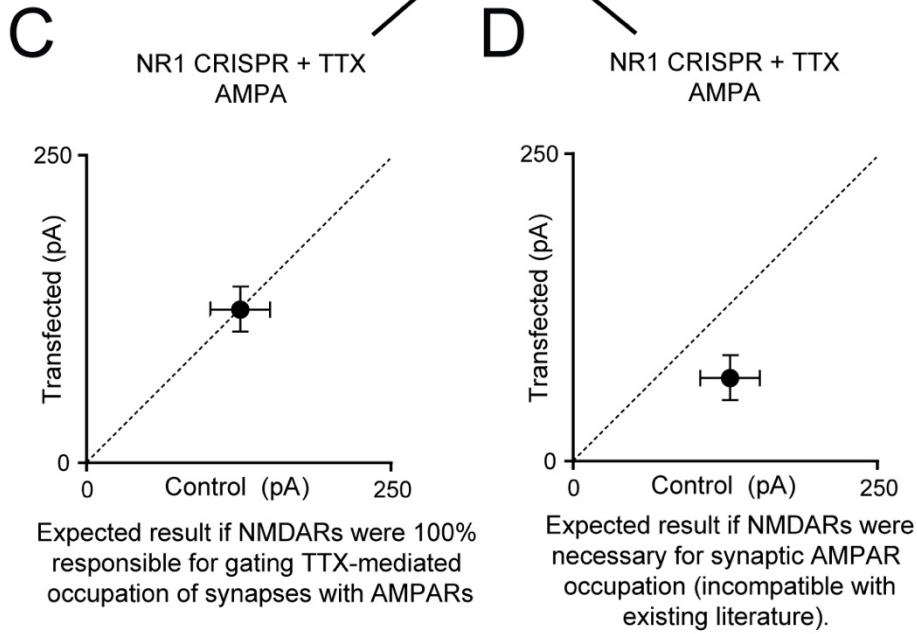


Figure S6. AMPAR synaptic accumulation after NMDAR ablation is not occluded by TTX-mediated synaptic scaling. (A) 3 weeks, or 21 days, after DIV1 transfection of GluN1 CRISPR into organotypic hippocampal rat slice cultures, paired synaptic AMPA and (B) NMDA currents were recorded, at -70mV and +40mV, respectively. n=3 pairs. (C) Model of possible alternative results depending on the relationship of NMDARs to synaptic scaling of AMPARs. Sample mean \pm s.e.m.

Chapter 4

Cell-intrinsic synaptic scaling

Introduction

Studying synaptic homeostasis with TTX incubation is like trying to study the migratory behavior of killer whales by observing them inside a tank at Sea World. In other words, while artificially silencing an entire network of neurons may induce activity dependent changes that also occur *in vivo* under subtler conditions, an experimental paradigm to study homeostatic plasticity in a more physiological way remains critically important for understanding the molecular mechanisms of synaptic scaling in individual neurons.

In the late 1990s, scientists first described a phenomenon whereby chronic incubation of neuronal cultures with synaptic or sodium channel blockers (NBQX+APV vs. TTX, respectively) elicited a homeostatic, or compensatory, increase in EPSC amplitude, and it was quickly determined to be mediated by both an increase in synaptic AMPARs as well as an increase in synaptic NMDARs (O'Brien et al., 1998; Turrigiano et al., 1998; Turrigiano and Nelson, 1998; Watt et al., 2000). Additionally, chronic incubation of neural cultures with toxins that block inhibitory postsynaptic channels (i.e. bicuculline blocking GABA receptors), which results in hyperactive cultures, elicited a compensatory decrease in EPSC amplitude (Turrigiano et al., 1998). Subsequently, this phenomenon of scaling-up was demonstrated *in vivo* (Desai et al., 2002; Goel et al., 2006; Maffei et al., 2004). In one study, binocular retinal lesion caused a compensatory increase in V1 activity levels in the 48 hours following lesion, a result of scaling of mEPSC amplitude (confirmed *in vitro*) and a correlated increase in spine size (confirmed *in vivo*) (Keck et al., 2013). Increased activity *in vivo* was monitored using the genetically-encoded calcium indicators, GCaMP3 and GCaMP5 (Keck et al., 2013).

The decision by Keck et al. (2013) to study this phenomenon *in vivo* using binocular retinal lesion is significant, as different effects have been observed after monocular activity deprivation (MD). In these MD experiments, a postsynaptic scaling-up of the deprived synapses does not occur. Instead, an activity-dependent competition between ipsilateral and contralateral inputs from the lateral geniculate nucleus (LGN) onto cell bodies in layer 4 in primary visual cortex occurs, in which deprived synapses are pruned away, favoring non-deprived inputs (Sipe et al., 2016; Wiesel and Hubel, 1963). This finding raises an intriguing question for the field of synaptic scaling: in scaling experiments, when we silence activity in an entire network of neurons – thereby blocking programs of activity-dependent competition – are we observing physiologically-relevant molecular mechanisms that govern scaling? Or not?

Few studies have attempted to look at silencing of individual neurons. In 2002, one group chronically hyperpolarized individual neurons by overexpressing the inwardly-rectifying potassium channel, Kir2.1, in dissociated cultures of hippocampal neurons, and described a homeostatic scaling-up of mEPSC frequency with no concomitant change in quantal amplitude, although this effect depended strongly on the timing of overexpression (Burrone et al., 2002). When neurons were transfected with the hyperpolarizing Kir2.1 prior to synapse formation (before DIV4) there was a reduction in synaptic input. Conversely, when neurons were transfected with Kir2.1 after synapse formation (after DIV 10), mEPSC frequency increased, with no change in mEPSC amplitude (Burrone et al., 2002). Of note, when young cultures were incubated with TTX, Kir2.1-expressing neurons did not experience a decrease in synaptic input, suggesting that a competitive, activity-dependent synaptic pruning program could be at play.

Indeed, the authors describe a presynaptic mechanism by which “fewer synapses were made onto neurons with reduced excitability” (Burrone et al., 2002).

Another group designed a micro-perfusion system to silence individual somata, and showed that single neurons were able to scale up over a period of about 5 hours when action potentials were blocked just at the soma (Ibata et al., 2008). However, this global scaling program was not elicited when individual dendrites were silenced, pointing to a possible role for a somatic activity sensor in global scaling of postsynaptic AMPAR occupation (Ibata et al., 2008). While this study suggests individually-silenced neurons are able to support “global” synaptic scaling, many unknowns remain. For example, was their micro-perfusion radius truly limited to single neurons? Furthermore, as microglia have been shown to play a critical role in activity-dependent synaptic pruning in V1 *in vivo* (Sipe et al., 2016), perhaps neuronally-enriched (microglia-deficient) dissociated hippocampal cultures do not present the most appropriate environment for single-cell scaling experiments.

If homeostatic synaptic scaling is able to operate within an individual neuron, and if we have the proper tools to perform scaling experiments in individual neurons, why, then, are we not using these tools to probe the molecular mechanisms of synaptic scaling with more physiological precision? Indeed, our lab has shown unequivocally that single-cell optogenetic excitation drives homeostatic scaling-down, and this tightly-controlled experiment allowed us to dissect the relevant molecular processes: namely, that scaling-down following chronic single-cell excitation depends on GluA2 and not GluA1 (Goold and Nicoll, 2010).

In this chapter, I explore four distinct mechanisms of reducing neural activity in single cells: 1) overexpression of the hyperpolarizing, inwardly-rectifying potassium channel, Kir2.1, 2) expression of the inhibitory DREADD, hM4Di and temporally-controlled membrane hyperpolarization during incubation with hM4Di's synthetic ligand, Clozapine-*N*-Oxide (CNO), 3) silencing of activity with a CRISPR targeting neuronal sodium channels Nav1.1, 1.2, 1.3, and 1.6, and finally 4) replacement of endogenous neuronal sodium channels with the skeletal sodium channel, Nav1.4, and temporally-controlled activity silencing during incubation with the Nav1.4-specific antagonist, μ -Conotoxin GIIIB.

Results

Kir2.1 overexpression does not increase synaptic currents

To achieve chronic hyperpolarization of individual neurons in slice culture, we first biolistically transfected the neurons with the inwardly-rectifying potassium channel, Kir2.1, encoded by the KCNJ2 gene. Organotypic slices were prepared from P6–P8 animals and transfected either the following day, 4 days after cultures were made, or 9 days after the cultures were made, to investigate effects of single cell genetic manipulations (Figures 2A, 3A, 4A). We first set out to verify in slice culture that Kir2.1 expression results in modest membrane hyperpolarization, recording (in current clamp) the excitability and the resting membrane potential of the neuron. When we first transfected pCaggs-Kir2.1-IRES-mcherry, expression of the potassium channel was toxic to the cells, so in order to reduce the expression of the Kir, we put the channel after the IRES, thus reducing its relative expression. The new pCaggs-mCherry-IRES-Kir2.1, when transfected at 7 DIV and recorded at 14 DIV, reduced neuronal excitability (Figure 1A, sample traces) via hyperpolarized resting membrane potential (Figure 1B). This hyperpolarization caused a significant increase in the rheobase current in pCaggs-mCherry-IRES-Kir2.1-transfected cells (Figure 1C), measured with a potassium methanesulfonate (KMeS)-based internal. After confirming membrane hyperpolarization, we stimulated Schaffer Collateral axons from CA3 and recorded EPSCs in CA1 pyramidal neurons after variable days of Kir2.1 expression (Figures 2-4).

We first asked what would occur if the Kir2.1 was overexpressed from a very early culture time point (DIV 1) until 11 days post transfection, at DIV 12 (Timeline, Figure 2A). Interestingly, and although the experimental n was relatively small ($n=6$ AMPA, $n=4$ NMDA, $n=4$ PPR), we did not

observe any enhancement or deficit in EPSC amplitude (Figure 2B and 2C). However, there is little evidence for a “homeostatic” synaptic phenomenon here, as EPSCs were unchanged, rather than scaled-up. One possible explanation is that younger neurons, prior to widespread synapse maturation, are better able to adjust or tune their intrinsic membrane properties to respond to a chronic hyperpolarization, i.e. through a compensatory removal of other endogenous potassium channels, or a silencing of a molecular program that removes iGluRs in response to chronic hyperpolarization. We also observed a hint of a change in the presynaptic probability of release, with a reduction in paired pulse ratio in 3 of 4 pairs recorded (Figure 2D).

We next sought to determine the extent to which this phenomenon might be timing specific, so we transfected slice cultures with pCaggs-mCherry-IRES-Kir2.1 at DIV 4, and recorded at DIV 7, thereby shortening the overexpression time window, and beginning the expression later as more functional synapses were forming (Figure 3A). Whereas before we saw no change in synaptic currents following chronic hyperpolarization from DIV 1-DIV 11 (Figure 2), we now observed a reduction when we transfected cultures at DIV 4 and recorded at DIV 7 (Figure 3B and 3C). Specifically, both AMPAR and NMDAR-mediated currents were significantly reduced following Kir2.1 overexpression.

To touch base with the TTX scaling experiments in chapter 3, we next decided to focus on overexpression of the inwardly-rectifying potassium channel from DIV 9-DIV 12, as this 3-day overexpression time window would more closely mimic the timeline of network-wide silencing with TTX treatment from DIV 8-DIV 10 (Figure 4A). After transfecting DIV 9 slice cultures with pCaggs-mCherry-IRES-Kir2.1, EPSCs were recorded following 3 days of overexpression. If

scaling-up was occurring in response to this single-cell hyperpolarizing manipulation, we would expect to see a compensatory increase in the size of the AMPAR-mediated EPSCs, on average. However, we observed the exact opposite: a statistically significant decrease in average EPSC amplitude, affecting both the AMPAR and NMDAR-mediated currents (Figure 4B and 4C). Paired pulse ratio was unaffected, with an $n=9$, suggesting that this reduction was not mediated via a retrograde signal that alters the presynaptic probability of release (Figure 4D).

These results, exploring the synaptic response to chronic hyperpolarization mediated by a modest overexpression of Kir2.1, argue against a cell-autonomous or cell-intrinsic model of synaptic homeostasis. Instead, there seems to be a more “Hebbian” molecular program by which hyperpolarized cells (perhaps similar to physiological situations in which certain neurons are not as frequently activated through other excitatory synapses or receive more inhibition) “lose out” in a manner similar to the synaptic pruning paradigm described in the ocular dominance columns of the visual cortex. However, as it is difficult to quantify the timeline and degree of Kir2.1 expression and hyperpolarization, we felt that a cleaner manipulation was required, with tighter temporal control over membrane hyperpolarization.

Single-cell hyperpolarization with hM4Di and CNO does not increase quantal size

We therefore turned to the engineered inhibitory DREADD (**D**esigner **R**eceptors **E**xclusively **A**ctivated by **D**esigner **D**rugs) hM4Di, a modified version of the human muscarinic receptor, M4 (Armbruster et al., 2007), and its accompanying, biologically-inert synthetic ligand, Clozapine-*N*-Oxide (CNO). hM4Di was engineered to be activated exclusively by CNO, and not by the endogenous ligand of muscarinic receptors, acetylcholine (ACh) or its synthetic analogue,

carbamylcholine (CCh) (Figure 5A). When hM4Di binds CNO, there is a resulting hyperpolarization of the membrane via increased activation of G-protein coupled inwardly-rectifying potassium channels (GIRKS) and a contemporaneous decrease in cyclic-AMP (cAMP) signaling (Rogan and Roth, 2011). This enabled us to modestly hyperpolarize individual transfected neurons only in the presence of CNO.

We first confirmed the acute effects of CNO on the resting membrane potential of neurons transfected with hM4di on DIV 7, recorded DIV 10 - DIV 11, and found that within minutes after 2 μ M CNO bath application, hM4Di-transfected neurons were hyperpolarized between 4-8 mV (Figure 5B, quantified in 5C). Of note, the rheobase current was consistently higher for transfected neurons, even in the absence of CNO, suggesting that there is leaky activity of this engineered GPCR (Figure 5D). Application of CNO consistently doubled the rheobase current of transfected neurons, with no change in the rheobase current of the control neuron (Figure 5D). The hyperpolarizing effect of CNO application remained for at least 20 minutes after washout across experiments, perhaps due to the dynamics of small molecule diffusion in slice culture preparations, and we did not always observe a return to pre-CNO membrane potentials following many minutes of CNO washout (Figure 5B). Despite these issues, we confirmed that this modest hyperpolarization had a significant effect on the excitability of the cell, by monitoring the action potential (AP) frequency for a given current injection in the control cell and transfected cell. For a given 0.5s current injection of 200 pA in one experiment, the transfected neuron's AP frequency dropped from 4 APs to 0 APs, with no discernible change in the AP frequency of the control cell, demonstrating that this single-cell hyperpolarizing technique is specific and efficient (Figure 5D).

Finally, we showed that AP frequency returned to pre-CNO levels after wash-out, and AP frequency was similar across multiple CNO wash-ins (Figure 5E).

After confirming the viability of this manipulation within a more acute time frame, we incubated hM4di-transfected hippocampal slices with 2 μ M CNO for 48 hours to mimic the time window of 48 hours of TTX incubation described in Chapter 3, refreshing the CNO after 24 hours in case of decreasing viability⁵ of the drug at 35 degrees Celsius (Figure 6A). We stimulated Schaffer Collateral axons from CA3 with a bipolar electrode and recorded asynchronous EPSCs (aEPSCs) in CA1 pyramidal neurons (see description of aEPSC recording paradigm in chapter 3). If scaling-up of aEPSCs were occurring in chronically-hyperpolarized individual neurons (hM4di-transfected + 48 hours CNO), then we might expect an approximately ~40% increase in aEPSC amplitude relative to untransfected neurons. However, aEPSC amplitudes were not changed in transfected cells (Figure 6B and 6C), suggesting that – as with the Kir2.1 overexpression – chronic and moderate hyperpolarization of individual neurons either leads to no synaptic scaling-up, or results in a scaling-down of the excitatory postsynaptic amplitude. In other words, we still had no evidence that scaling-up could occur in a cell-autonomous, or cell-intrinsic manner.

However, critical differences remained between these methods of single cell silencing and the mechanism of silencing in TTX sodium channel block. Namely, TTX blocks all voltage-gated sodium channel activity, with smaller membrane depolarizations occurring only through calcium

⁵ Characterization of chronic CNO application, especially with an accompanied dose-response curve, has not yet been performed Smith, K. S., Bucci, D. J., Luikart, B. W., and Mahler, S. V. (2016). DREADDs: Use and application in behavioral neuroscience. *Behav Neurosci* *130*, 137-155.. We are, therefore, unable to unequivocally confirm a sustained activation of GIRKs through the transfected DREADD.

channels. In the case of Kir2.1 overexpression or hM4di activation with a synthetic ligand, moderate hyperpolarization of the resting membrane potential will serve to increase the rheobase current and decrease action potential frequency, but we would not expect these manipulations to fully block action potentials.

Genetic ablation of all neuronal voltage-sensitive sodium channels drives synaptic depression

Thus, we set out to find a method of completely eliminating depolarizing membrane currents that could support action-potential propagation. We therefore turned to CRISPR technology to target all voltage-dependent sodium channels endogenous to hippocampal CA1 neurons, designing a single CRISPR to target rat sodium channels, and two CRISPRs to target the same channels in mouse, although no consensus sequence for all four sodium channels was found: Nav1.1, Nav1.2, 1.3 and Nav1.6 (Figure 7A; gRNA sequences in methods). Mouse sodium channel CRISPR was validated by M. Horn in manuscript currently in review at *Cell Reports*. We first transfected the neuronal sodium channel CRISPR (“nNav 1.X CRISPR”) at DIV 1, and found that after 14-21 days after transfection of nNav 1.X CRISPR (>DIV15), there was a robust and replicable ablation of sodium channel current, although there was often a very small “action potential-like” depolarization that could occur with large current injections at earlier time points (Figure 7B). After confirming consistent genetic ablation of neuronal sodium channels, we examined synaptic currents between DIV 10-DIV 14 in both mouse and rat (n=4 rat, n=6 mouse), finding a significant reduction in synaptic AMPA currents and a reduction in NMDA currents (Figure 7C and 7D).

Yet again, we find no evidence for a cell-intrinsic homeostatic scaling mechanism following chronic reduction (and later, ablation) of action potentials, instead recapitulating the more

“Hebbian-like” phenomenon in our Kir2.1 and hM4Di+CNO experiments. However, critical differences remain between this manipulation and our TTX treatment paradigm. Namely, the TTX-mediated ablation of voltage-dependent sodium channel current occurred over a well-defined 48-hour timeline, whereas our nNav 1.X CRISPR manipulation likely reduced sodium currents gradually over 14 days. It was therefore critical to look for a means of completely blocking sodium channels in individual neurons for just 48 hours.

Nav1.4 replacement and temporally-controlled single-cell silencing with μ -Conotoxin GIIIB leads to synaptic depression

Thanks to both the sequence specificity of our nNav 1.X CRISPR and the diversity of non-neuronal sodium channels, we decided to rescue action potentials (sodium channel-mediated current) on the nNav 1.X CRISPR background with Nav1.4, encoded by the *SCN4A* gene, expressed exclusively in skeletal muscles (Wang et al., 1992) (Figure 8A). We chose Nav1.4 because it was the most pharmacologically accessible amongst the other non-neuronal sodium channels, blocked by a specific conotoxin, μ -Conotoxin GIIIB, which carries a 1000-fold specificity for muscle over neuronal sodium channels (Ruiz et al., 2011) (Model in Figure 8B). We then transfected this Nav1.4 cDNA along with the nNav 1.X CRISPR. After 14 days of expression following transfection, we recorded in current clamp to examine the utility and feasibility of this approach, first looking for evidence of action potential rescue with the skeletal sodium channel. Indeed, in a preliminary proof-of-concept screen, we found a robust rescue of action potentials with the skeletal sodium channel Nav1.4 (Figure 9A), although action potential waveforms were distinct in these Nav1.4-replacement neurons: AP slope was significantly smaller than control APs (Figure 9C), AP rise time was significantly slower in Nav1.4-replacement neurons (Figure 9D), and AP height

significantly smaller (Figure 9E) (n=2 pairs). Application of 600nM μ -Conotoxin GIIIB resulted in a slow reduction of action potential frequency and height, eventually eliminating all action potentials after 20 minutes of wash-in (Figure 10A and quantified in Figure 10C). Control action potential frequency and height were unaffected by application of μ -Conotoxin GIIIB (Figure 10B), suggesting that, at 600nM, this conotoxin was not blocking endogenous neuronal sodium channels in control neurons.

We then examined synaptic AMPAR-mediated currents with this Nav1.4 replacement strategy (with no Conotoxin treatment), to see if rescuing some basic form of action potential propagation was able to rescue synaptic currents as well. Indeed, Nav1.4 replacement on the nNav 1.X CRISPR background was able to support normal AMPAR-mediated synaptic currents, as there was no appreciable difference between transfected neurons and their paired controls (Figure 11A). Additionally, NMDAR-mediated currents were comparable to controls in neurons containing only Nav1.4 (Figure 12A). After confirming normal synaptic currents with Nav1.4 rescue, we incubated Nav1.4/ nNav1.X CRISPR-transfected slices with 600nM μ -Conotoxin GIIIB for 24 or 48 hours, at 2 weeks or 3 weeks post transfection, respectively, and the data were combined. Paired pulse ratio (PPR) was unchanged after Conotoxin treatment in transfected neurons (Figure 11C). After Conotoxin treatment, AMPAR-mediated currents in transfected neurons were significantly lower than their paired controls (Figure 11B), again recapitulating a more “Hebbian-like” phenomenon, in which a less-active neuron does not initiate the necessary molecular program to scale-up synaptic AMPARs ($p < 0.02$). Similarly, NMDAR-mediated currents in Nav1.4/ nNav1.X CRISPR-transfected neurons trended toward scaling down ($p = 0.058$) in response to chronic μ -Conotoxin GIIIB treatment (Figure 12B).

As we only confirmed definitive Nav1.4 rescue in 2 cells, we cannot be sure that this skeletal sodium channel is able to functionally replace endogenous sodium channels in a consistent manner. However, when we compared the synaptic AMPAR-mediated currents in the Nav1.4/nNav1.x CRISPR rescue to the nNav1.x CRISPR alone, we found that Nav1.4 expression consistently supported synaptic AMPAR currents at levels similar to controls, which likely reflects a functional rescue of neuronal excitability through Nav1.4. In future, we would perform a control experiment in which we confirm action potential rescue with Nav1.4, although we feel that the synaptic rescue is a more informative control, as the kinetics and dynamics of Nav1.4-mediated action potentials are so distinct from neuronal sodium channels Nav1.1, 1.2, 1.3 and 1.6, and cannot be directly compared.

Discussion

Based on our results, it seems increasingly unlikely that scaling-up occurs in response to membrane hyperpolarization or genetic ablation of sodium channels at the level of individual cells. Instead, this negative result, while difficult to prove unconditionally, argues for the existence of a scaling paradigm that requires either a secreted, “network-wide” signal, or a suppression of activity-regulated programs of synaptic competition, although further experiments are necessary to develop a strong enough case to challenge scaling dogma. An extended discussion of experiments performed in this chapter can be found in General Conclusions in Chapter 5.

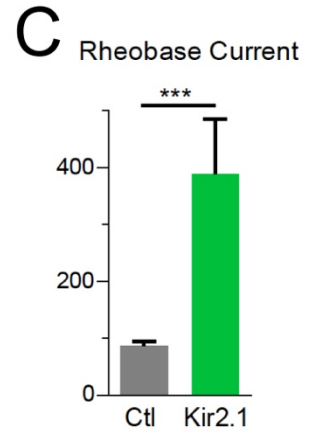
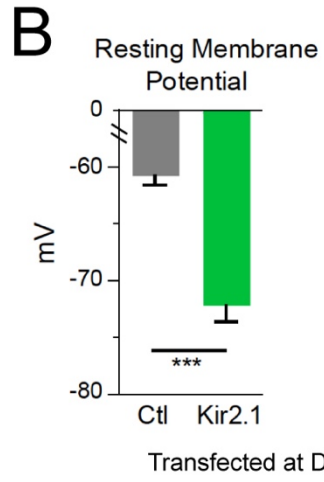
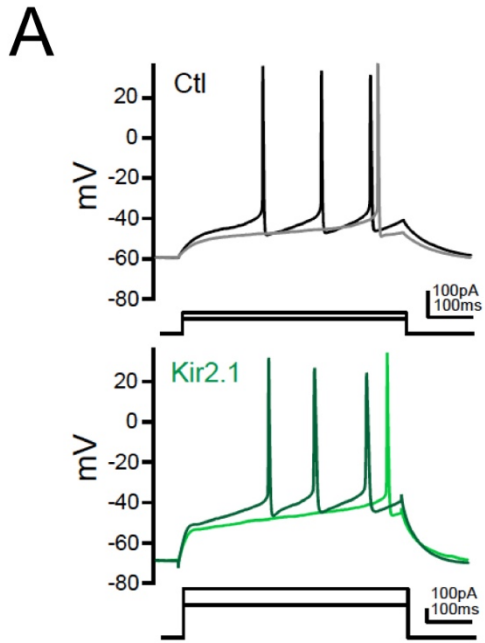


Figure 1. pCaggs-mCherry-IRES-Kir2.1 characterization. (A) Sample trace of control neuron in current clamp (above) and pCaggs-mCherry-IRES-Kir2.1 transfected neuron in green (below) with current pulses to evoke either a single action potential for subsequent rheobase calculation (grey and light green trace), or multiple action potentials (black and dark green traces). (B) Resting membrane potential of control and pCaggs-mCherry-IRES-Kir2.1+ neurons \pm s.e.m ($P < 0.001$, $n = 20$ control neurons, $n = 10$ Kir2.1). (C) Rheobase current of control and pCaggs-mCherry-IRES-Kir2.1+ neurons \pm s.e.m ($P < 0.001$, $n = 20$ control neurons, $n = 9$ Kir2.1).

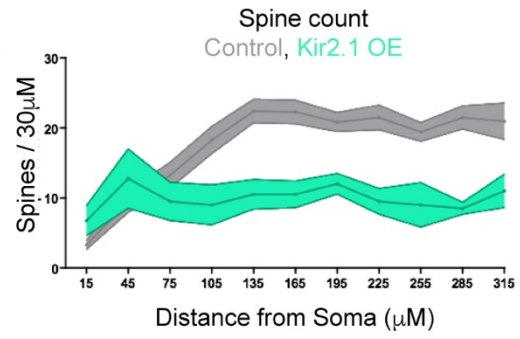
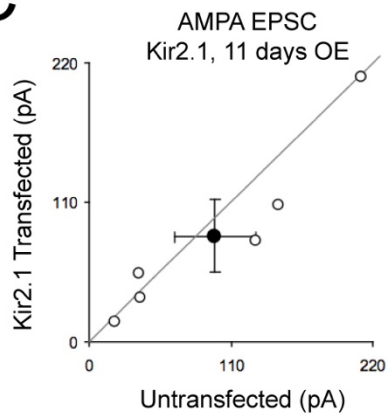
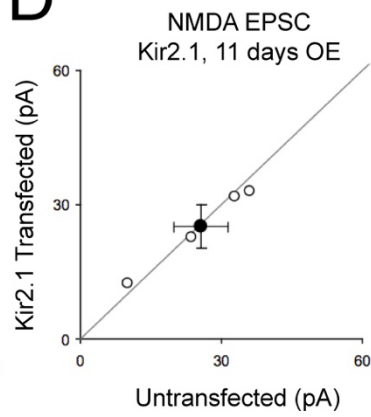
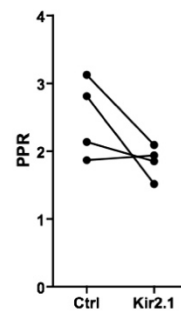
A**B****C****D****E**

Figure 2. Synaptic effects of long-term overexpression of pCaggs-mCherry-IRES-Kir2.1.

(A) Experimental timeline, rat. (B) Spine count in control (grey) and pCaggs-mCherry-IRES-Kir2.1 transfected neurons (green) as a function of distance from soma. Reduction in spine density, especially further from the soma. Spine count per 30 μm \pm s.e.m., n = 4 neurons. (C) Paired AMPA EPSC, Kir2.1 vs. control, n=6 pairs. Open circles are individual pairs, closed circle is mean \pm s.e.m. (Control 97.70 pA \pm 31.19, Kir2.1 83.39 pA \pm 28.29. p = 0.21, n.s.). (D) Paired NMDA EPSC, Kir2.1 vs. control, n=4 pairs. (Control 20.66 pA \pm 6.75, Kir2.1 25.08 pA \pm 4.8, p=0.64, n.s.) (E) Paired pulse ratio Kir2.1 vs. control, n=4 pairs, (Control 2.48 \pm 0.29, Kir2.1 1.85 \pm 0.12 p=0.09, n.s.). Statistics are paired student's T-Test.

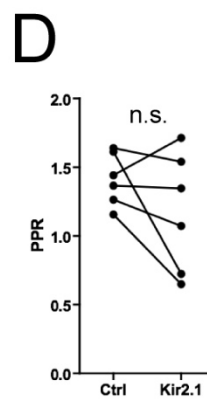
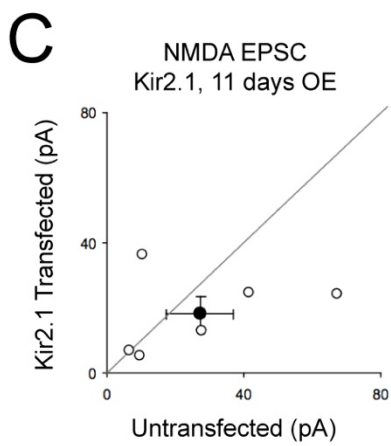
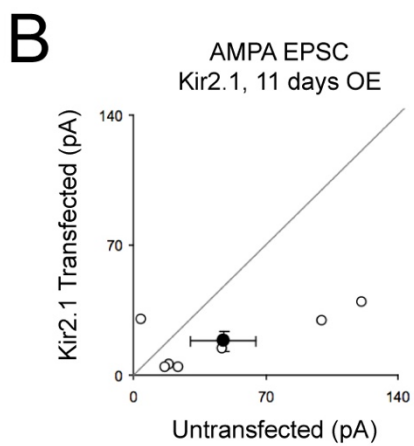
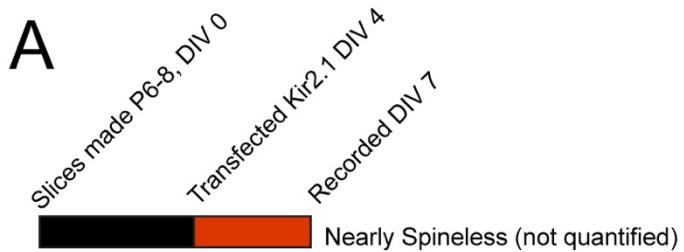


Figure 3. Synaptic effects of pCaggs-mCherry-IRES-Kir2.1 early overexpression from DIV4-7. (A) Experimental timeline, rat. (B) Paired AMPA EPSC, Kir2.1 vs. control, n=7 pairs. Open circles are individual pairs, closed circle is mean \pm s.e.m. (Control 21.70 pA \pm 4.56, Kir2.1 13.08pA \pm 2.55, p=0.03*). (D) Paired NMDA EPSC, Kir2.1 vs. control, n=6 pairs (Control 24.65 pA \pm 6.06, Kir2.1 26.74 pA \pm 6.78, p=0.88, n.s.). (E) Paired pulse ratio Kir2.1 vs. control, n=6 pairs (Control 1.75 \pm 0.22, Kir2.1 1.88 \pm 0.13, p=0.84, n.s.). Statistics are paired student's T-Test.

A

Slices made P6-8, DIV 0

Transfected Kir2.1 DIV 9

Recorded DIV 12

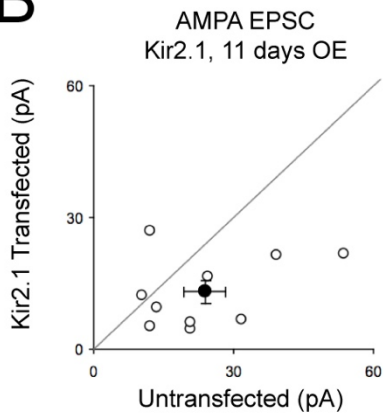
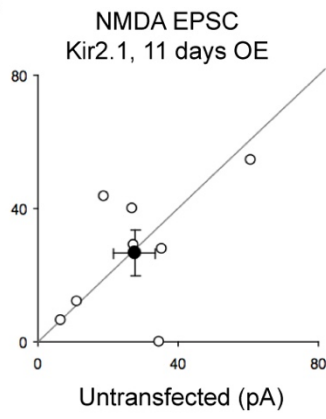
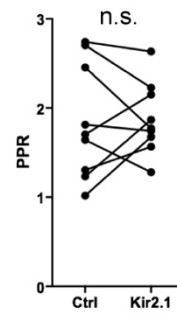
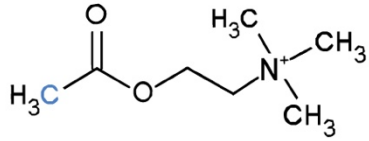
 Very few spines (not quantified)**B****C****D**

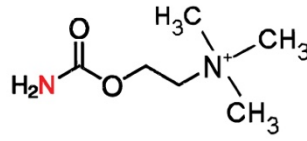
Figure 4. Synaptic effects of late pCaggs-mCherry-IRES-Kir2.1 overexpression from DIV9-12. (A) Experimental timeline, rat. (B) Paired AMPA EPSC, Kir2.1 vs. control, n=10 pairs. Open circles are individual pairs, closed circle is mean \pm s.e.m. (Control $41.56 \text{ pA} \pm 15.97$, Kir2.1 $18.28 \text{ pA} \pm 5.45$, $p=0.03^*$). (D) Paired NMDA EPSC, Kir2.1 vs. control, n=8 pairs. (Control $23.33 \text{ pA} \pm 9.06$, Kir2.1 $18.38 \text{ pA} \pm 4.93$, $p=0.39$, n.s.). (E) Paired pulse ratio Kir2.1 vs. control, n=9 pairs (Control 1.24 ± 0.18 , Kir2.1 1.17 ± 0.18 , $p=0.21$, n.s.). Statistics are paired student's T-Test.

+CNO

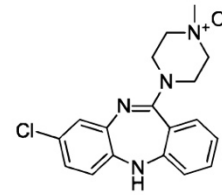
A



i. Acetylcholine (ACh)



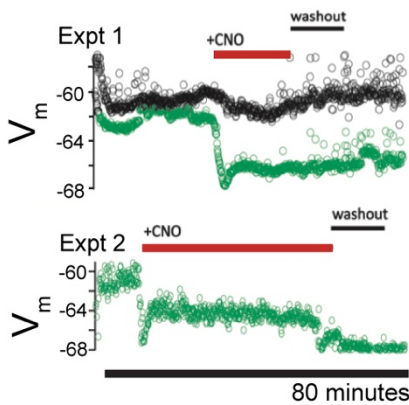
ii. Carbamylcholine (CCh)



iii. Clozapine-N-Oxide

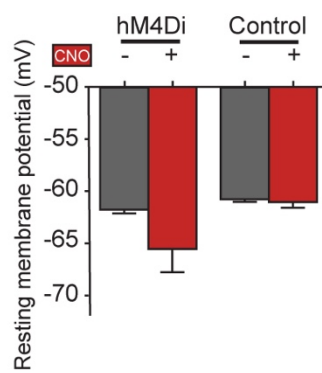
B

V_m of 2 hM4Di Cells (Green)



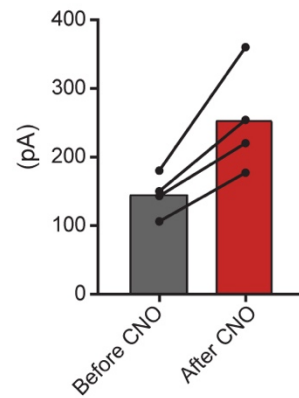
C

V_m (n=4 pairs)



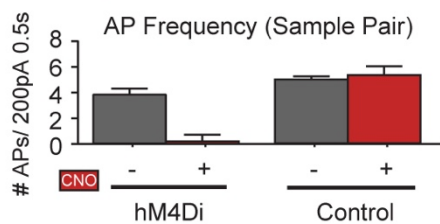
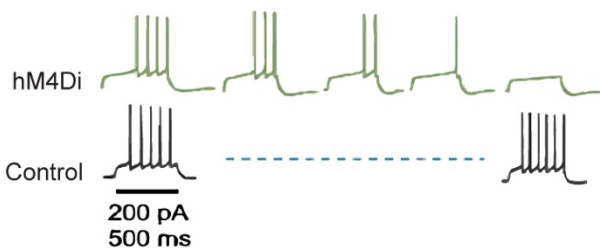
D

hM4Di+ Rheobase Current Before-After Acute CNO



E

+2 μ M CNO - 3 minute wash-in



F

Sample hM4Di-Transfected Neuron AP # Similar after 1st and 2nd CNO Wash

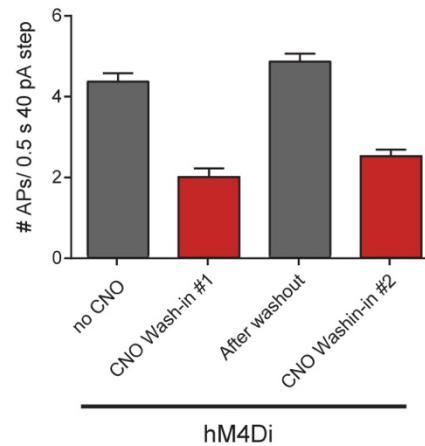


Figure 5. Characterization of acute effects of synthetic ligand CNO on Vm of inhibitory DREADD hM4Di-transfected cells. Transfected DIV 7, Recorded DIV 12. (A) Structural comparison of natural muscarinic acetylcholine receptor ligand, acetylcholine (Ai), with synthetic ligand, Carbamylcholine (Aii), and synthetic DREADD ligand Clozapine-N-Oxide (Aiii). (B) 2 sample recordings of hyperpolarized membrane potentials in hM4Di-transfected cells following application of +2mM CNO for varying times, quantified in (C). (C) n=4 pairs, acutely hyperpolarized membrane potential after application of CNO. Values before and after CNO application averaged from >30 time points in each experiment. Summary graph is mean \pm s.e.m. (D) Plot of rheobase currents for 4 hM4Di-transfected neurons before/after CNO wash-in. (E) Top: Sample trace of action potentials in control neuron (black) and hM4Di-transfected neuron (green) for a given current injection (200 pA, 500 ms). hM4Di+ neurons no longer fire action potentials after just 3 minutes of CNO wash-in, while control neuron AP frequency is unaffected by CNO wash-in. Bottom: Quantification of action potential # taken from one experiment, mean \pm s.e.m. (F) Bar graph of a different hM4di-transfected neuron showing a halving of action potential frequency for a given current injection that is consistent with multiple wash-in/ wash-out cycles of CNO. Action potential frequency returns to pre-CNO levels with wash-out, although this was not always reflected by a return in resting potential (see 5B).

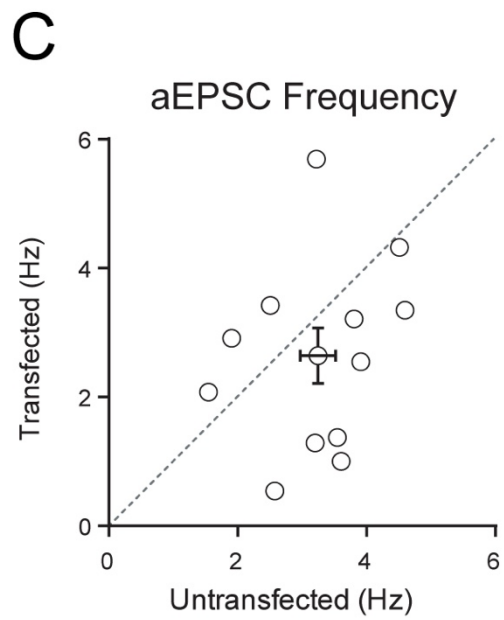
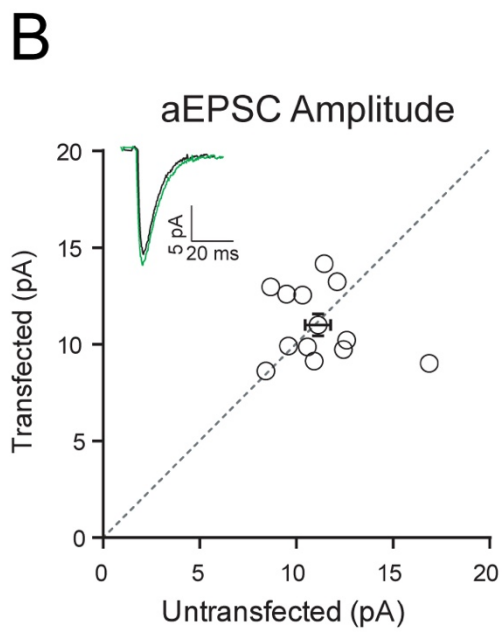
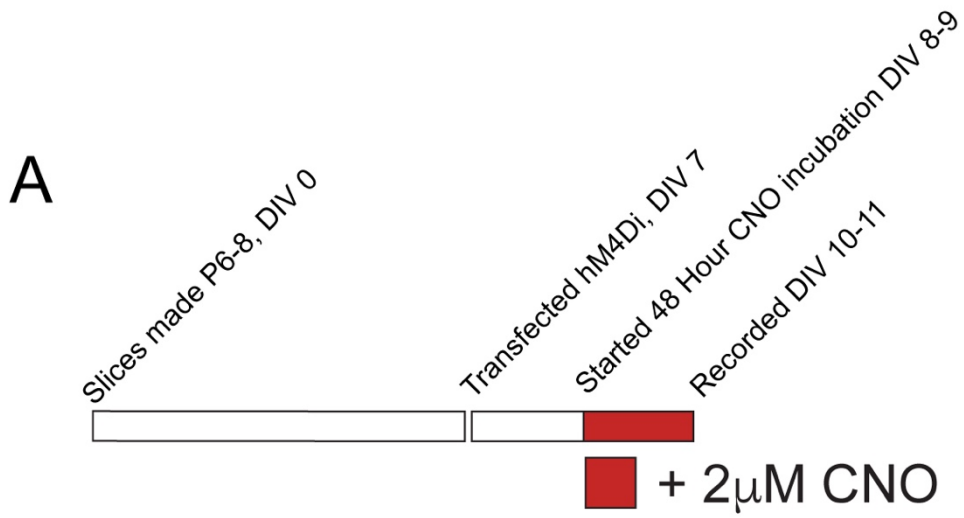
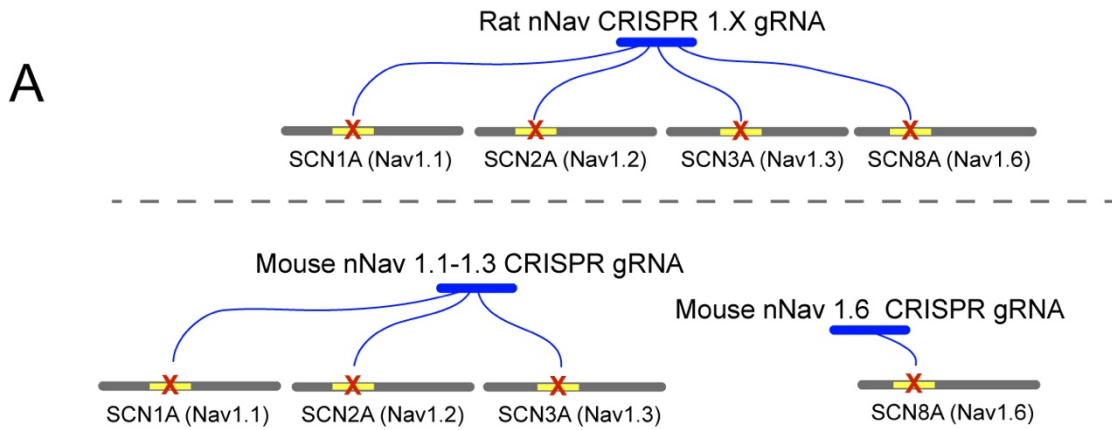


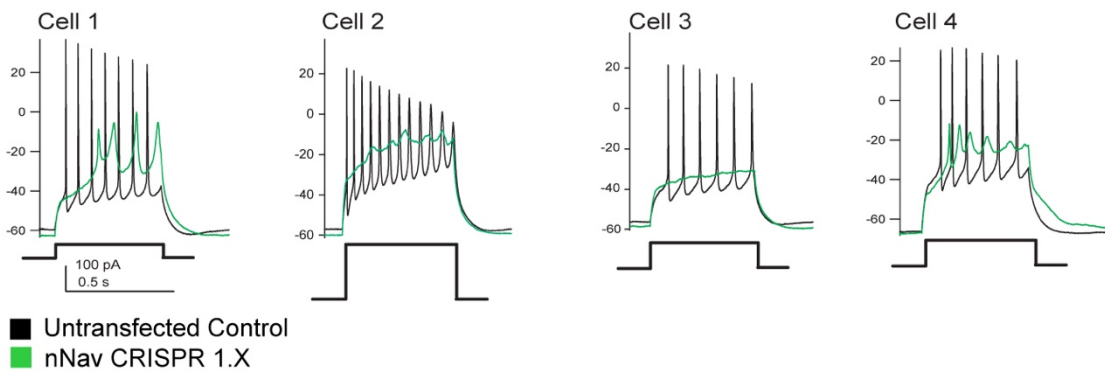
Figure 6. Synaptic effects of inhibitory DREADD hM4di and synthetic ligand CNO.

(A) Experimental timeline. (B) Paired asynchronous EPSC amplitude in hM4Di vs. control neurons after 48 hours of 2mM CNO incubation, not significant (n.s.), indicating no scaling-up of quantal amplitude in an individually chronically hyperpolarized neuron. (C) Paired asynchronous EPSC frequency in hM4Di vs. control neurons after 48 hours of 2mM CNO incubation, not significant (n.s.), indicating no scaling-up of quantal content in an individually chronically hyperpolarized neuron.



B

Sample Action Potential Waveforms : nNav 1.X CRISPR 13 Days Transfection



nNav CRISPR 1.X; 10-14 div, Rat and Mouse ○ = rat 12 div
○ = mouse 10-14 div

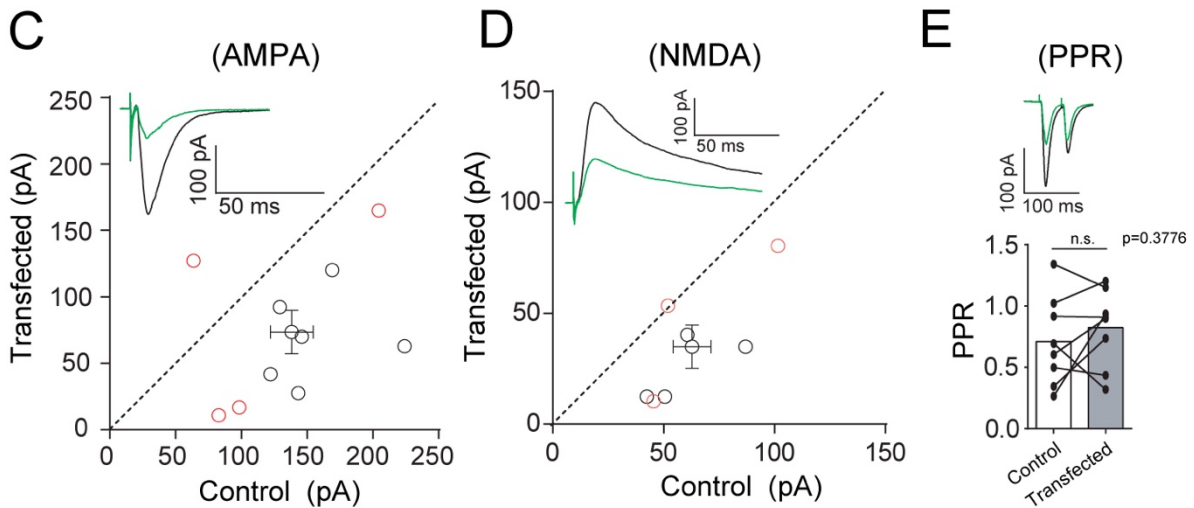
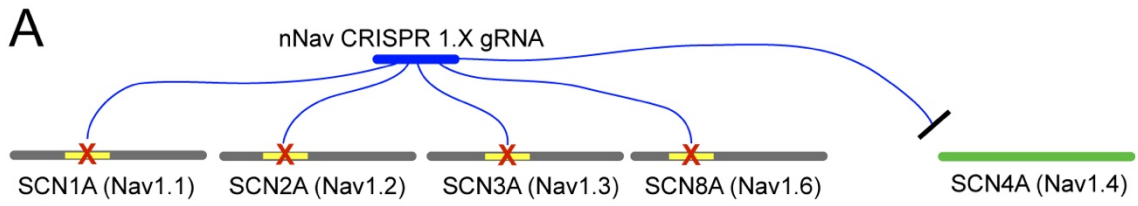
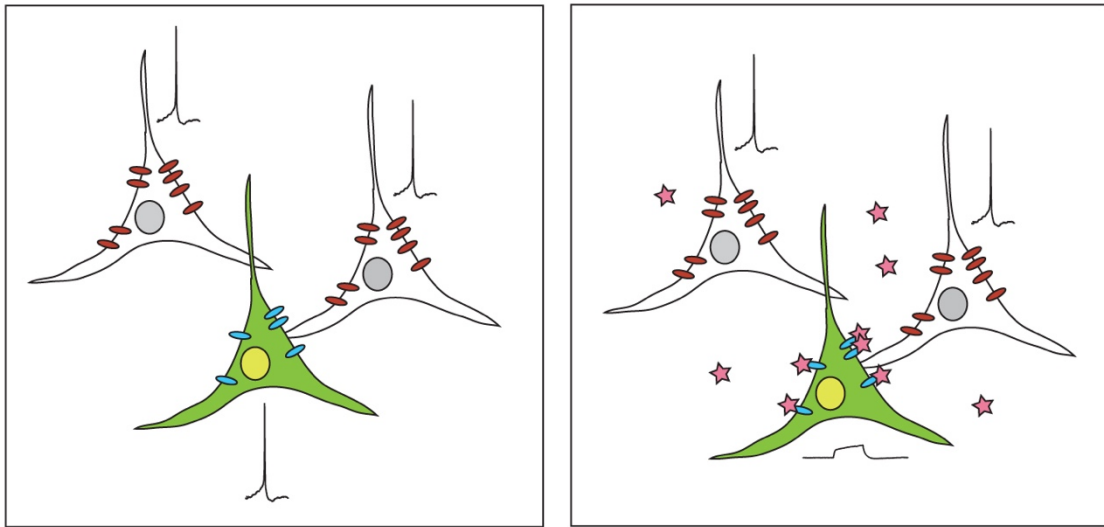




Figure 7. Synaptic effects of long-term sodium channel genetic ablation. (A) Schematic of nNav 1.X CRISPR gRNA scheme in rat (top) and mouse (bottom). (B) Sample traces of evoked action potentials in control neurons (rat, black trace) and paired rat nNav 1.X CRISPR-transfected neurons (rat, green trace) after 13 days CRISPR expression. Even with large current injections, we were unable to elicit any true action potentials in all nNav CRISPR 1.X-transfected neurons tested after this time point (data not shown). (C) Paired synaptic AMPAR currents after 10-14 days of CRISPR expression following transfection at DIV1. Rat pairs were recorded at 12 DIV and are shown here as open red circles. Mouse pairs were recorded at 10-14 DIV and are shown here as open black circles, with average pair shown on scatter plot with standard error bars (n=10, p=0.0066**, t-test). (D) Paired synaptic NMDAR currents after 10-14 days of CRISPR expression following transfection at DIV1. Rat pairs were recorded at 12 DIV and are shown here as open red circles. Mouse pairs were recorded at 10-14 DIV and are shown here as open black circles, with average pair shown on scatter plot with standard error bars (n=7, p=0.0047**, t-test). (E) Paired pulse ratio of paired nNav 1.X CRISPR-transfected vs. control neurons, rat and mouse combined (n=8, n.s p=0.38).



B



 Transfected (nNav CRISPR + Nav1.4)
 Untransfected Neuron




 Neuronal Sodium Channel
 Skeletal Sodium Channel Nav1.4
 μ -Conotoxin GIIIB

Figure 8. Nav1.4 replacement experiment design. (A) Schematic of rat nNav 1.X CRISPR and skeletal Nav1.4 replacement experiment, in which neuronal sodium channel CRISPR is not able to target skeletal Nav1.4. (B) Left: Drawing showing experimental design. Green neurons are transfected with CRISPR and replacement skeletal sodium channel Nav1.4. Clear neurons are control neurons. Pink ovals represent endogenous neuronal sodium channels, while blue ovals represent exogenous, overexpressed, replacement skeletal sodium channels, “Nav1.4.” Sample action potential traces are next to their corresponding neuron. Note: Neurons expressing only skeletal voltage sensitive sodium channel Nav1.4 are able to reach threshold and achieve action potential propagation with membrane depolarization. Right: After acute bath-application of 600 mM of the Nav1.4 specific conotoxin, m-Conotoxin GIIIB, action potentials in neurons expressing Nav1.4 (but no endogenous neuronal sodium channels) are unable to reach action potential threshold after less than 20 minutes of bath application of Conotoxin, confirming acute block of sodium channels.

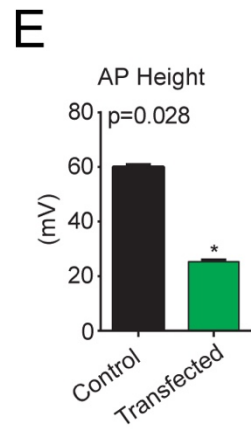
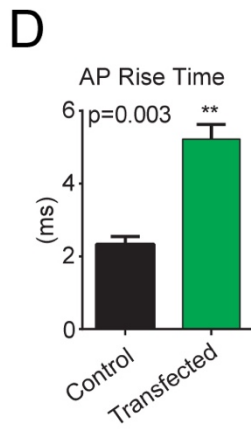
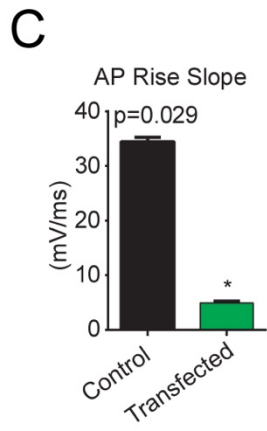
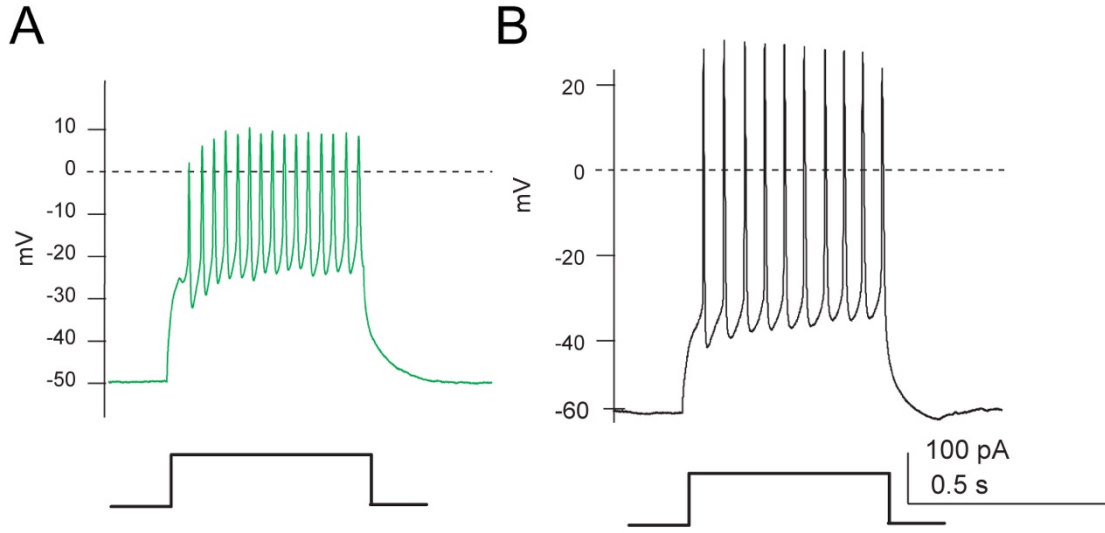


Figure 9. Acute characterization of skeletal sodium channel replacement on nNav 1.X CRISPR background. (A) Sample action potentials from transfected neuron (green trace) and (B) control neuron (black trace) with a given current injection (100pA, 0.5s). (C) Nav1.4 replacement AP slope, (D) rise time, and (E) height quantified.

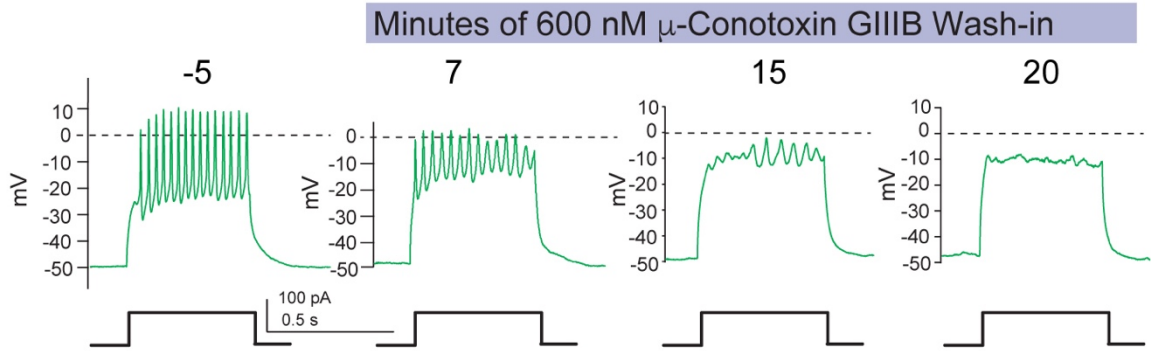
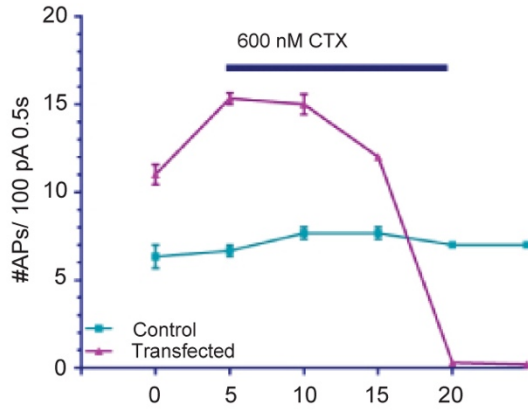
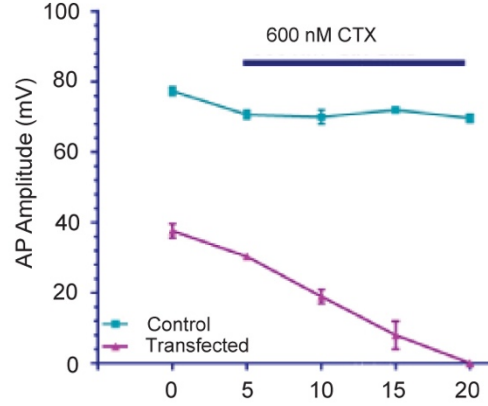
A**B****C**

Figure 10. Acute characterization of skeletal sodium channel replacement on nNav 1.X CRISPR background, with Nav1.4-specific Conotoxin block. (A) Sample trace from the same transfected neuron (in Figure 9) after Conotoxin application. (B) Action potential frequency for a given current injection in control (blue) and transfected (pink) neurons. Action potentials are more frequent in transfected neuron but disappear after conotoxin wash-in. (C) Action potential amplitude for a given current injection in control (blue) and transfected (pink) neurons. Action potential amplitudes are shorter in transfected neuron fall to zero after conotoxin wash-in. Line charts show mean \pm s.e.m.

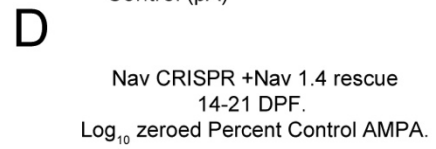
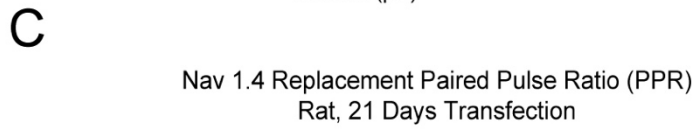
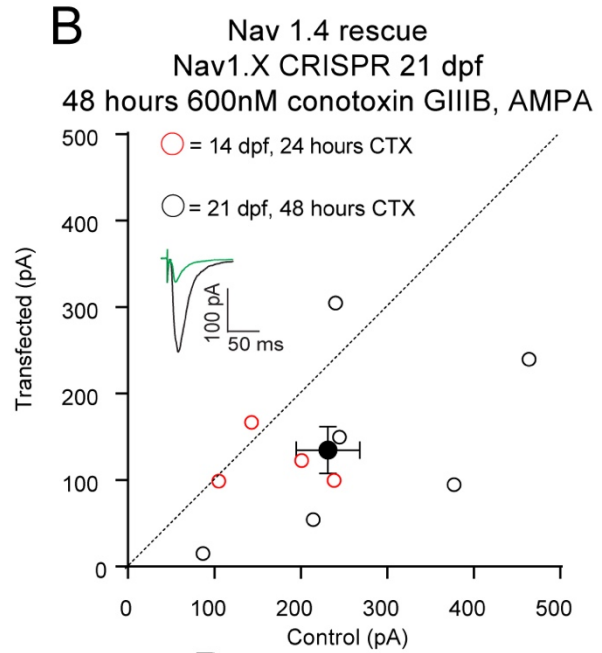
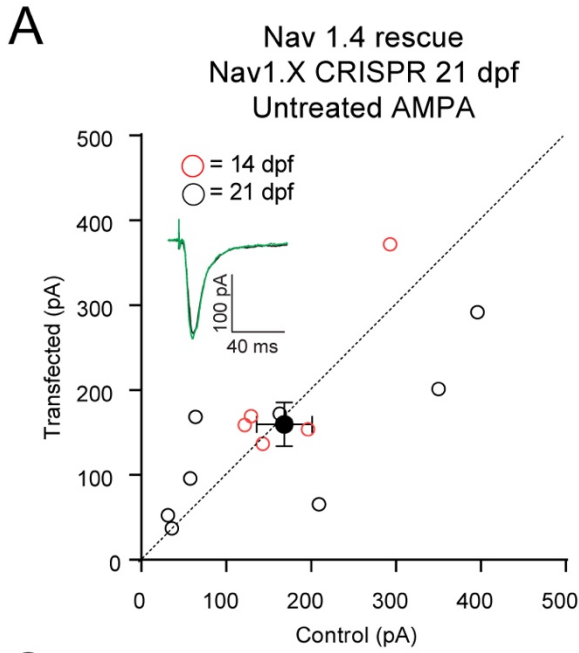


Figure 11. Synaptic (AMPA) characterization of Nav 1.4 replacement and chronic Conotoxin (CTX) block. (A) After 2 or 3 weeks of Nav1.4 replacement on the nNav 1.X CRISPR background, synaptic AMPA currents appear unaffected (n=13, n.s.). (B) After 2 or 3 weeks of Nav1.4 replacement on the nNav 1.X CRISPR background, synaptic AMPA currents were recorded after chronic μ -conotoxin GIIIB treatment for 24 or 48 hours, respectively (n=10, p=0.02*, Paired student's T-Test). (C) Paired pulse ratio was obtained in 4 pairs of control vs. transfected neurons after 21 days of expression and 48 hours of conotoxin treatment. No difference was observed. Summary graph is mean \pm s.e.m. (n=4, n.s.). (D) Log₁₀ normalized summary graph comparing transfected as % control in CTX-treated and untreated conditions. Mean \pm s.e.m. p=0.02*, Mann-Whitney).

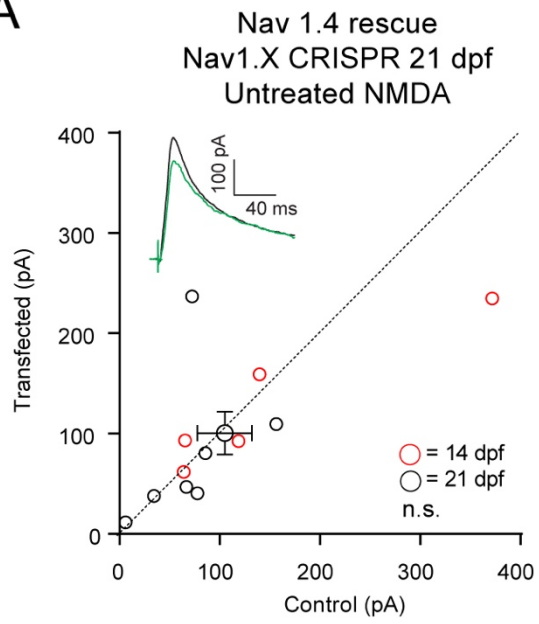
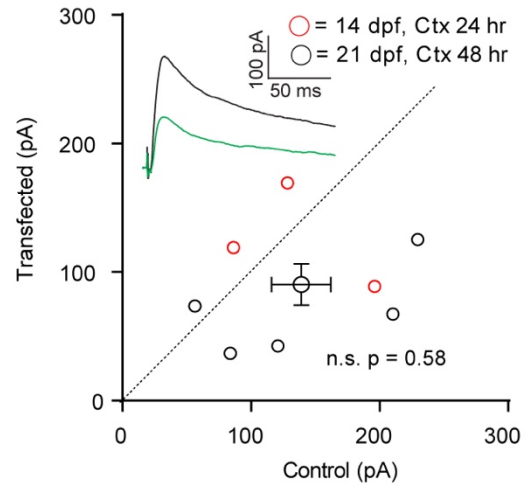
A**B**

Figure 12. Synaptic (NMDA) characterization of Nav 1.4 replacement and chronic Conotoxin (CTX) block. (A) After 2 or 3 weeks of Nav1.4 replacement on the nNav 1.X CRISPR background, synaptic NMDA currents appear unaffected (n=12, n.s.). (B) After 2 or 3 weeks of Nav1.4 replacement on the nNav 1.X CRISPR background, synaptic NMDA currents were recorded after chronic μ -conotoxin GIIIB treatment for 24 or 48 hours, respectively (n=8, n.s. p=0.058, Paired student's t-test).

Chapter 5

General Conclusions

GluA2 is necessary and sufficient for the expression of postsynaptic scaling-up

The results of my thesis support a model of synaptic scaling that not only requires the GluA2 AMPAR subunit, but is also entirely supported by GluA2 in the absence of other endogenous AMPAR subunits. Using RNAi technology to remove individual AMPAR subunits, I found that only GluA2 knockdown blocked scaling-up in organotypic hippocampal cultures. In addition, using a molecular replacement strategy in which all endogenous AMPARs are conditionally replaced with specific transfected AMPAR subunits, I found that GluA2, but not GluA1, is sufficient to mediate scaling-up following chronic activity deprivation.

In contrast to previous results suggesting that GluA2-lacking receptors are critical for scaling, we found that GluA2 is essential for scaling-up, reinforcing the GluA2-centric model of synaptic homeostasis supported by evidence from multiple studies. For example, GluA2 is required for homeostatic scaling-down following chronic, cell-autonomous optogenetic excitation (Goold and Nicoll, 2010). In addition, GluA2 is necessary for distance-dependent scaling of AMPARs along the dendrite (Shipman et al., 2013). Finally, we previously (Levy et al., 2015) identified a requirement for the GluA2 subunit in AMPAR consolidation following loss of synaptic scaffolding proteins. Together, these findings lay the groundwork for a model of bi-directional homeostatic control of postsynaptic strength through the GluA2 AMPAR subunit.

The membrane-proximal GluA2 CTD is necessary for scaling

While many of the findings described in chapter 3 of this thesis are in agreement with the GluA2-centric scaling literature, certain results are at odds with the preexisting model of GluA2-mediated scaling, in which the distal GluA2 C-tail controls the expression of synaptic AMPAR insertion via

competitive binding of GRIP1 and PICK1 to the distal C-tail. Specifically, although my work identified a requirement for the GluA2 C-tail by rescuing knockdown of endogenous GluA2 with chimeric GluA2-GluA1 or CTD-truncated GluA2 receptors, I discovered no requirement for the distal GluA2 C-tail. Indeed, I found no requirement for any part of the GluA2 C-tail after K847. This is very much at odds with work from the Turrigiano and Hugarir labs, which have zeroed in on a scaling program involving the competitive and reversible binding of GRIP1 and PICK1. Work in Gainey et al. (2015) shows that a distal GluA2 serine (S880) undergoes activity-dependent phosphorylation that affects the relative occupation of the distal C-tail by GRIP1 and PICK1. In their model, phosphorylation of GluA2 S880 blocks GRIP1 binding and promotes association with PICK1. Additionally, they report GRIP1 knockdown prevents scaling-up and GRIP1 overexpression “mimicked” scaling-up. In support of this model, the Hugarir lab showed that germline PICK1 knockout occludes synaptic scaling, suggesting that in the absence of a competitive binding environment, GRIP1 is constitutively trafficking GluA2-containing AMPARs to synapses and creating a constantly-scaled-up state (Anggono et al., 2011).

Many interactions have been described in the GluA2 C-tail, especially close to the distal PDZ domain. In testing various C-tail truncated GluA2 rescues, I was therefore surprised when the GluA2 Δ 847 fully rescued scaling, as there are few known protein-protein interactions in the membrane proximal C-tail, and more recently, studies have demonstrated a role for the distal C-tail (Anggono et al., 2011; Gainey et al., 2015). How, then, can I reconcile my findings with the literature? While some of the discrepancy could be attributed to different culture conditions (previous studies rely primarily on dissociated cultures, while we turned to organotypic cultures), other caveats to these studies exist, and I will discuss specific caveats in two papers, Gainey et al.

(2009) and Gainey et al. (2015). Of note, caveats exist concerning the likely redundancy of the GRIP family proteins, the quality of the GluA2 shRNAs used in these two studies, and the shRNA expression timeline, discussed below.

GRIP1 and GRIP2, ~130 kDa each, coexist at excitatory synapses in the hippocampus and are both known to bind AMPARs, although their expression time courses are markedly distinct (Dong et al., 1999). GRIP1 is expressed at higher levels embryonically, prior to AMPAR expression, and expression decreases as synapses mature. Conversely, GRIP2 expression more closely follows AMPAR expression, with higher levels of GRIP2 following synapse maturation (Dong et al., 1999). Additionally, our lab has previously attempted to validate the GluA2 shRNA used in Gainey et al. (2009 & 2015), where we did not observe inward rectification, even after many days of shRNA expression (data not shown).

Another concern with their use of the shRNA is the length of shRNA expression: they report either 1 day shRNA expression (Gainey et al., 2009) or 2 day shRNA expression (Gainey et al., 2015) in either dissociated or organotypic cultures, which is arguably far too short of an expression window to achieve complete knockdown of GluA2. The complete turnover of AMPARs occurs on the order of multiple days, if not weeks, as the metabolic half-life of GluA2 has been reported to be on the order of >140 hours *in vivo* (Archibald et al., 1998; Huh and Wenthold, 1999; Kjoller and Diemer, 2000; Mammen et al., 1997).

Interestingly, while the authors report that GRIP1 overexpression “mimicked” scaling-up, they did not perform a critically important (and somewhat obvious) follow-up experiment to determine

whether or not the effect they observed was an occlusion of scaling-up or an additional enhancement that could be observed on top of scaling induced by activity blockade. Specifically, the authors should have overexpressed GRIP1, incubated transfected cultures in TTX, and compared the degree of scaling in control neurons to the degree of enhancement in GRIP1-overexpressing neurons to determine if scaling is occluded or enhanced with higher levels of GRIP1. The fact that the authors omitted this critical experiment is concerning. A final caveat to their finding that GRIP1 knockdown blocks scaling (due to a putative activity-dependent removal of GluA2-containing AMPARs mediated by PICK1), is that absence of GRIP1 could promote a hyper-phosphorylated state of GluA2 S880, thereby promoting a more active internalization of GluA2 by PICK1. This could potentially obscure other, physiological scaling programs, perhaps involving the membrane proximal GluA2 C-tail.

A single amino acid residue within the membrane proximal CTD of GluA2 is necessary for scaling

In studying the role of the GluA2 membrane-proximal C-tail, I identified a specific amino acid residue that seems to be necessary and sufficient for synaptic scaling. When GluA2 A843 is replaced with a “phosphorylatable” and “GluA1-like” serine (GluA2* A843S and GluA2*Δ847 A843S), scaling-up is blocked. Additionally, when S818 in the otherwise nearly-identical GluA1 membrane proximal C-tail is mutated to an alanine (S818A), chimeric AMPA receptor subunits containing the GluA2 ATD and the mutant GluA1 C-tail (GluA2*:A1CTD S818A) are able to support scaling-up. Taken together, these results could point toward a mechanism by which GluA2 is stabilized at synapses following chronic silencing through some modification or interaction of

residues in the proximal CTD, thus ensuring that GluA2-containing, calcium-impermeable AMPARs are preferentially targeted to synapses following global scaling-up.

Phosphorylation of GluA1S818 by PKC is known to affect binding of the cytoskeletal-associated protein, Band4.1 (also known as 4.1N), although an interaction between Band4.1 and GluA2 has not yet been described (Chen et al., 2005; Coleman et al., 2003; Lin et al., 2009). Interestingly, another group found an important stabilizing interaction between Band4.1 and the membrane proximal C-tail of GluK2 (Kainate receptor) subunits, which is negatively regulated by PKC phosphorylation of a nearby serine (Copits and Swanson, 2013). However, 4.1N is unlikely to be playing a critically important role in neuronal homeostasis, as germline KO of 4.1N and its family member 4.1G has no effect on baseline transmission or LTP (Wozny et al., 2009). These results are discussed in more detail in the discussion of chapter 3 of this thesis.

Other explanations, while less parsimonious, are nevertheless possible. For example, phosphorylation of the corresponding residue in the membrane proximal GluA1 C-tail, S818, may serve as a weak synaptic exclusion or ER retention signal in the absence of an associated GluA2 subunit. The occupation of synapses by AMPARs is a tightly-regulated process, and under basal conditions, preventing excess AMPARs from entering synapses is likely critical for preserving cellular patterns of information storage. Further experiments are necessary to uncover the protein or proteins upstream of synaptic AMPAR insertion that interact with the membrane proximal C-tail of GluA2

Scaling in single neurons?

In chapter 4 of this thesis, I describe experiments that assess the intrinsic ability of a single neuron to engage synaptic scaling programs after chronic hyperpolarization or sodium channel block. Despite employing four distinct techniques to chronically reduce the activity of individual neurons, I saw no evidence for a cell-intrinsic scaling program. An interesting juxtaposition emerges between scaling-down (which can be robustly induced in individual neurons) and scaling-up (which has yet to be definitively shown by more than one group) (Burrone et al., 2002; Goold and Nicoll, 2010; Iyata et al., 2008). Why might a neuron be able to scale-down synaptic strength in response to chronic optogenetic excitation, yet unable to scale-up synaptic strength in response to chronic activity blockade? To some extent, the answer might still be more philosophical than empirical: it's perhaps more important to silence a hyperactive neuron within an otherwise healthy network than to enhance the activity of an unusually silent one. In a given non-pathological neuronal environment, "Hebbian" activity-dependent synaptic pruning phenomena might supersede or drown-out homeostatic pathways following chronic single-cell silencing, as the remaining neurons within the network compensate for the less-active neuron, while, conversely, a pathologically-excited cell might robustly engage homeostatic feedback programs to reduce activity back to a set-point.

Future directions

The findings reported in chapter 4 of this thesis are preliminary, at best, and much validation is required when proving a null hypothesis, so I feel compelled to offer suggestions for experiments to help guide future studies. Significant work was done by a former lab member, Seth Shipman, to characterize the effects of Kir2.1-mediated single-cell hyperpolarization over development, both

prior to robust synapse formation and after. I would then propose an experiment exploring the effects of pharmacological hM4Di activation at different time points: earlier days *in vitro*, late days *in vitro*, and by activating the inhibitory DREADD for either more than 48 hours or less than 24. In addition, using the pan-neuronal sodium channel CRISPR, I would knockout sodium channels earlier, perhaps *in utero*, to assess the effects of early sodium channel genetic ablation.

Evidence for *other* forms of homeostatic compensation following early loss of voltage-dependent ion channels comes from studies comparing acute functional KO of the Kv4.2 channel with germline deletion of the same channel. Kv4.2 channels, which are the primary source of I_A in the mammalian brain, are known to localize to inhibitory synapses in somatodendritic compartments in both cortical and hippocampal pyramidal neurons (Burkhalter et al., 2006; Nerbonne et al., 2008; Yuan et al., 2005). A-type current (I_A) is critical for appropriate repolarization following an AP, the rapid repolarization during repetitive firing, and the regulation of back-propagating action potentials into dendrites. Acute functional KO of Kv4.2 with a dominant negative Kv4.2 leads to hyper-excitable cultures, while germline Kv4.2 KO neurons were functionally indistinguishable from their WT counterparts (apart from persistent hyper-excitability in the dendritic compartments). Thus, it would be worth assessing intrinsic excitability homeostasis in individual neurons following early genetic ablation of voltage-dependent sodium channels. For similar reasons, I would repeat the Nav1.4 replacement and pharmacological-silencing experiments at multiple time points, and I would explore the effects of replacing endogenous neuronal sodium channels with Nav1.4 *in utero*, thereby allowing more time for additional forms of activity normalization prior to AMPA receptor incorporation into synapses.

But what about trying to silence the synapses directly? After all, chronic network-wide pharmacological block of synaptic receptors triggers the same homeostatic programs as sodium channel block (Thiagarajan et al., 2005). The problem with trying to study the effects of direct synaptic silencing *on* synaptic scaling in single neurons is that – any manipulation you might be able to design to acutely silence synapses results in a scenario in which synapses could not incorporate synaptic AMPARs even if there were some cell-intrinsic program driving the surface targeting of AMPARs to mediate scaling. By way of example, one could imagine expressing the genetically encoded PSD95 recombinant antibody (Gross et al., 2013), attached to an E3 Ubiquitin ligase under doxycycline control, to rapidly and reversibly reduce synaptic activity (similar to the acute and reversible targeted degradation of gephyrin in (Gross et al., 2016)). Other means of eliminating expression of proteins – like shRNA or CRISPR technology – work by cutting off the supply of the protein (either by targeting mRNA or gene) and are therefore only effective once the existing protein has degraded, which can take up to 3 weeks (Gross et al., 2016). Conversely, a genetically-encoded intracellular antibody could escort an attached ubiquitin ligase to a protein of interest, allowing the ubiquitin ligase to mark the protein for immediate transport to – and degradation in – the proteasome. The protein turnover would likely occur within a 24-hour period as near-complete degradation has been demonstrated to occur in a (much shorter) 6-hour window (Gross et al., 2016). However, we arrive at the catch-22: the problem with a manipulation like this, of course, is that eliminating PSD95 *ipso facto* eliminates AMPAR docking sites, or “slots,” within synaptic PSD95, thus preventing any significant synaptic AMPAR-incorporation following chronic synaptic-PSD95 ablation.

Concluding remarks

Homeostatic synaptic scaling, operating at a much slower time-scale than more acute forms of plasticity, such as LTP and LTD, is a critical mechanism by which the cell tunes the strength of its synaptic inputs up or down to counteract normal or pathological activity perturbations, contributing to the restoration of baseline neuronal output. Even subtle deficits in a neuron's ability to maintain a fine-tuning of activity in response to a chronic perturbation would result in catastrophic degradation of salient information. Thus, accurately characterizing the molecular interactions of downstream effectors – including the postsynaptic receptors themselves – that drive synaptic scaling is of critical importance in developing a thorough understanding of the mechanism by which a cell is able to maintain a set-point of activity.

As scaling is likely to exist as a subtle phenomenon in a non-pathological neuronal environment, it may be impossible for any scientist to observe the phenomenon without using more extreme manipulations – i.e. blocking all action potentials in a cell or network of neurons. While the field of scaling is likely using an experimental sledgehammer to crack open a nut⁶, the work described in chapter 3 of my thesis, as well as the myriad scaling experiments performed previously in other labs, are nevertheless critically important for uncovering the underlying mechanisms of synaptic scaling and synaptic AMPA receptor targeting, even if it is unclear how these mechanisms are used *in vivo* by the cell.

⁶ To use excessive or extravagant means to accomplish something requiring subtler coercion.

References

- Abbott, L. F., and Nelson, S. B. (2000). Synaptic plasticity: taming the beast. *Nat Neurosci 3 Suppl*, 1178-1183.
- Adesnik, H., Li, G., Durling, M. J., Pleasure, S. J., and Nicoll, R. A. (2008). NMDA receptors inhibit synapse unsilencing during brain development. *Proc Natl Acad Sci U S A 105*, 5597-5602.
- Altimimi, H. F., and Stellwagen, D. (2013). Persistent synaptic scaling independent of AMPA receptor subunit composition. *J Neurosci 33*, 11763-11767.
- Anggono, V., Clem, R. L., and Huganir, R. L. (2011). PICK1 loss of function occludes homeostatic synaptic scaling. *J Neurosci 31*, 2188-2196.
- Anggono, V., and Huganir, R. L. (2012). Regulation of AMPA receptor trafficking and synaptic plasticity. *Curr Opin Neurobiol 22*, 461-469.
- Aoto, J., Nam, C. I., Poon, M. M., Ting, P., and Chen, L. (2008). Synaptic signaling by all-trans retinoic acid in homeostatic synaptic plasticity. *Neuron 60*, 308-320.
- Archibald, K., Perry, M. J., Molnar, E., and Henley, J. M. (1998). Surface expression and metabolic half-life of AMPA receptors in cultured rat cerebellar granule cells. *Neuropharmacology 37*, 1345-1353.
- Arendt, K. L., Sarti, F., and Chen, L. (2013). Chronic inactivation of a neural circuit enhances LTP by inducing silent synapse formation. *J Neurosci 33*, 2087-2096.
- Armbruster, B. N., Li, X., Pausch, M. H., Herlitze, S., and Roth, B. L. (2007). Evolving the lock to fit the key to create a family of G protein-coupled receptors potently activated by an inert ligand. *Proc Natl Acad Sci U S A 104*, 5163-5168.
- Armstrong, N., Jasti, J., Beich-Frandsen, M., and Gouaux, E. (2006). Measurement of conformational changes accompanying desensitization in an ionotropic glutamate receptor. *Cell 127*, 85-97.
- Bear, M. F. (2003). Bidirectional synaptic plasticity: from theory to reality. *Philos Trans R Soc Lond B Biol Sci 358*, 649-655.

- Bemben, M. A., Shipman, S. L., Hirai, T., Herring, B. E., Li, Y., Badger, J. D., 2nd, Nicoll, R. A., Diamond, J. S., and Roche, K. W. (2014). CaMKII phosphorylation of neuroligin-1 regulates excitatory synapses. *Nat Neurosci* 17, 56-64.
- Bienenstock, E. L., Cooper, L. N., and Munro, P. W. (1982). Theory for the development of neuron selectivity: orientation specificity and binocular interaction in visual cortex. *J Neurosci* 2, 32-48.
- Bliss, T. V., and Lomo, T. (1973). Long-lasting potentiation of synaptic transmission in the dentate area of the anaesthetized rabbit following stimulation of the perforant path. *J Physiol* 232, 331-356.
- Braithwaite, S. P., Xia, H., and Malenka, R. C. (2002). Differential roles for NSF and GRIP/ABP in AMPA receptor cycling. *Proc Natl Acad Sci U S A* 99, 7096-7101.
- Burkhalter, A., Gonchar, Y., Mellor, R. L., and Nerbonne, J. M. (2006). Differential expression of I(A) channel subunits Kv4.2 and Kv4.3 in mouse visual cortical neurons and synapses. *J Neurosci* 26, 12274-12282.
- Burrone, J., O'Byrne, M., and Murthy, V. N. (2002). Multiple forms of synaptic plasticity triggered by selective suppression of activity in individual neurons. *Nature* 420, 414-418.
- Cannon, W. B. (1932). *The wisdom of the body*, (New York,: W.W. Norton & Company).
- Chang, M. C., Park, J. M., Pelkey, K. A., Grabenstatter, H. L., Xu, D., Linden, D. J., Sutula, T. P., McBain, C. J., and Worley, P. F. (2010). Narp regulates homeostatic scaling of excitatory synapses on parvalbumin-expressing interneurons. *Nat Neurosci* 13, 1090-1097.
- Chen, K., Merino, C., Sigrist, S. J., and Featherstone, D. E. (2005). The 4.1 protein coracle mediates subunit-selective anchoring of Drosophila glutamate receptors to the postsynaptic actin cytoskeleton. *J Neurosci* 25, 6667-6675.
- Coleman, S. K., Cai, C., Mottershead, D. G., Haapalahti, J. P., and Keinanen, K. (2003). Surface expression of GluR-D AMPA receptor is dependent on an interaction between its C-terminal domain and a 4.1 protein. *J Neurosci* 23, 798-806.
- Collingridge, G. L., Isaac, J. T., and Wang, Y. T. (2004). Receptor trafficking and synaptic plasticity. *Nat Rev Neurosci* 5, 952-962.

- Collingridge, G. L., Kehl, S. J., and McLennan, H. (1983). Excitatory amino acids in synaptic transmission in the Schaffer collateral-commissural pathway of the rat hippocampus. *J Physiol* 334, 33-46.
- Copits, B. A., and Swanson, G. T. (2013). Kainate receptor post-translational modifications differentially regulate association with 4.1N to control activity-dependent receptor endocytosis. *J Biol Chem* 288, 8952-8965.
- Davis, G. W. (2013). Homeostatic signaling and the stabilization of neural function. *Neuron* 80, 718-728.
- Desai, N. S., Cudmore, R. H., Nelson, S. B., and Turrigiano, G. G. (2002). Critical periods for experience-dependent synaptic scaling in visual cortex. *Nat Neurosci* 5, 783-789.
- Dong, H., Zhang, P., Song, I., Petralia, R. S., Liao, D., and Huganir, R. L. (1999). Characterization of the glutamate receptor-interacting proteins GRIP1 and GRIP2. *J Neurosci* 19, 6930-6941.
- Fox, K., and Stryker, M. (2017). Integrating Hebbian and homeostatic plasticity: introduction. *Philos Trans R Soc Lond B Biol Sci* 372.
- Gainey, M. A., Hurvitz-Wolff, J. R., Lambo, M. E., and Turrigiano, G. G. (2009). Synaptic scaling requires the GluR2 subunit of the AMPA receptor. *J Neurosci* 29, 6479-6489.
- Gainey, M. A., Tataavarty, V., Nahmani, M., Lin, H., and Turrigiano, G. G. (2015). Activity-dependent synaptic GRIP1 accumulation drives synaptic scaling up in response to action potential blockade. *Proc Natl Acad Sci U S A* 112, E3590-3599.
- Garcia-Bereguian, M. A., Gonzalez-Islas, C., Lindsly, C., Butler, E., Hill, A. W., and Wenner, P. (2013). In vivo synaptic scaling is mediated by GluA2-lacking AMPA receptors in the embryonic spinal cord. *J Neurosci* 33, 6791-6799.
- Giese, K. P., Fedorov, N. B., Filipkowski, R. K., and Silva, A. J. (1998). Autophosphorylation at Thr286 of the alpha calcium-calmodulin kinase II in LTP and learning. *Science* 279, 870-873.
- Goel, A., Jiang, B., Xu, L. W., Song, L., Kirkwood, A., and Lee, H. K. (2006). Cross-modal regulation of synaptic AMPA receptors in primary sensory cortices by visual experience. *Nat Neurosci* 9, 1001-1003.

- Goold, C. P., and Nicoll, R. A. (2010). Single-cell optogenetic excitation drives homeostatic synaptic depression. *Neuron* 68, 512-528.
- Granger, A. J., and Nicoll, R. A. (2014). LTD expression is independent of glutamate receptor subtype. *Front Synaptic Neurosci* 6, 15.
- Granger, A. J., Shi, Y., Lu, W., Cerpas, M., and Nicoll, R. A. (2013). LTP requires a reserve pool of glutamate receptors independent of subunit type. *Nature* 493, 495-500.
- Gray, J. A., Shi, Y., Usui, H., During, M. J., Sakimura, K., and Nicoll, R. A. (2011). Distinct modes of AMPA receptor suppression at developing synapses by GluN2A and GluN2B: single-cell NMDA receptor subunit deletion in vivo. *Neuron* 71, 1085-1101.
- Greger, I. H., Khatri, L., Kong, X., and Ziff, E. B. (2003). AMPA receptor tetramerization is mediated by Q/R editing. *Neuron* 40, 763-774.
- Greger, I. H., Ziff, E. B., and Penn, A. C. (2007). Molecular determinants of AMPA receptor subunit assembly. *Trends Neurosci* 30, 407-416.
- Gross, G. G., Junge, J. A., Mora, R. J., Kwon, H. B., Olson, C. A., Takahashi, T. T., Liman, E. R., Ellis-Davies, G. C., McGee, A. W., Sabatini, B. L., *et al.* (2013). Recombinant probes for visualizing endogenous synaptic proteins in living neurons. *Neuron* 78, 971-985.
- Gross, G. G., Straub, C., Perez-Sanchez, J., Dempsey, W. P., Junge, J. A., Roberts, R. W., Trinh, A., Fraser, S. E., De Koninck, Y., De Koninck, P., *et al.* (2016). An E3-ligase-based method for ablating inhibitory synapses. *Nat Methods* 13, 673-678.
- Groth, R. D., Lindskog, M., Thiagarajan, T. C., Li, L., and Tsien, R. W. (2011). Beta Ca²⁺/CaM-dependent kinase type II triggers upregulation of GluA1 to coordinate adaptation to synaptic inactivity in hippocampal neurons. *Proc Natl Acad Sci U S A* 108, 828-833.
- Harris, N., Braiser, D. J., Dickman, D. K., Fetter, R. D., Tong, A., and Davis, G. W. (2015). The Innate Immune Receptor PGRP-LC Controls Presynaptic Homeostatic Plasticity. *Neuron* 88, 1157-1164.
- Hebb, D. O. (1949). *The organization of behavior; a neuropsychological theory*, (New York,: Wiley).

- Hollmann, M., and Heinemann, S. (1994). Cloned glutamate receptors. *Annu Rev Neurosci* 17, 31-108.
- Hoover, K. B., and Bryant, P. J. (2000). The genetics of the protein 4.1 family: organizers of the membrane and cytoskeleton. *Curr Opin Cell Biol* 12, 229-234.
- Huganir, R. L., and Nicoll, R. A. (2013). AMPARs and synaptic plasticity: the last 25 years. *Neuron* 80, 704-717.
- Huh, K. H., and Wenthold, R. J. (1999). Turnover analysis of glutamate receptors identifies a rapidly degraded pool of the N-methyl-D-aspartate receptor subunit, NR1, in cultured cerebellar granule cells. *J Biol Chem* 274, 151-157.
- Ibata, K., Sun, Q., and Turrigiano, G. G. (2008). Rapid synaptic scaling induced by changes in postsynaptic firing. *Neuron* 57, 819-826.
- Incontro, S., Asensio, C. S., Edwards, R. H., and Nicoll, R. A. (2014). Efficient, complete deletion of synaptic proteins using CRISPR. *Neuron* 83, 1051-1057.
- Keck, T., Keller, G. B., Jacobsen, R. I., Eysel, U. T., Bonhoeffer, T., and Hubener, M. (2013). Synaptic scaling and homeostatic plasticity in the mouse visual cortex in vivo. *Neuron* 80, 327-334.
- Keinanen, K., Wisden, W., Sommer, B., Werner, P., Herb, A., Verdoorn, T. A., Sakmann, B., and Seeburg, P. H. (1990). A family of AMPA-selective glutamate receptors. *Science* 249, 556-560.
- Kerchner, G. A., and Nicoll, R. A. (2008). Silent synapses and the emergence of a postsynaptic mechanism for LTP. *Nat Rev Neurosci* 9, 813-825.
- Kjoller, C., and Diemer, N. H. (2000). GluR2 protein synthesis and metabolism in rat hippocampus following transient ischemia and ischemic tolerance induction. *Neurochem Int* 37, 7-15.
- Lee, H. K., Takamiya, K., Han, J. S., Man, H., Kim, C. H., Rumbaugh, G., Yu, S., Ding, L., He, C., Petralia, R. S., *et al.* (2003). Phosphorylation of the AMPA receptor GluR1 subunit is required for synaptic plasticity and retention of spatial memory. *Cell* 112, 631-643.

- Lee, H. K., Takamiya, K., He, K., Song, L., and Huganir, R. L. (2010). Specific roles of AMPA receptor subunit GluR1 (GluA1) phosphorylation sites in regulating synaptic plasticity in the CA1 region of hippocampus. *J Neurophysiol* *103*, 479-489.
- Lee, S. H., Liu, L., Wang, Y. T., and Sheng, M. (2002). Clathrin adaptor AP2 and NSF interact with overlapping sites of GluR2 and play distinct roles in AMPA receptor trafficking and hippocampal LTD. *Neuron* *36*, 661-674.
- Letellier, M., Elramah, S., Mondin, M., Soula, A., Penn, A., Choquet, D., Landry, M., Thoumine, O., and Favereaux, A. (2014). miR-92a regulates expression of synaptic GluA1-containing AMPA receptors during homeostatic scaling. *Nat Neurosci* *17*, 1040-1042.
- Levy, J. M., Chen, X., Reese, T. S., and Nicoll, R. A. (2015). Synaptic Consolidation Normalizes AMPAR Quantal Size following MAGUK Loss. *Neuron* *87*, 534-548.
- Lin, D. T., Makino, Y., Sharma, K., Hayashi, T., Neve, R., Takamiya, K., and Huganir, R. L. (2009). Regulation of AMPA receptor extrasynaptic insertion by 4.1N, phosphorylation and palmitoylation. *Nat Neurosci* *12*, 879-887.
- Lindskog, M., Li, L., Groth, R. D., Poburko, D., Thiagarajan, T. C., Han, X., and Tsien, R. W. (2010). Postsynaptic GluA1 enables acute retrograde enhancement of presynaptic function to coordinate adaptation to synaptic inactivity. *Proc Natl Acad Sci U S A* *107*, 21806-21811.
- Lu, W., Shi, Y., Jackson, A. C., Bjorgan, K., Doring, M. J., Sprengel, R., Seeburg, P. H., and Nicoll, R. A. (2009). Subunit composition of synaptic AMPA receptors revealed by a single-cell genetic approach. *Neuron* *62*, 254-268.
- Maffei, A., Nelson, S. B., and Turrigiano, G. G. (2004). Selective reconfiguration of layer 4 visual cortical circuitry by visual deprivation. *Nat Neurosci* *7*, 1353-1359.
- Malenka, R. C., and Bear, M. F. (2004). LTP and LTD: an embarrassment of riches. *Neuron* *44*, 5-21.
- Malinow, R., and Malenka, R. C. (2002). AMPA receptor trafficking and synaptic plasticity. *Annu Rev Neurosci* *25*, 103-126.
- Mammen, A. L., Huganir, R. L., and O'Brien, R. J. (1997). Redistribution and stabilization of cell surface glutamate receptors during synapse formation. *J Neurosci* *17*, 7351-7358.

- Matsuzaki, M., Honkura, N., Ellis-Davies, G. C., and Kasai, H. (2004). Structural basis of long-term potentiation in single dendritic spines. *Nature* *429*, 761-766.
- Matta, J. A., Pelkey, K. A., Craig, M. T., Chittajallu, R., Jeffries, B. W., and McBain, C. J. (2013). Developmental origin dictates interneuron AMPA and NMDA receptor subunit composition and plasticity. *Nat Neurosci* *16*, 1032-1041.
- Muller, M., Liu, K. S., Sigrist, S. J., and Davis, G. W. (2012). RIM controls homeostatic plasticity through modulation of the readily-releasable vesicle pool. *J Neurosci* *32*, 16574-16585.
- Navarro-Quiroga, I., Chittajallu, R., Gallo, V., and Haydar, T. F. (2007). Long-term, selective gene expression in developing and adult hippocampal pyramidal neurons using focal in utero electroporation. *J Neurosci* *27*, 5007-5011.
- Nerbonne, J. M., Gerber, B. R., Norris, A., and Burkhalter, A. (2008). Electrical remodelling maintains firing properties in cortical pyramidal neurons lacking KCND2-encoded A-type K⁺ currents. *J Physiol* *586*, 1565-1579.
- Nicoll, R. A. (2017). A Brief History of Long-Term Potentiation. *Neuron* *93*, 281-290.
- Noel, J., Ralph, G. S., Pickard, L., Williams, J., Molnar, E., Uney, J. B., Collingridge, G. L., and Henley, J. M. (1999). Surface expression of AMPA receptors in hippocampal neurons is regulated by an NSF-dependent mechanism. *Neuron* *23*, 365-376.
- O'Brien, R. J., Kamboj, S., Ehlers, M. D., Rosen, K. R., Fischbach, G. D., and Huganir, R. L. (1998). Activity-dependent modulation of synaptic AMPA receptor accumulation. *Neuron* *21*, 1067-1078.
- Oliet, S. H., Malenka, R. C., and Nicoll, R. A. (1996). Bidirectional control of quantal size by synaptic activity in the hippocampus. *Science* *271*, 1294-1297.
- Osten, P., Srivastava, S., Inman, G. J., Vilim, F. S., Khatri, L., Lee, L. M., States, B. A., Einheber, S., Milner, T. A., Hanson, P. I., and Ziff, E. B. (1998). The AMPA receptor GluR2 C terminus can mediate a reversible, ATP-dependent interaction with NSF and alpha- and beta-SNAPs. *Neuron* *21*, 99-110.
- Panicker, S., Brown, K., and Nicoll, R. A. (2008). Synaptic AMPA receptor subunit trafficking is independent of the C terminus in the GluR2-lacking mouse. *Proc Natl Acad Sci U S A* *105*, 1032-1037.

- Paradis, S., Sweeney, S. T., and Davis, G. W. (2001). Homeostatic control of presynaptic release is triggered by postsynaptic membrane depolarization. *Neuron* 30, 737-749.
- Parrish, J. Z., Kim, C. C., Tang, L., Bergquist, S., Wang, T., Derisi, J. L., Jan, L. Y., Jan, Y. N., and Davis, G. W. (2014). Kruppel mediates the selective rebalancing of ion channel expression. *Neuron* 82, 537-544.
- Penn, A. C., Zhang, C. L., Georges, F., Royer, L., Breillat, C., Hosy, E., Petersen, J. D., Humeau, Y., and Choquet, D. (2017). Hippocampal LTP and contextual learning require surface diffusion of AMPA receptors. *Nature* 549, 384-388.
- Perez-Otano, I., and Ehlers, M. D. (2005). Homeostatic plasticity and NMDA receptor trafficking. *Trends Neurosci* 28, 229-238.
- Pettit, D. L., Perlman, S., and Malinow, R. (1994). Potentiated transmission and prevention of further LTP by increased CaMKII activity in postsynaptic hippocampal slice neurons. *Science* 266, 1881-1885.
- Roche, K. W., O'Brien, R. J., Mammen, A. L., Bernhardt, J., and Huganir, R. L. (1996). Characterization of multiple phosphorylation sites on the AMPA receptor GluR1 subunit. *Neuron* 16, 1179-1188.
- Rogan, S. C., and Roth, B. L. (2011). Remote control of neuronal signaling. *Pharmacol Rev* 63, 291-315.
- Rosenmund, C., Stern-Bach, Y., and Stevens, C. F. (1998). The tetrameric structure of a glutamate receptor channel. *Science* 280, 1596-1599.
- Ruiz, R., Cano, R., Casanas, J. J., Gaffield, M. A., Betz, W. J., and Tabares, L. (2011). Active zones and the readily releasable pool of synaptic vesicles at the neuromuscular junction of the mouse. *J Neurosci* 31, 2000-2008.
- Rutherford, L. C., Nelson, S. B., and Turrigiano, G. G. (1998). BDNF has opposite effects on the quantal amplitude of pyramidal neuron and interneuron excitatory synapses. *Neuron* 21, 521-530.
- Schnell, E., Sizemore, M., Karimzadegan, S., Chen, L., Brecht, D. S., and Nicoll, R. A. (2002). Direct interactions between PSD-95 and stargazin control synaptic AMPA receptor number. *Proc Natl Acad Sci U S A* 99, 13902-13907.

- Scoville, W. B., and Milner, B. (1957). Loss of recent memory after bilateral hippocampal lesions. *J Neurol Neurosurg Psychiatry* *20*, 11-21.
- Shen, L., Liang, F., Walensky, L. D., and Huganir, R. L. (2000). Regulation of AMPA receptor GluR1 subunit surface expression by a 4. 1N-linked actin cytoskeletal association. *J Neurosci* *20*, 7932-7940.
- Sheng, M., and Kim, M. J. (2002). Postsynaptic signaling and plasticity mechanisms. *Science* *298*, 776-780.
- Shepherd, J. D., Rumbaugh, G., Wu, J., Chowdhury, S., Plath, N., Kuhl, D., Huganir, R. L., and Worley, P. F. (2006). Arc/Arg3.1 mediates homeostatic synaptic scaling of AMPA receptors. *Neuron* *52*, 475-484.
- Shi, S., Hayashi, Y., Esteban, J. A., and Malinow, R. (2001). Subunit-specific rules governing AMPA receptor trafficking to synapses in hippocampal pyramidal neurons. *Cell* *105*, 331-343.
- Shipman, S. L., Herring, B. E., Suh, Y. H., Roche, K. W., and Nicoll, R. A. (2013). Distance-dependent scaling of AMPARs is cell-autonomous and GluA2 dependent. *J Neurosci* *33*, 13312-13319.
- Sipe, G. O., Lowery, R. L., Tremblay, M. E., Kelly, E. A., Lamantia, C. E., and Majewska, A. K. (2016). Microglial P2Y12 is necessary for synaptic plasticity in mouse visual cortex. *Nat Commun* *7*, 10905.
- Smith, K. S., Bucci, D. J., Luikart, B. W., and Mahler, S. V. (2016). DREADDS: Use and application in behavioral neuroscience. *Behav Neurosci* *130*, 137-155.
- Soares, C., Lee, K. F., Nassrallah, W., and Beique, J. C. (2013). Differential subcellular targeting of glutamate receptor subtypes during homeostatic synaptic plasticity. *J Neurosci* *33*, 13547-13559.
- Sobolevsky, A. I., Rosconi, M. P., and Gouaux, E. (2009). X-ray structure, symmetry and mechanism of an AMPA-subtype glutamate receptor. *Nature* *462*, 745-756.
- Sommer, B., Kohler, M., Sprengel, R., and Seeburg, P. H. (1991). RNA editing in brain controls a determinant of ion flow in glutamate-gated channels. *Cell* *67*, 11-19.

- Stellwagen, D., and Malenka, R. C. (2006). Synaptic scaling mediated by glial TNF- α . *Nature* *440*, 1054-1059.
- Sutton, M. A., Ito, H. T., Cressy, P., Kempf, C., Woo, J. C., and Schuman, E. M. (2006). Miniature neurotransmission stabilizes synaptic function via tonic suppression of local dendritic protein synthesis. *Cell* *125*, 785-799.
- Thiagarajan, T. C., Lindskog, M., and Tsien, R. W. (2005). Adaptation to synaptic inactivity in hippocampal neurons. *Neuron* *47*, 725-737.
- Turrigiano, G., Abbott, L. F., and Marder, E. (1994). Activity-dependent changes in the intrinsic properties of cultured neurons. *Science* *264*, 974-977.
- Turrigiano, G. G. (2008). The self-tuning neuron: synaptic scaling of excitatory synapses. *Cell* *135*, 422-435.
- Turrigiano, G. G., Leslie, K. R., Desai, N. S., Rutherford, L. C., and Nelson, S. B. (1998). Activity-dependent scaling of quantal amplitude in neocortical neurons. *Nature* *391*, 892-896.
- Turrigiano, G. G., and Nelson, S. B. (1998). Thinking globally, acting locally: AMPA receptor turnover and synaptic strength. *Neuron* *21*, 933-935.
- Turrigiano, G. G., and Nelson, S. B. (2004). Homeostatic plasticity in the developing nervous system. *Nat Rev Neurosci* *5*, 97-107.
- Wang, J. Z., Rojas, C. V., Zhou, J. H., Schwartz, L. S., Nicholas, H., and Hoffman, E. P. (1992). Sequence and genomic structure of the human adult skeletal muscle sodium channel alpha subunit gene on 17q. *Biochem Biophys Res Commun* *182*, 794-801.
- Watt, A. J., and Desai, N. S. (2010). Homeostatic Plasticity and STDP: Keeping a Neuron's Cool in a Fluctuating World. *Front Synaptic Neurosci* *2*, 5.
- Watt, A. J., van Rossum, M. C., MacLeod, K. M., Nelson, S. B., and Turrigiano, G. G. (2000). Activity coregulates quantal AMPA and NMDA currents at neocortical synapses. *Neuron* *26*, 659-670.
- Wenthold, R. J., Petralia, R. S., Blahos, J., II, and Niedzielski, A. S. (1996). Evidence for multiple AMPA receptor complexes in hippocampal CA1/CA2 neurons. *J Neurosci* *16*, 1982-1989.

- Wiesel, T. N., and Hubel, D. H. (1963). Single-Cell Responses in Striate Cortex of Kittens Deprived of Vision in One Eye. *J Neurophysiol* 26, 1003-1017.
- Woods, S. C., and Ramsay, D. S. (2007). Homeostasis: beyond Curt Richter. *Appetite* 49, 388-398.
- Wozny, C., Breustedt, J., Wolk, F., Varoqueaux, F., Boretius, S., Zivkovic, A. R., Neeb, A., Frahm, J., Schmitz, D., Brose, N., and Ivanovic, A. (2009). The function of glutamatergic synapses is not perturbed by severe knockdown of 4.1N and 4.1G expression. *J Cell Sci* 122, 735-744.
- Xue, M., Atallah, B. V., and Scanziani, M. (2014). Equalizing excitation-inhibition ratios across visual cortical neurons. *Nature* 511, 596-600.
- Younger, M. A., Muller, M., Tong, A., Pym, E. C., and Davis, G. W. (2013). A presynaptic ENaC channel drives homeostatic plasticity. *Neuron* 79, 1183-1196.
- Yuan, W., Burkhalter, A., and Nerbonne, J. M. (2005). Functional role of the fast transient outward K⁺ current I_A in pyramidal neurons in (rat) primary visual cortex. *J Neurosci* 25, 9185-9194.
- Zamanillo, D., Sprengel, R., Hvalby, O., Jensen, V., Burnashev, N., Rozov, A., Kaiser, K. M., Koster, H. J., Borchardt, T., Worley, P., *et al.* (1999). Importance of AMPA receptors for hippocampal synaptic plasticity but not for spatial learning. *Science* 284, 1805-1811.

Publishing Agreement

It is the policy of the University to encourage the distribution of all theses, dissertations, and manuscripts. Copies of all UCSF theses, dissertations, and manuscripts will be routed to the library via the Graduate Division. The library will make all theses, dissertations, and manuscripts accessible to the public and will preserve these to the best of their abilities, in perpetuity.

Please sign the following statement:

I hereby grant permission to the Graduate Division of the University of California, San Francisco to release copies of my thesis, dissertation, or manuscript to the Campus Library to provide access and preservation, in whole or in part, in perpetuity.

Samantha Anona Esselmann
Author Signature

11/13/17
Date